

# Block-structured Adaptive Mesh Refinement Methods for Conservation Laws

Theory, Implementation and Application

Ralf Deiterding

Computer Science and Mathematics Division  
Oak Ridge National Laboratory  
P.O. Box 2008 MS6367, Oak Ridge, TN 37831, USA

E-mail: [deiterdingr@ornl.gov](mailto:deiterdingr@ornl.gov)

# Structure of the lectures

1. Fundamentals
  - ▶ Finite volume schemes for hyperbolic problems
  - ▶ Discussion of mesh adaptation approaches
2. Structured AMR for hyperbolic problems
  - ▶ Presentation of all algorithmic components
  - ▶ Parallelization
3. Complex hyperbolic structured AMR applications
  - ▶ Shock-induced combustion
  - ▶ Fluid-structure interaction
4. Further topics
  - ▶ Using the SAMR approach for multigrid methods
  - ▶ Practical implementation, discussion of SAMR systems

# Useful references I

## Finite volume methods for hyperbolic problems

- ▶ LeVeque, R. J. (2002). *Finite volume methods for hyperbolic problems*. Cambridge University Press, Cambridge, New York.
- ▶ Godlewski, E. and Raviart, P.-A. (1996). *Numerical approximation of hyperbolic systems of conservation laws*. Springer Verlag, New York.
- ▶ Toro, E. F. (1999). *Riemann solvers and numerical methods for fluid dynamics*. Springer-Verlag, Berlin, Heidelberg, 2nd edition.
- ▶ Laney, C. B. (1998). *Computational gasdynamics*. Cambridge University Press, Cambridge.

## Structured Adaptive Mesh Refinement

- ▶ Berger, M. and Colella, P. (1988). Local adaptive mesh refinement for shock hydrodynamics. *J. Comput. Phys.*, 82:64–84.
- ▶ Bell, J., Berger, M., Saltzman, J., and Welcome, M. (1994). Three-dimensional adaptive mesh refinement for hyperbolic conservation laws. *SIAM J. Sci. Comp.*, 15(1):127–138.
- ▶ Berger, M. and LeVeque, R. (1998). Adaptive mesh refinement using wave-propagation algorithms for hyperbolic systems. *SIAM J. Numer. Anal.*, 35(6):2298–2316.

## Useful references II

Adaptive multigrid (finite difference and finite element based in textbooks)

- ▶ Hackbusch, W. (1985). *Multi-Grid Methods and Applications*. Springer Verlag, Berlin, Heidelberg.
- ▶ Briggs, W. L., Henson, V. E., and McCormick, S. F. (2001). *A Multigrid Tutorial*. Society for Industrial and Applied Mathematics, 2nd edition.
- ▶ Trottenberg, U., Oosterlee, C., and Schüller, A. (2001). *Multigrid*. Academic Press, San Antonio.
- ▶ Martin, D. F. (1998). *A cell-centered adaptive projection method for the incompressible Euler equations*. PhD thesis, University of California at Berkeley.

Implementation, parallelization

- ▶ Hornung, R. D., Wissink, A. M., and Kohn, S. H. (2006). Managing complex data and geometry in parallel structured AMR applications. *Engineering with Computers*, 22:181–195.
- ▶ Rendleman, C. A., Beckner, V. E., Lijewski, M., Crutchfield, W., and Bell, J. B. (2000). Parallelization of structured, hierarchical adaptive mesh refinement algorithms. *Computing and Visualization in Science*, 3:147–157.

## Useful references III

- ▶ Deiterding, R. (2005). Construction and application of an AMR algorithm for distributed memory computers. In Plewa, T., Linde, T., and Weirs, V. G., editors, *Adaptive Mesh Refinement - Theory and Applications*, volume 41 of *Lecture Notes in Computational Science and Engineering*, pages 361–372. Springer.
- ▶ Deiterding, R. (2003). *Parallel adaptive simulation of multi-dimensional detonation structures*. PhD thesis, Brandenburgische Technische Universität Cottbus.

### Applications (from my own work)

- ▶ Deiterding, R. (2009). A parallel adaptive method for simulating shock-induced combustion with detailed chemical kinetics in complex domains. *Computers & Structures*, 87:769–783.
- ▶ Deiterding, R., Radovitzky, R., Mauch, S. P., Noels, L., Cummings, J. C., and Meiron, D. I. (2006). A virtual test facility for the efficient simulation of solid materials under high energy shock-wave loading. *Engineering with Computers*, 22(3-4):325–347.
- ▶ Pantano, C., Deiterding, R., Hill, D. J., and Pullin, D. I. (2007). A low-numerical dissipation patch-based adaptive mesh refinement method for large-eddy simulation of compressible flows. *J. Comput. Phys.*, 221(1):63–87.

# Lecture 1

## Fundamentals: Used schemes and mesh adaptation

Course *Block-structured Adaptive Mesh Refinement Methods for Conservation Laws*  
*Theory, Implementation and Application*

Ralf Deiterding

Computer Science and Mathematics Division  
Oak Ridge National Laboratory  
P.O. Box 2008 MS6367, Oak Ridge, TN 37831, USA

E-mail: [deiterdingr@ornl.gov](mailto:deiterdingr@ornl.gov)

# Outline

## Conservation laws

- Mathematical background
- Examples

## Finite volume methods

- Basics of finite difference methods
- Splitting methods, second derivatives

## Upwind schemes

- Flux-difference splitting
- Flux-vector splitting
- High-resolution methods

## Meshes and adaptation

- Elements of adaptive algorithms
- Adaptivity on unstructured meshes
- Structured mesh refinement techniques

# Outline

## Conservation laws

Mathematical background

Examples

## Finite volume methods

Basics of finite difference methods

Splitting methods, second derivatives

## Upwind schemes

Flux-difference splitting

Flux-vector splitting

High-resolution methods

## Meshes and adaptation

Elements of adaptive algorithms

Adaptivity on unstructured meshes

Structured mesh refinement techniques



# Hyperbolic Conservation Laws

$$\frac{\partial}{\partial t} \mathbf{q}(\mathbf{x}, t) + \sum_{n=1}^d \frac{\partial}{\partial x_n} \mathbf{f}_n(\mathbf{q}(\mathbf{x}, t)) = \mathbf{s}(\mathbf{q}(\mathbf{x}, t)), \quad D \subset \{(\mathbf{x}, t) \in \mathbb{R}^d \times \mathbb{R}_0^+\}$$

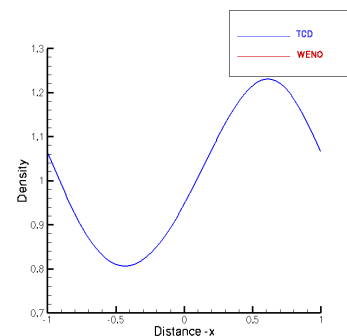
$\mathbf{q} = \mathbf{q}(\mathbf{x}, t) \in S \subset \mathbb{R}^M$  - vector of state,  $\mathbf{f}_n(\mathbf{q}) \in C^1(S, \mathbb{R}^M)$  - flux functions,  $\mathbf{s}(\mathbf{q}) \in C^1(S, \mathbb{R}^M)$  - source term

## Definition (Hyperbolicity)

$\mathbf{A}(\mathbf{q}, \nu) = \nu_1 \mathbf{A}_1(\mathbf{q}) + \dots + \nu_d \mathbf{A}_d(\mathbf{q})$  with  $\mathbf{A}_n(\mathbf{q}) = \partial \mathbf{f}_n(\mathbf{q}) / \partial \mathbf{q}$  has  $M$  real eigenvalues  $\lambda_1(\mathbf{q}, \nu) \leq \dots \leq \lambda_M(\mathbf{q}, \nu)$  and  $M$  linear independent right eigenvectors  $\mathbf{r}_m(\mathbf{q}, \nu)$ .

If  $\mathbf{f}_n(\mathbf{q})$  is nonlinear, classical solutions  $\mathbf{q}(\mathbf{x}, t) \in C^1(D, S)$  do not generally exist, not even for  $\mathbf{q}_0(\mathbf{x}) \in C^1(\mathbb{R}^d, S)$  [Majda, 1984], [Godlewski and Raviart, 1996], [Kröner, 1997]

Example: Euler equations



# Weak solutions

Integral form (Gauss's theorem):

$$\int_{\Omega} \mathbf{q}(\mathbf{x}, t + \Delta t) d\mathbf{x} - \int_{\Omega} \mathbf{q}(\mathbf{x}, t) d\mathbf{x} + \sum_{n=1}^d \int_t^{t+\Delta t} \int_{\partial\Omega} \mathbf{f}_n(\mathbf{q}(\mathbf{o}, t)) \sigma_n(\mathbf{o}) d\mathbf{o} dt = \int_t^{t+\Delta t} \int_{\Omega} \mathbf{s}(\mathbf{q}(\mathbf{x}, t)) d\mathbf{x}$$

## Theorem (Weak solution)

$\mathbf{q}_0 \in L_{loc}^{\infty}(\mathbb{R}^d, S)$ .  $\mathbf{q} \in L_{loc}^{\infty}(D, S)$  is weak solution if  $\mathbf{q}$  satisfies

$$\int_0^{\infty} \int_{\mathbb{R}^d} \left[ \frac{\partial \varphi}{\partial t} \cdot \mathbf{q} + \sum_{n=1}^d \frac{\partial \varphi}{\partial x_n} \cdot \mathbf{f}_n(\mathbf{q}) - \varphi \cdot \mathbf{s}(\mathbf{q}) \right] d\mathbf{x} dt + \int_{\mathbb{R}^d} \varphi(\mathbf{x}, 0) \cdot \mathbf{q}_0(\mathbf{x}) d\mathbf{x} = 0$$

for any test function  $\varphi \in C_0^1(D, S)$

# Entropy solutions

Select physical weak solution as  $\lim_{\varepsilon \rightarrow 0} \mathbf{q}_\varepsilon = \mathbf{q}$  almost everywhere in  $D$  of

$$\frac{\partial \mathbf{q}_\varepsilon}{\partial t} + \sum_{n=1}^d \frac{\partial \mathbf{f}_n(\mathbf{q}_\varepsilon)}{\partial x_n} - \varepsilon \sum_{n=1}^d \frac{\partial^2 \mathbf{q}_\varepsilon}{\partial x_n^2} = \mathbf{s}(\mathbf{q}_\varepsilon), \quad \mathbf{x} \in \mathbb{R}^d, \quad t > 0$$

## Theorem (Entropy condition)

Assume existence of entropy  $\eta \in C^2(S, \mathbb{R})$  and entropy fluxes  $\psi_n \in C^1(S, \mathbb{R})$  that satisfy

$$\frac{\partial \eta(\mathbf{q})}{\partial \mathbf{q}}^T \cdot \frac{\partial \mathbf{f}_n(\mathbf{q})}{\partial \mathbf{q}} = \frac{\partial \psi_n(\mathbf{q})}{\partial \mathbf{q}}^T, \quad n = 1, \dots, d$$

then  $\lim_{\varepsilon \rightarrow 0} \mathbf{q}_\varepsilon = \mathbf{q}$  almost everywhere in  $D$  is weak solution and satisfies

$$\frac{\partial \eta(\mathbf{q})}{\partial t} + \sum_{n=1}^d \frac{\partial \psi_n(\mathbf{q})}{\partial x_n} \leq \frac{\partial \eta(\mathbf{q})}{\partial \mathbf{q}}^T \cdot \mathbf{s}(\mathbf{q})$$

in the sense of distributions. Proof: [Godlewski and Raviart, 1996]

# Entropy solutions II

## Definition (Entropy solution)

Weak solution  $\mathbf{q}$  is called an entropy solution if  $\mathbf{q}$  satisfies

$$\int_0^\infty \int_{\mathbb{R}^d} \left[ \frac{\partial \varphi}{\partial t} \eta(\mathbf{q}) + \sum_{n=1}^d \frac{\partial \varphi}{\partial x_n} \psi_n(\mathbf{q}) - \varphi \frac{\partial \eta(\mathbf{q})}{\partial \mathbf{q}}^T \cdot \mathbf{s}(\mathbf{q}) \right] d\mathbf{x} dt + \int_{\mathbb{R}^d} \varphi(\mathbf{x}, 0) \eta(\mathbf{q}_0(\mathbf{x})) d\mathbf{x} \geq 0$$

for all entropy functions  $\eta(\mathbf{q})$  and all test functions  $\varphi \in C_0^1(D, \mathbb{R}_0^+)$ ,  $\varphi \geq 0$

## Theorem (Jump conditions)

An entropy solution  $\mathbf{q}$  is a classical solution  $\mathbf{q} \in C^1(D, S)$  almost everywhere and satisfies the Rankine-Hugoniot (RH) jump condition

$$(\mathbf{q}^+ - \mathbf{q}^-) \sigma_t + \sum_{n=1}^d (\mathbf{f}_n(\mathbf{q}^+) - \mathbf{f}_n(\mathbf{q}^-)) \sigma_n = \mathbf{0}$$

and the jump inequality

$$(\eta(\mathbf{q}^+) - \eta(\mathbf{q}^-)) \sigma_t + \sum_{n=1}^d (\psi_n(\mathbf{q}^+) - \psi_n(\mathbf{q}^-)) \sigma_n \leq 0$$

along discontinuities. Proof: [Godlewski and Raviart, 1996]

# Examples

Euler equations

$$\frac{\partial \rho}{\partial t} + \frac{\partial}{\partial x_n} (\rho u_n) = 0$$

$$\frac{\partial}{\partial t} (\rho u_k) + \frac{\partial}{\partial x_n} (\rho u_k u_n + \delta_{kn} p) = 0, \quad k = 1, \dots, d$$

$$\frac{\partial}{\partial t} (\rho E) + \frac{\partial}{\partial x_n} (u_n (\rho E + p)) = 0$$

with polytrope gas equation of state

$$p = (\gamma - 1) \left( \rho E - \frac{1}{2} \rho u_n u_n \right)$$

have structure

$$\partial_t \mathbf{q}(\mathbf{x}, t) + \nabla \cdot \mathbf{f}(\mathbf{q}(\mathbf{x}, t)) = 0$$

# Examples II

Navier-Stokes equations

$$\frac{\partial \rho}{\partial t} + \frac{\partial}{\partial x_n} (\rho u_n) = 0$$

$$\frac{\partial}{\partial t} (\rho u_k) + \frac{\partial}{\partial x_n} (\rho u_k u_n + \delta_{kn} p - \tau_{kn}) = 0, \quad k = 1, \dots, d$$

$$\frac{\partial}{\partial t} (\rho E) + \frac{\partial}{\partial x_n} (u_n (\rho E + p) + q_n - \tau_{nj} u_j) = 0$$

with stress tensor

$$\tau_{kn} = \mu \left( \frac{\partial u_n}{\partial x_k} + \frac{\partial u_k}{\partial x_n} \right) - \frac{2}{3} \mu \frac{\partial u_j}{\partial x_j} \delta_{kn}$$

and heat conduction

$$q_n = -\lambda \frac{\partial T}{\partial x_n}$$

have structure

$$\partial_t \mathbf{q}(\mathbf{x}, t) + \nabla \cdot \mathbf{f}(\mathbf{q}(\mathbf{x}, t)) + \nabla \cdot \mathbf{h}(\mathbf{q}(\mathbf{x}, t), \nabla \mathbf{q}(\mathbf{x}, t)) = 0$$

Type can be either hyperbolic or parabolic

# Outline

## Conservation laws

- Mathematical background
- Examples

## Finite volume methods

- Basics of finite difference methods
- Splitting methods, second derivatives

## Upwind schemes

- Flux-difference splitting
- Flux-vector splitting
- High-resolution methods

## Meshes and adaptation

- Elements of adaptive algorithms
- Adaptivity on unstructured meshes
- Structured mesh refinement techniques

# Derivation

Assume  $\partial_t \mathbf{q} + \partial_x \mathbf{f}(\mathbf{q}) + \partial_x \mathbf{h}(\mathbf{q}(\cdot, \partial_x \mathbf{q})) = \mathbf{s}(\mathbf{q})$

Time discretization  $t_n = n\Delta t$ , discrete volumes

$$I_j = [x_j - \frac{1}{2}\Delta x, x_j + \frac{1}{2}\Delta x] =: [x_{j-1/2}, x_{j+1/2}]$$

Using approximations  $\mathbf{Q}_j(t) \approx \frac{1}{|I_j|} \int_{I_j} \mathbf{q}(\mathbf{x}, t) dx$ ,  $\mathbf{s}(\mathbf{Q}_j(t)) \approx \frac{1}{|I_j|} \int_{I_j} \mathbf{s}(\mathbf{q}(\mathbf{x}, t)) dx$

and numerical fluxes

$$\mathbf{F}(\mathbf{Q}_j(t), \mathbf{Q}_{j+1}(t)) \approx \mathbf{f}(\mathbf{q}(x_{j+1/2}, t)), \quad \mathbf{H}(\mathbf{Q}_j(t), \mathbf{Q}_{j+1}(t)) \approx \mathbf{h}(\mathbf{q}(x_{j+1/2}, t), \nabla \mathbf{q}(x_{j+1/2}, t))$$

yields after integration (Gauss theorem)

$$\begin{aligned} \mathbf{Q}_j(t_{n+1}) = \mathbf{Q}_j(t_n) - \frac{1}{\Delta x} \int_{t_n}^{t_{n+1}} [\mathbf{F}(\mathbf{Q}_j(t), \mathbf{Q}_{j+1}(t)) - \mathbf{F}(\mathbf{Q}_{j-1}(t), \mathbf{Q}_j(t))] dt - \\ \frac{1}{\Delta x} \int_{t_n}^{t_{n+1}} [\mathbf{H}(\mathbf{Q}_j(t), \mathbf{Q}_{j+1}(t)) - \mathbf{H}(\mathbf{Q}_{j-1}(t), \mathbf{Q}_j(t))] dt + \int_{t_n}^{t_{n+1}} \mathbf{s}(\mathbf{Q}_j(t)) dt \end{aligned}$$

For instance:

$$\begin{aligned} \mathbf{Q}_j^{n+1} = \mathbf{Q}_j^n - \frac{\Delta t}{\Delta x} [\mathbf{F}(\mathbf{Q}_j^n, \mathbf{Q}_{j+1}^n) - \mathbf{F}(\mathbf{Q}_{j-1}^n, \mathbf{Q}_j^n)] - \\ \frac{\Delta t}{\Delta x} [\mathbf{H}(\mathbf{Q}_j^n, \mathbf{Q}_{j+1}^n) - \mathbf{H}(\mathbf{Q}_{j-1}^n, \mathbf{Q}_j^n)] + \Delta t \mathbf{s}(\mathbf{Q}_j^n) \end{aligned}$$



# Some classical definitions

$(2s + 1)$ -point difference scheme of the form

$$\mathbf{Q}_j^{n+1} = \mathcal{H}^{(\Delta t)}(\mathbf{Q}_{j-s}^n, \dots, \mathbf{Q}_{j+s}^n)$$

## Definition (Stability)

For each time  $\tau$  there is a constant  $C_S$  and a value  $n_0 \in \mathbb{N}$  such that  $\|\mathcal{H}^{(\Delta t)}(\mathbf{Q}^n)\| \leq C_S$  for all  $n\Delta t \leq \tau$ ,  $n < n_0$

## Definition (Consistency)

If the local truncation error

$$\mathcal{L}^{(\Delta t)}(\mathbf{x}, t) := \frac{1}{\Delta t} \left[ \mathbf{q}(\mathbf{x}, t + \Delta t) - \mathcal{H}^{(\Delta t)}(\mathbf{q}(\cdot, t)) \right]$$

satisfies  $\|\mathcal{L}^{(\Delta t)}(\cdot, t)\| \rightarrow 0$  as  $\Delta t \rightarrow 0$

## Definition (Convergence)

If the global error  $\mathcal{E}^{(\Delta t)}(\mathbf{x}, t) := \mathbf{Q}(\mathbf{x}, t) - \mathbf{q}(\mathbf{x}, t)$  satisfies  $\|\mathcal{E}^{(\Delta t)}(\cdot, t)\| \rightarrow 0$  as  $\Delta t \rightarrow 0$  for all admissible initial data  $\mathbf{q}_0(\mathbf{x})$

# Some classical definitions II

## Definition (Order of accuracy)

$\mathcal{H}(\cdot)$  is accurate of order  $o$  if for all sufficiently smooth initial data  $\mathbf{q}_0(\mathbf{x})$ , there is a constant  $C_L$ , such that the local truncation error satisfies

$$\|\mathcal{L}^{(\Delta t)}(\cdot, t)\| \leq C_L \Delta t^o \text{ for all } \Delta t < \Delta t_0, t \leq \tau$$

## Definition (Conservative form)

If  $\mathcal{H}(\cdot)$  can be written in the form

$$\mathbf{Q}_j^{n+1} = \mathbf{Q}_j^n - \frac{\Delta t}{\Delta x} (\mathbf{F}(\mathbf{Q}_{j-s+1}^n, \dots, \mathbf{Q}_{j+s}^n) - \mathbf{F}(\mathbf{Q}_{j-s}^n, \dots, \mathbf{Q}_{j+s-1}^n))$$

A conservative scheme satisfies

$$\sum_{j \in \mathbb{Z}} \mathbf{Q}_j^{n+1} = \sum_{j \in \mathbb{Z}} \mathbf{Q}_j^n$$

## Definition (Consistency of a conservative method)

If the numerical flux satisfies  $\mathbf{F}(\mathbf{q}, \dots, \mathbf{q}) = \mathbf{f}(\mathbf{q})$  for all  $\mathbf{q} \in S$

# Splitting methods

Solve homogeneous PDE and ODE successively!

$$\begin{aligned}\mathcal{H}^{(\Delta t)} : \quad & \partial_t \mathbf{q} + \nabla \cdot \mathbf{f}(\mathbf{q}) = 0, \quad \text{IC: } \mathbf{Q}(t_m) \xrightarrow{\Delta t} \tilde{\mathbf{Q}} \\ \mathcal{S}^{(\Delta t)} : \quad & \partial_t \mathbf{q} = \mathbf{s}(\mathbf{q}), \quad \text{IC: } \tilde{\mathbf{Q}} \xrightarrow{\Delta t} \mathbf{Q}(t_m + \Delta t)\end{aligned}$$

1st-order Godunov splitting:  $\mathbf{Q}(t_m + \Delta t) = \mathcal{S}^{(\Delta t)} \mathcal{H}^{(\Delta t)}(\mathbf{Q}(t_m))$ ,

2nd-order Strang splitting :  $\mathbf{Q}(t_m + \Delta t) = \mathcal{S}^{(\frac{1}{2}\Delta t)} \mathcal{H}^{(\Delta t)} \mathcal{S}^{(\frac{1}{2}\Delta t)}(\mathbf{Q}(t_m))$

1st-order dimensional splitting for  $\mathcal{H}^{(\cdot)}$ :

$$\begin{aligned}\mathcal{X}_1^{(\Delta t)} : \quad & \partial_t \mathbf{q} + \partial_{x_1} \mathbf{f}_1(\mathbf{q}) = 0, \quad \text{IC: } \mathbf{Q}(t_m) \xrightarrow{\Delta t} \tilde{\mathbf{Q}}^{1/2} \\ \mathcal{X}_2^{(\Delta t)} : \quad & \partial_t \mathbf{q} + \partial_{x_2} \mathbf{f}_2(\mathbf{q}) = 0, \quad \text{IC: } \tilde{\mathbf{Q}}^{1/2} \xrightarrow{\Delta t} \tilde{\mathbf{Q}}\end{aligned}$$

[Toro, 1999]

# Conservative scheme for diffusion equation

Consider  $\partial_t q - c \Delta q = 0$  with  $c \in \mathbb{R}^+$ , which is readily discretized as

$$Q_{jk}^{n+1} = Q_{jk}^n + c \frac{\Delta t}{\Delta x_1^2} (Q_{j+1,k}^n - 2Q_{jk}^n + Q_{j-1,k}^n) + c \frac{\Delta t}{\Delta x_2^2} (Q_{j,k+1}^n - 2Q_{jk}^n + Q_{j,k-1}^n)$$

or conservatively

$$Q_{jk}^{n+1} = Q_{jk}^n + c \frac{\Delta t}{\Delta x_1} \left( H_{j+\frac{1}{2},k}^1 - H_{j-\frac{1}{2},k}^1 \right) + c \frac{\Delta t}{\Delta x_2} \left( H_{j,k+\frac{1}{2}}^2 - H_{j,k-\frac{1}{2}}^2 \right)$$

Von Neumann stability analysis: Insert single eigenmode  $\hat{Q}(t)e^{ik_1 x_1} e^{ik_2 x_2}$  into discretization

$$\hat{Q}^{n+1} = \hat{Q}^n + C_1 (\hat{Q}^n e^{ik_1 \Delta x_1} - 2\hat{Q}^n + \hat{Q}^n e^{-ik_1 \Delta x_1}) + C_2 (\hat{Q}^n e^{ik_2 \Delta x_2} - 2\hat{Q}^n + \hat{Q}^n e^{-ik_2 \Delta x_2})$$

with  $C_\ell = c \frac{\Delta t}{\Delta x_\ell^2}$ ,  $\ell = 1, 2$ , which gives after inserting  $e^{ik_\ell x_\ell} = \cos(k_\ell x_\ell) + i \sin(k_\ell x_\ell)$

$$\hat{Q}^{n+1} = \hat{Q}^n (1 + 2C_1(\cos(k_1 \Delta x_1) - 1) + 2C_2(\cos(k_2 \Delta x_2) - 1))$$

Stability requires

$$|1 + 2C_1(\cos(k_1 \Delta x_1) - 1) + 2C_2(\cos(k_2 \Delta x_2) - 1)| \leq 1$$

i.e.

$$|1 - 4C_1 - 4C_2| \leq 1$$

from which we derive the stability condition

$$0 \leq c \left( \frac{\Delta t}{\Delta x_1^2} + \frac{\Delta t}{\Delta x_2^2} \right) \leq \frac{1}{2}$$

# Linear upwind schemes

Consider Riemann problem

$$\frac{\partial}{\partial t} \mathbf{q}(x, t) + \mathbf{A} \frac{\partial}{\partial x} \mathbf{q}(x, t) = \mathbf{0}, \quad x \in \mathbb{R}, \quad t > 0$$

Has exact solution

$$\mathbf{q}(x, t) = \mathbf{q}_L + \sum_{\lambda_m < x/t} a_m \mathbf{r}_m = \mathbf{q}_R - \sum_{\lambda_m \geq x/t} a_m \mathbf{r}_m = \sum_{\lambda_m \geq x/t} \delta_m \mathbf{r}_m + \sum_{\lambda_m < x/t} \beta_m \mathbf{r}_m$$

Use Riemann problem to evaluate numerical flux  $\mathbf{F}(\mathbf{q}_L, \mathbf{q}_R) := \mathbf{f}(\mathbf{q}(0, t)) = \mathbf{A}\mathbf{q}(0, t)$  as

$$\mathbf{F}(\mathbf{q}_L, \mathbf{q}_R) = \mathbf{A}\mathbf{q}_L + \sum_{\lambda_m < 0} a_m \lambda_m \mathbf{r}_m = \mathbf{A}\mathbf{q}_R - \sum_{\lambda_m \geq 0} a_m \lambda_m \mathbf{r}_m = \sum_{\lambda_m \geq 0} \delta_m \lambda_m \mathbf{r}_m + \sum_{\lambda_m < 0} \beta_m \lambda_m \mathbf{r}_m$$

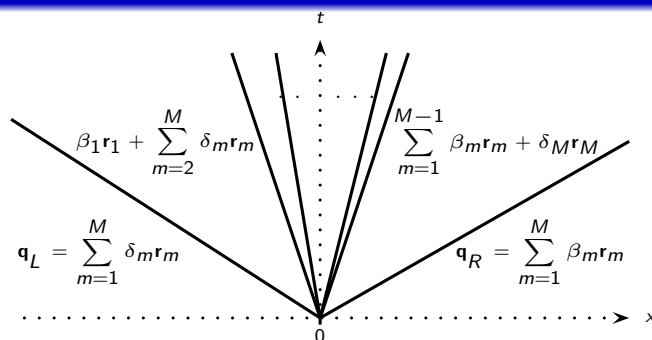
Use  $\lambda_m^+ = \max(\lambda_m, 0)$ ,  $\lambda_m^- = \min(\lambda_m, 0)$

to define  $\mathbf{\Lambda}^+ := \text{diag}(\lambda_1^+, \dots, \lambda_M^+)$ ,  $\mathbf{\Lambda}^- := \text{diag}(\lambda_1^-, \dots, \lambda_M^-)$

and  $\mathbf{A}^+ := \mathbf{R} \mathbf{\Lambda}^+ \mathbf{R}^{-1}$ ,  $\mathbf{A}^- := \mathbf{R} \mathbf{\Lambda}^- \mathbf{R}^{-1}$  which gives

$$\mathbf{F}(\mathbf{q}_L, \mathbf{q}_R) = \mathbf{A}\mathbf{q}_L + \mathbf{A}^- \Delta \mathbf{q} = \mathbf{A}\mathbf{q}_R - \mathbf{A}^+ \Delta \mathbf{q} = \mathbf{A}^+ \mathbf{q}_L + \mathbf{A}^- \mathbf{q}_R$$

with  $\Delta \mathbf{q} = \mathbf{q}_R - \mathbf{q}_L$



# Flux difference splitting

Godunov-type scheme with  $\Delta \mathbf{Q}_{j+1/2}^n = \mathbf{Q}_{j+1}^n - \mathbf{Q}_j^n$

$$\mathbf{Q}_j^{n+1} = \mathbf{Q}_j^n - \frac{\Delta t}{\Delta x} \left( \mathbf{A}^- \Delta \mathbf{Q}_{j+1/2}^n + \mathbf{A}^+ \Delta \mathbf{Q}_{j-1/2}^n \right)$$

Use linearization  $\bar{\mathbf{f}}(\bar{\mathbf{q}}) = \hat{\mathbf{A}}(\mathbf{q}_L, \mathbf{q}_R) \bar{\mathbf{q}}$  and construct scheme for nonlinear problem as

$$\mathbf{Q}_j^{n+1} = \mathbf{Q}_j^n - \frac{\Delta t}{\Delta x} \left( \hat{\mathbf{A}}^-(\mathbf{Q}_j^n, \mathbf{Q}_{j+1}^n) \Delta \mathbf{Q}_{j+\frac{1}{2}}^n + \hat{\mathbf{A}}^+(\mathbf{Q}_{j-1}^n, \mathbf{Q}_j^n) \Delta \mathbf{Q}_{j-\frac{1}{2}}^n \right)$$

stability condition

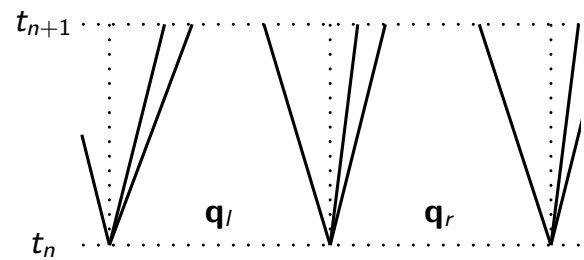
$$\max_{j \in \mathbb{Z}} |\hat{\lambda}_{m,j+\frac{1}{2}}| \frac{\Delta t}{\Delta x} \leq 1, \quad \text{for all } m = 1, \dots, M$$

[LeVeque, 1992]

# Roe's approximate Riemann solver

Choosing  $\hat{\mathbf{A}}(\mathbf{q}_L, \mathbf{q}_R)$  [Roe, 1981]:

- (i)  $\hat{\mathbf{A}}(\mathbf{q}_L, \mathbf{q}_R)$  has real eigenvalues
- (ii)  $\hat{\mathbf{A}}(\mathbf{q}_L, \mathbf{q}_R) \rightarrow \frac{\partial \mathbf{f}(\mathbf{q})}{\partial \mathbf{q}}$  as  $\mathbf{q}_L, \mathbf{q}_R \rightarrow \mathbf{q}$
- (iii)  $\hat{\mathbf{A}}(\mathbf{q}_L, \mathbf{q}_R) \Delta \mathbf{q} = \mathbf{f}(\mathbf{q}_R) - \mathbf{f}(\mathbf{q}_L)$



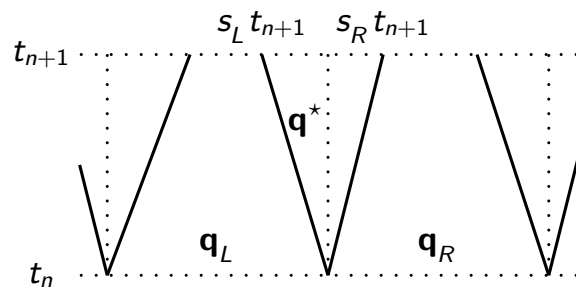
For Euler equations:

$$\hat{\rho} = \frac{\sqrt{\rho_L \rho_R} + \sqrt{\rho_R \rho_L}}{\sqrt{\rho_L} + \sqrt{\rho_R}} = \sqrt{\rho_L \rho_R} \quad \text{and} \quad \hat{v} = \frac{\sqrt{\rho_L} v_L + \sqrt{\rho_R} v_R}{\sqrt{\rho_L} + \sqrt{\rho_R}} \quad \text{for } v = u_n, H$$

Wave decomposition:  $\Delta \mathbf{q} = \mathbf{q}_r - \mathbf{q}_l = \sum_m a_m \hat{\mathbf{r}}_m$

$$\begin{aligned} \mathbf{F}(\mathbf{q}_L, \mathbf{q}_R) &= \mathbf{f}(\mathbf{q}_L) + \sum_{\hat{\lambda}_m < 0} \hat{\lambda}_m a_m \hat{\mathbf{r}}_m = \mathbf{f}(\mathbf{q}_R) - \sum_{\hat{\lambda}_m \geq 0} \hat{\lambda}_m a_m \hat{\mathbf{r}}_m \\ &= \frac{1}{2} \left( \mathbf{f}(\mathbf{q}_L) + \mathbf{f}(\mathbf{q}_R) - \sum_m |\hat{\lambda}_m| a_m \hat{\mathbf{r}}_m \right) \end{aligned}$$

# Harten-Lax-Van Leer (HLL) approximate Riemann solver



$$\bar{q}(x, t) = \begin{cases} q_L, & x < s_L t \\ q^*, & s_L t \leq x \leq s_R t \\ q_R, & x > s_R t \end{cases}$$

$$F_{HLL}(q_L, q_R) = \begin{cases} f(q_L), & 0 < s_L, \\ \frac{s_R f(q_L) - s_L f(q_R) + s_L s_R (q_R - q_L)}{s_R - s_L}, & s_L \leq 0 \leq s_R, \\ f(q_R), & 0 > s_R, \end{cases}$$

Euler equations:

$$s_L = \min(u_{1,L} - c_L, u_{1,R} - c_R), \quad s_R = \max(u_{1,L} + c_L, u_{1,R} + c_R)$$

[Toro, 1999], HLLC: [Toro et al., 1994]



# Flux vector splitting

## Splitting

$$\mathbf{f}(\mathbf{q}) = \mathbf{f}^+(\mathbf{q}) + \mathbf{f}^-(\mathbf{q})$$

derived under restriction  $\hat{\lambda}_m^+ \geq 0$  and  $\hat{\lambda}_m^- \leq 0$  for all  $m = 1, \dots, M$  for

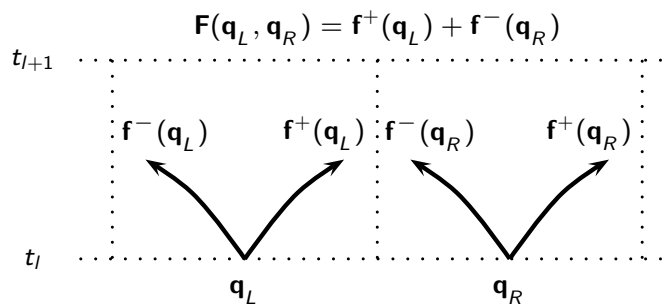
$$\hat{\mathbf{A}}^+(\mathbf{q}) = \frac{\partial \mathbf{f}^+(\mathbf{q})}{\partial \mathbf{q}}, \quad \hat{\mathbf{A}}^-(\mathbf{q}) = \frac{\partial \mathbf{f}^-(\mathbf{q})}{\partial \mathbf{q}}$$

plus reproduction of regular upwinding

$$\begin{aligned} \mathbf{f}^+(\mathbf{q}) &= \mathbf{f}(\mathbf{q}), & \mathbf{f}^-(\mathbf{q}) &= \mathbf{0} & \text{if } \lambda_m \geq 0 & \text{for all } m = 1, \dots, M \\ \mathbf{f}^+(\mathbf{q}) &= \mathbf{0}, & \mathbf{f}^-(\mathbf{q}) &= \mathbf{f}(\mathbf{q}) & \text{if } \lambda_m \leq 0 & \text{for all } m = 1, \dots, M \end{aligned}$$

Then use

$$\mathbf{F}(\mathbf{q}_L, \mathbf{q}_R) = \mathbf{f}^+(\mathbf{q}_L) + \mathbf{f}^-(\mathbf{q}_R)$$



# Steger-Warming

Required  $\mathbf{f}(\mathbf{q}) = \mathbf{A}(\mathbf{q}) \mathbf{q}$

$$\lambda_m^+ = \frac{1}{2} (\lambda_m + |\lambda_m|) \quad \lambda_m^- = \frac{1}{2} (\lambda_m - |\lambda_m|)$$

$$\mathbf{A}^+(\mathbf{q}) := \mathbf{R}(\mathbf{q}) \mathbf{\Lambda}^+(\mathbf{q}) \mathbf{R}^{-1}(\mathbf{q}), \quad \mathbf{A}^-(\mathbf{q}) := \mathbf{R}(\mathbf{q}) \mathbf{\Lambda}^-(\mathbf{q}) \mathbf{R}^{-1}(\mathbf{q})$$

Gives

$$\mathbf{f}(\mathbf{q}) = \mathbf{A}^+(\mathbf{q}) \mathbf{q} + \mathbf{A}^-(\mathbf{q}) \mathbf{q}$$

and the numerical flux

$$\mathbf{F}(\mathbf{q}_L, \mathbf{q}_R) = \mathbf{A}^+(\mathbf{q}_L) \mathbf{q}_L + \mathbf{A}^-(\mathbf{q}_R) \mathbf{q}_R$$

Jacobians of the split fluxes are identical to  $\mathbf{A}^\pm(\mathbf{q})$  only in linear case

$$\frac{\partial \mathbf{f}^\pm(\mathbf{q})}{\partial \mathbf{q}} = \frac{\partial (\mathbf{A}^\pm(\mathbf{q}) \mathbf{q})}{\partial \mathbf{q}} = \mathbf{A}^\pm(\mathbf{q}) + \frac{\partial \mathbf{A}^\pm(\mathbf{q})}{\partial \mathbf{q}} \mathbf{q}$$

Further methods: Van Leer FVS [Toro, 1999], AUSM [Wada and Liou, 1997]

# High-resolution methods

Objective: Higher-order accuracy in smooth solution regions but no spurious oscillations near large gradients

Consistent monotone methods converge toward the entropy solution, but

## Theorem

*A monotone method is at most first order accurate.*

Proof: [Harten et al., 1976]

## Definition (TVD property)

Scheme  $\mathcal{H}^{(\Delta t)}(\mathbf{Q}^n; j)$  TVD if  $TV(\mathbf{Q}^{l+1}) \leq TV(\mathbf{Q}^l)$  is satisfied for all discrete sequences  $\mathbf{Q}^n$ . Herein,  $TV(\mathbf{Q}^l) := \sum_{j \in \mathbb{Z}} |\mathbf{Q}_{j+1}^l - \mathbf{Q}_j^l|$ .

TVD schemes: no new extrema, local minima are non-decreasing, local maxima are non-increasing (termed *monotonicity-preserving*). *Monotonicity-preserving* higher-order schemes are at least 5-point methods. Proofs: [Harten, 1983]

TVD concept is proven [Godlewski and Raviart, 1996] for scalar schemes only but nevertheless used to construct *high resolution* schemes.

*Monotonicity-preserving scheme can converge toward non-physical weak solutions.*

# MUSCL slope limiting

Monotone Upwind Schemes for Conservation Laws [van Leer, 1979]

$$\tilde{Q}_{j+\frac{1}{2}}^L = Q_j^n + \frac{1}{4} \left[ (1 - \omega) \Phi_{j-\frac{1}{2}}^+ \Delta_{j-\frac{1}{2}} + (1 + \omega) \Phi_{j+\frac{1}{2}}^- \Delta_{j+\frac{1}{2}} \right],$$

$$\tilde{Q}_{j-\frac{1}{2}}^R = Q_j^n - \frac{1}{4} \left[ (1 - \omega) \Phi_{j+\frac{1}{2}}^- \Delta_{j+\frac{1}{2}} + (1 + \omega) \Phi_{j-\frac{1}{2}}^+ \Delta_{j-\frac{1}{2}} \right]$$

with  $\Delta_{j-1/2} = Q_j^n - Q_{j-1}^n$ ,  $\Delta_{j+1/2} = Q_{j+1}^n - Q_j^n$ .

$$\Phi_{j-\frac{1}{2}}^+ := \Phi \left( r_{j-\frac{1}{2}}^+ \right), \quad \Phi_{j+\frac{1}{2}}^- := \Phi \left( r_{j+\frac{1}{2}}^- \right) \quad \text{with} \quad r_{j-\frac{1}{2}}^+ := \frac{\Delta_{j+\frac{1}{2}}}{\Delta_{j-\frac{1}{2}}}, \quad r_{j+\frac{1}{2}}^- := \frac{\Delta_{j-\frac{1}{2}}}{\Delta_{j+\frac{1}{2}}}$$

and *slope limiters*, e.g., *Minmod*

$$\Phi(r) = \max(0, \min(r, 1))$$

Using a midpoint rule for temporal integration, e.g.,

$$Q_j^* = Q_j^n - \frac{1}{2} \frac{\Delta t}{\Delta x} \left( F(Q_{j+1}^n, Q_j^n) - F(Q_j^n, Q_{j-1}^n) \right)$$

and constructing limited values from  $Q^*$  to be used in FV scheme gives a TVD method if

$$\frac{1}{2} \left[ (1 - \omega) \Phi(r) + (1 + \omega) r \Phi \left( \frac{1}{r} \right) \right] < \min(2, 2r)$$

is satisfied for  $r > 0$ . Proof: [Hirsch, 1988]

# Wave Propagation with flux limiting

Wave Propagation Method [LeVeque, 1997] is built on the flux differencing approach  $\mathcal{A}^\pm \Delta := \hat{\mathbf{A}}^\pm(\mathbf{q}_L, \mathbf{q}_R) \Delta \mathbf{q}$  and the waves  $\mathcal{W}_m := a_m \hat{\mathbf{r}}_m$ , i.e.

$$\mathcal{A}^- \Delta \mathbf{q} = \sum_{\hat{\lambda}_m < 0} \hat{\lambda}_m \mathcal{W}_m, \quad \mathcal{A}^+ \Delta \mathbf{q} = \sum_{\hat{\lambda}_m \geq 0} \hat{\lambda}_m \mathcal{W}_m$$

Wave Propagation 1D:

$$\mathbf{Q}^{n+1} = \mathbf{Q}_j^n - \frac{\Delta t}{\Delta x} \left( \mathcal{A}^- \Delta_{j+\frac{1}{2}} + \mathcal{A}^+ \Delta_{j-\frac{1}{2}} \right) - \frac{\Delta t}{\Delta x} \left( \tilde{\mathbf{F}}_{j+\frac{1}{2}} - \tilde{\mathbf{F}}_{j-\frac{1}{2}} \right)$$

with

$$\tilde{\mathbf{F}}_{j+\frac{1}{2}} = \frac{1}{2} |\mathcal{A}| \left( 1 - \frac{\Delta t}{\Delta x} |\mathcal{A}| \right) \Delta_{j+\frac{1}{2}} = \frac{1}{2} \sum_{m=1}^M |\hat{\lambda}_{j+\frac{1}{2}}^m| \left( 1 - \frac{\Delta t}{\Delta x} \right) |\hat{\lambda}_{j+\frac{1}{2}}^m| \tilde{\mathcal{W}}_{j+\frac{1}{2}}^m$$

and wave limiter

$$\tilde{\mathcal{W}}_{j+\frac{1}{2}}^m = \Phi(\Theta_{j+\frac{1}{2}}^m) \mathcal{W}_{j+\frac{1}{2}}^m$$

with

$$\Theta_{j+\frac{1}{2}}^m = \begin{cases} a_{j-\frac{1}{2}}^m / a_{j+\frac{1}{2}}^m, & \hat{\lambda}_{j+\frac{1}{2}}^m \geq 0, \\ a_{j+\frac{3}{2}}^m / a_{j+\frac{1}{2}}^m, & \hat{\lambda}_{j+\frac{1}{2}}^m < 0 \end{cases}$$

# Wave Propagation Method in 2D

Writing  $\tilde{\mathcal{A}}^{\pm} \Delta_{j\pm 1/2} := \mathcal{A}^{\pm} \Delta_{j\pm 1/2} + \tilde{\mathbf{F}}_{j\pm 1/2}$  one can develop a truly two-dimensional one-step method [Langseth and LeVeque, 2000]

$$\begin{aligned} \mathbf{Q}_{jk}^{n+1} = \mathbf{Q}_{jk}^n &- \frac{\Delta t}{\Delta x_1} \left( \tilde{\mathcal{A}}^{-} \Delta_{j+\frac{1}{2},k} - \frac{1}{2} \frac{\Delta t}{\Delta x_2} \left[ \mathcal{A}^{-} \tilde{\mathcal{B}}^{-} \Delta_{j+1,k+\frac{1}{2}} + \mathcal{A}^{-} \tilde{\mathcal{B}}^{+} \Delta_{j+1,k-\frac{1}{2}} \right] + \right. \\ &\quad \left. \tilde{\mathcal{A}}^{+} \Delta_{j-\frac{1}{2},k} - \frac{1}{2} \frac{\Delta t}{\Delta x_2} \left[ \mathcal{A}^{+} \tilde{\mathcal{B}}^{-} \Delta_{j-1,k+\frac{1}{2}} + \mathcal{A}^{+} \tilde{\mathcal{B}}^{+} \Delta_{j-1,k-\frac{1}{2}} \right] \right) \\ &- \frac{\Delta t}{\Delta x_2} \left( \tilde{\mathcal{B}}^{-} \Delta_{j,k+\frac{1}{2}} - \frac{1}{2} \frac{\Delta t}{\Delta x_1} \left[ \mathcal{B}^{-} \tilde{\mathcal{A}}^{-} \Delta_{j+\frac{1}{2},k+1} + \mathcal{B}^{-} \tilde{\mathcal{A}}^{+} \Delta_{j-\frac{1}{2},k+1} \right] + \right. \\ &\quad \left. \tilde{\mathcal{B}}^{+} \Delta_{j,k-\frac{1}{2}} - \frac{1}{2} \frac{\Delta t}{\Delta x_1} \left[ \mathcal{B}^{+} \tilde{\mathcal{A}}^{-} \Delta_{j+\frac{1}{2},k-1} + \mathcal{B}^{+} \tilde{\mathcal{A}}^{+} \Delta_{j-\frac{1}{2},k-1} \right] \right) \end{aligned}$$

that is stable for

$$\left\{ \max_{j \in \mathbb{Z}} |\hat{\lambda}_{m,j+\frac{1}{2}}| \frac{\Delta t}{\Delta x_1}, \max_{k \in \mathbb{Z}} |\hat{\lambda}_{m,k+\frac{1}{2}}| \frac{\Delta t}{\Delta x_2} \right\} \leq 1, \quad \text{for all } m = 1, \dots, M$$

## Further high-resolution methods

Some further high-resolution methods (good overview in [Laney, 1998]):

- ▶ FCT: 2nd order [Oran and Boris, 2001]
- ▶ ENO/WENO: 3rd order [Shu, 97]
- ▶ PPM: 3rd order [Colella and Woodward, 1984]

3rd order methods must make use of strong-stability preserving Runge-Kutta methods [Gottlieb et al., 2001] for time integration that use a multi-step update

$$\tilde{\mathbf{Q}}_j^v = \alpha_v \mathbf{Q}_j^n + \beta_v \tilde{\mathbf{Q}}_j^{v-1} + \gamma_v \frac{\Delta t}{\Delta x} \left( \mathbf{F}_{j+\frac{1}{2}}(\tilde{\mathbf{Q}}^{v-1}) - \mathbf{F}_{j-\frac{1}{2}}(\tilde{\mathbf{Q}}^{v-1}) \right)$$

with  $\tilde{\mathbf{Q}}^0 := \mathbf{Q}^n$ ,  $\alpha_1 = 1$ ,  $\beta_1 = 0$ ; and  $\mathbf{Q}^{n+1} := \tilde{\mathbf{Q}}^\Upsilon$  after final stage  $\Upsilon$

Typical storage-efficient SSPRK(3,3):

$$\begin{aligned} \tilde{\mathbf{Q}}^1 &= \mathbf{Q}^n + \Delta t \mathcal{F}(\mathbf{Q}^n), & \tilde{\mathbf{Q}}^2 &= \frac{3}{4} \mathbf{Q}^n + \frac{1}{4} \tilde{\mathbf{Q}}^1 + \frac{1}{4} \Delta t \mathcal{F}(\tilde{\mathbf{Q}}^1), \\ \mathbf{Q}^{n+1} &= \frac{1}{3} \mathbf{Q}^n + \frac{2}{3} \tilde{\mathbf{Q}}^2 + \frac{2}{3} \Delta t \mathcal{F}(\tilde{\mathbf{Q}}^2) \end{aligned}$$

# Outline

## Conservation laws

- Mathematical background
- Examples

## Finite volume methods

- Basics of finite difference methods
- Splitting methods, second derivatives

## Upwind schemes

- Flux-difference splitting
- Flux-vector splitting
- High-resolution methods

## Meshes and adaptation

- Elements of adaptive algorithms
- Adaptivity on unstructured meshes
- Structured mesh refinement techniques

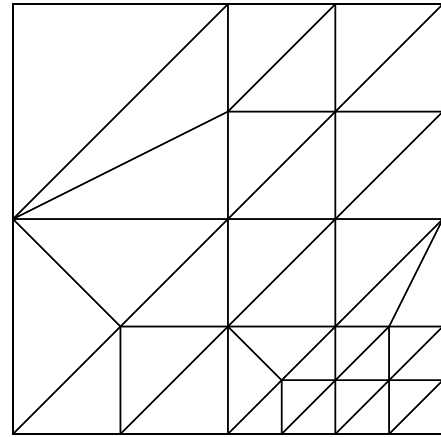


# Elements of adaptive algorithms

- ▶ Base grid
- ▶ Solver
- ▶ Error indicators
- ▶ Grid manipulation
- ▶ Interpolation (restriction and prolongation)
- ▶ Load-balancing

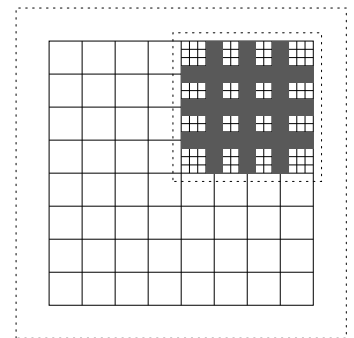
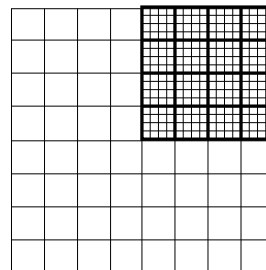
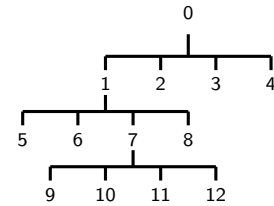
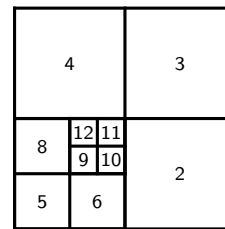
# Adaptivity on unstructured meshes

- ▶ Coarse cells replaced by finer ones
- ▶ Global time-step
- ▶ Cell-based data structures
- ▶ Neighborhoods have to stored
- + Geometric flexible
- + No hanging nodes
- + Easy to implement
  - Higher order difficult to achieve
  - Cell aspect ratio must be considered
  - Fragmented data
  - Cache-reuse / vectorization nearly impossible
  - Complex load-balancing
  - Complex synchronization



# Structured mesh refinement techniques

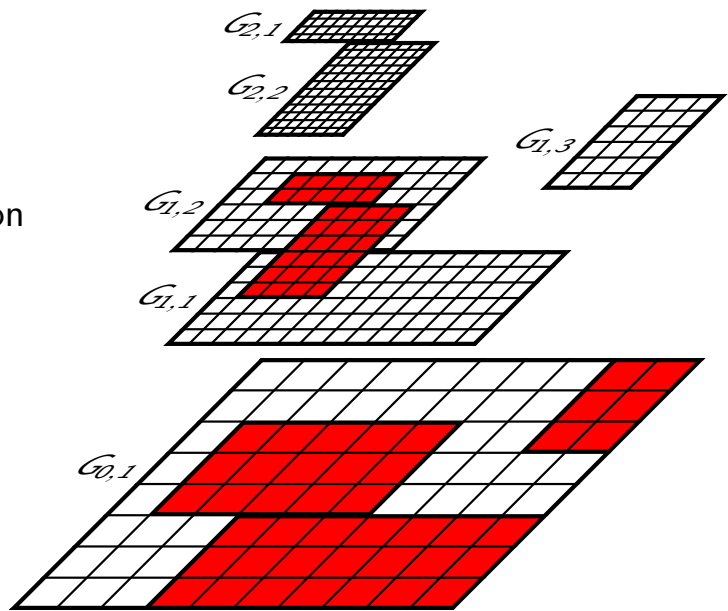
- ▶ Block-based data of equal size
- ▶ Block stored in a quad-tree
- ▶ Time-step refinement
- ▶ Global index coordinate system
- ▶ Neighborhoods need not be stored
- + Numerical scheme only for single regular block necessary
- + Easy to implement
- + Simple load-balancing
- + Parent/Child relations according to tree
- +/- Cache-reuse / vectorization only in data block



Wasted boundary space in a quad-tree

# Block-structured adaptive mesh refinement (SAMR)

- ▶ Refined block overlay coarser ones
- ▶ Time-step refinement
- ▶ Block (aka patch) based data structures
- ▶ Global index coordinate system
- + Numerical scheme only for single patch necessary
- + Efficient cache-reuse / vectorization possible
- + Simple load-balancing
- + Minimal synchronization overhead
  - Cells without mark are refined
  - Hanging nodes unavoidable
  - Cluster-algorithm necessary
  - Difficult to implement



# References I

- [Colella and Woodward, 1984] Colella, P. and Woodward, P. (1984). The piecewise parabolic method (PPM) for gas-dynamical simulations. *J. Comput. Phys.*, 54:174–201.
- [Godlewski and Raviart, 1996] Godlewski, E. and Raviart, P.-A. (1996). *Numerical approximation of hyperbolic systems of conservation laws*. Springer Verlag, New York.
- [Gottlieb et al., 2001] Gottlieb, S., Shu, C.-W., and Tadmor, E. (2001). Strong stability-preserving high-order time discretization methods. *SIAM Review*, 43(1):89–112.
- [Harten, 1983] Harten, A. (1983). High resolution schemes for hyperbolic conservation laws. *J. Comput. Phys.*, 49:357–393.
- [Harten et al., 1976] Harten, A., Hyman, J. M., and Lax, P. D. (1976). On finite-difference approximations and entropy conditions for shocks. *Comm. Pure Appl. Math.*, 29:297–322.
- [Hirsch, 1988] Hirsch, C. (1988). *Numerical computation of internal and external flows*. John Wiley & Sons, Chichester.

## References II

- [Kröner, 1997] Kröner, D. (1997). *Numerical schemes for conservation laws*. John Wiley & Sons and B. G. Teubner, New York, Leipzig.
- [Laney, 1998] Laney, C. B. (1998). *Computational gasdynamics*. Cambridge University Press, Cambridge.
- [Langseth and LeVeque, 2000] Langseth, J. and LeVeque, R. (2000). A wave propagation method for three dimensional conservation laws. *J. Comput. Phys.*, 165:126–166.
- [LeVeque, 1992] LeVeque, R. J. (1992). *Numerical methods for conservation laws*. Birkhäuser, Basel.
- [LeVeque, 1997] LeVeque, R. J. (1997). Wave propagation algorithms for multidimensional hyperbolic systems. *J. Comput. Phys.*, 131(2):327–353.
- [Majda, 1984] Majda, A. (1984). *Compressible fluid flow and systems of conservation laws in several space variables*. Applied Mathematical Sciences Vol. 53. Springer-Verlag, New York.
- [Oran and Boris, 2001] Oran, E. S. and Boris, J. P. (2001). *Numerical simulation of reactive flow*. Cambridge Univ. Press, Cambridge, 2nd edition.

## References III

- [Roe, 1981] Roe, P. L. (1981). Approximate Riemann solvers, parameter vectors and difference schemes. *J. Comput. Phys.*, 43:357–372.
- [Shu, 97] Shu, C.-W. (97). Essentially non-oscillatory and weighted essentially non-oscillatory schemes for hyperbolic conservation laws. Technical Report CR-97-206253, NASA.
- [Toro, 1999] Toro, E. F. (1999). *Riemann solvers and numerical methods for fluid dynamics*. Springer-Verlag, Berlin, Heidelberg, 2nd edition.
- [Toro et al., 1994] Toro, E. F., Spruce, M., and Speares, W. (1994). Restoration of the contact surface in the HLL-Riemann solver. *Shock Waves*, 4:25–34.
- [van Leer, 1979] van Leer, B. (1979). Towards the ultimate conservative difference scheme V. A second order sequel to Godunov's method. *J. Comput. Phys.*, 32:101–136.
- [Wada and Liou, 1997] Wada, Y. and Liou, M.-S. (1997). An accurate and robust flux splitting scheme for shock and contact discontinuities. *SIAM J. Sci. Comp.*, 18(3):633–657.

# Lecture 2

## The SAMR method for hyperbolic problems

Course *Block-structured Adaptive Mesh Refinement Methods for Conservation Laws*  
*Theory, Implementation and Application*

Ralf Deiterding

Computer Science and Mathematics Division  
Oak Ridge National Laboratory  
P.O. Box 2008 MS6367, Oak Ridge, TN 37831, USA

E-mail: [deiterdingr@ornl.gov](mailto:deiterdingr@ornl.gov)



# Outline

## The serial Berger-Colella SAMR method

- Block-based data structures
- Numerical update
- Conservative flux correction
- Level transfer operators
- The basic recursive algorithm
- Cluster algorithm
- Refinement criteria

## Parallel SAMR method

- Domain decomposition
- A parallel SAMR algorithm
- Partitioning

## Examples

- Euler equations

# Outline

## The serial Berger-Colella SAMR method

- Block-based data structures
- Numerical update
- Conservative flux correction
- Level transfer operators
- The basic recursive algorithm
- Cluster algorithm
- Refinement criteria

## Parallel SAMR method

- Domain decomposition
- A parallel SAMR algorithm
- Partitioning

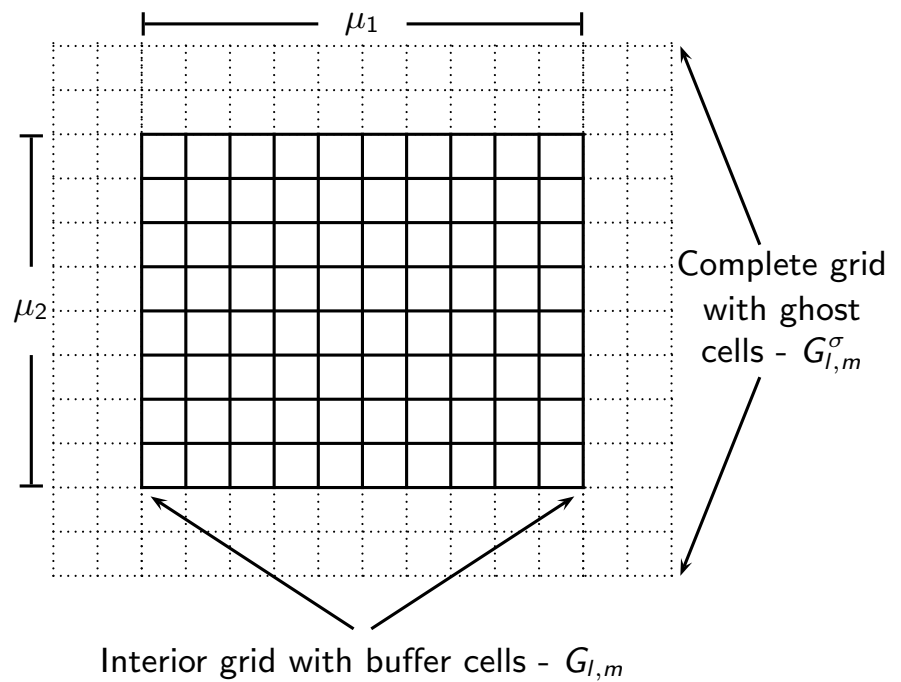
## Examples

- Euler equations

# The $m$ th refinement grid on level $l$

Notations:

- ▶ Boundary:  $\partial G_{l,m}$
- ▶ Hull:  
 $\bar{G}_{l,m} = G_{l,m} \cup \partial G_{l,m}$
- ▶ Ghost cell region:  
 $\tilde{G}_{l,m}^\sigma = G_{l,m}^\sigma \setminus \bar{G}_{l,m}$



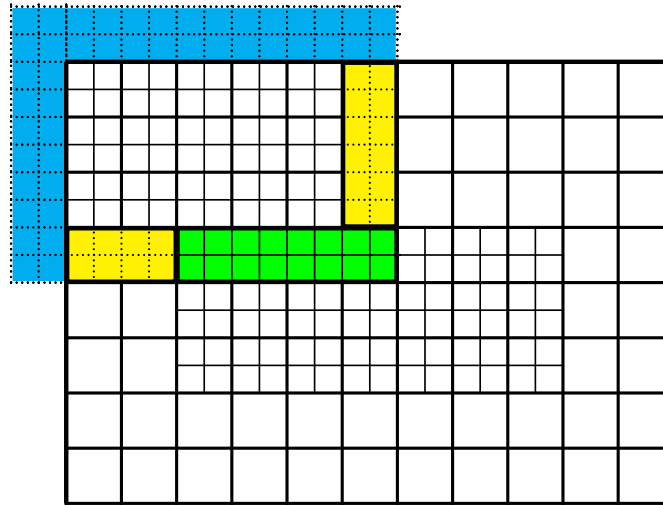
## Refinement data

- ▶ Resolution:  $\Delta t_l := \frac{\Delta t_{l-1}}{r_l}$  and  $\Delta x_{n,l} := \frac{\Delta x_{n,l-1}}{r_l}$
- ▶ Refinement factor:  $r_l \in \mathbb{N}$ ,  $r_l \geq 2$  for  $l > 0$  and  $r_0 = 1$
- ▶ Integer coordinate system for internal organization [Bell et al., 1994]:

$$\Delta x_{n,l} \cong \prod_{\kappa=l+1}^{l_{\max}} r_{\kappa}$$

- ▶ Computational Domain:  $G_0 = \bigcup_{m=1}^{M_0} G_{0,m}$
- ▶ Domain of level  $l$ :  $G_l := \bigcup_{m=1}^{M_l} G_{l,m}$  with  $G_{l,m} \cap G_{l,n} = \emptyset$  for  $m \neq n$
- ▶ Refinements are properly nested:  $G_l^1 \subset G_{l-1}$
- ▶ Assume a FD scheme with stencil radius  $s$ . Necessary data:
  - ▶ Vector of state:  $\mathbf{Q}^l := \bigcup_m \mathbf{Q}(G_{l,m}^s)$
  - ▶ Numerical fluxes:  $\mathbf{F}^{n,l} := \bigcup_m \mathbf{F}^n(\bar{G}_{l,m})$
  - ▶ Flux corrections:  $\delta \mathbf{F}^{n,l} := \bigcup_m \delta \mathbf{F}^n(\partial G_{l,m})$

# Setting of ghost cells



- Synchronization with  $G_l$  -  $\tilde{S}_{l,m}^s = \tilde{G}_{l,m}^s \cap G_l$
- Physical boundary conditions -  $\tilde{P}_{l,m}^s = \tilde{G}_{l,m}^s \setminus G_0$
- Interpolation from  $G_{l-1}$  -  $\tilde{I}_{l,m}^s = \tilde{G}_{l,m}^s \setminus (\tilde{S}_{l,m}^s \cup \tilde{P}_{l,m}^s)$

# Numerical update

Time-explicit conservative finite volume scheme

$$\mathcal{H}^{(\Delta t)} : \mathbf{Q}_{jk}(t+\Delta t) = \mathbf{Q}_{jk}(t) - \frac{\Delta t}{\Delta x_1} \left( \mathbf{F}_{j+\frac{1}{2},k}^1 - \mathbf{F}_{j-\frac{1}{2},k}^1 \right) - \frac{\Delta t}{\Delta x_2} \left( \mathbf{F}_{j,k+\frac{1}{2}}^2 - \mathbf{F}_{j,k-\frac{1}{2}}^2 \right)$$

UpdateLevel( $l$ )

For all  $m = 1$  To  $M_l$  Do

$$\mathbf{Q}(G_{l,m}^s, t) \xrightarrow{\mathcal{H}^{(\Delta t_l)}} \mathbf{Q}(G_{l,m}, t + \Delta t_l), \mathbf{F}^n(\bar{G}_{l,m}, t)$$

If level  $l > 0$

Add  $\mathbf{F}^n(\partial G_{l,m}, t)$  to  $\delta \mathbf{F}^{n,l}$

If level  $l+1$  exists

Init  $\delta \mathbf{F}^{n,l+1}$  with  $\mathbf{F}^n(\bar{G}_{l,m} \cap \partial G_{l+1}, t)$

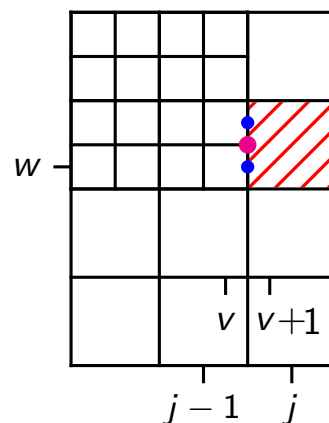
# Conservative flux correction

Example: Cell  $j, k$

$$\begin{aligned} \check{Q}_{jk}^l(t + \Delta t_l) = & Q_{jk}^l(t) - \frac{\Delta t_l}{\Delta x_{1,l}} \left( F_{j+\frac{1}{2},k}^{1,l} - \frac{1}{r_{l+1}^2} \sum_{\kappa=0}^{r_{l+1}-1} \sum_{\iota=0}^{r_{l+1}-1} F_{v+\frac{1}{2},w+\iota}^{1,l+1}(t + \kappa \Delta t_{l+1}) \right) \\ & - \frac{\Delta t_l}{\Delta x_{2,l}} \left( F_{j,k+\frac{1}{2}}^{2,l} - F_{j,k-\frac{1}{2}}^{2,l} \right) \end{aligned}$$

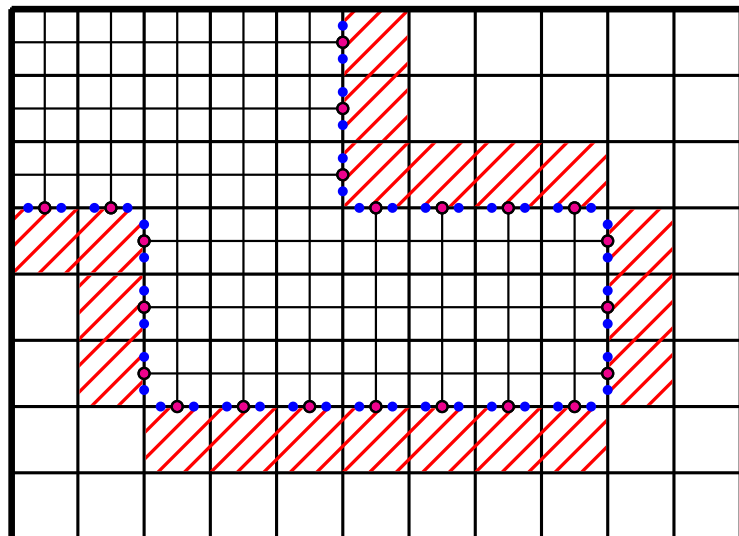
Correction pass:

1.  $\delta F_{j-\frac{1}{2},k}^{1,l+1} := -F_{j-\frac{1}{2},k}^{1,l}$
2.  $\delta F_{j-\frac{1}{2},k}^{1,l+1} := \delta F_{j-\frac{1}{2},k}^{1,l+1} + \frac{1}{r_{l+1}^2} \sum_{\iota=0}^{r_{l+1}-1} F_{v+\frac{1}{2},w+\iota}^{1,l+1}(t + \kappa \Delta t_{l+1})$
3.  $\check{Q}_{jk}^l(t + \Delta t_l) := Q_{jk}^l(t + \Delta t_l) + \frac{\Delta t_l}{\Delta x_{1,l}} \delta F_{j-\frac{1}{2},k}^{1,l+1}$



## Conservative flux correction II

- ▶ Level  $l$  cells needing correction  $(G_{l+1}^{r_{l+1}} \setminus G_{l+1}) \cap G_l$
- ▶ Corrections  $\delta \mathbf{F}^{n,l+1}$  stored on level  $l+1$  along  $\partial G_{l+1}$  (lower-dimensional data coarsened by  $r_{l+1}$ )
- ▶ Init  $\delta \mathbf{F}^{n,l+1}$  with level  $l$  fluxes  $\mathbf{F}^{n,l}(\bar{G}_l \cap \partial G_{l+1})$
- ▶ Add level  $l+1$  fluxes  $\mathbf{F}^{n,l+1}(\partial G_{l+1})$  to  $\delta \mathbf{F}^{n,l}$



 Cells to correct    
   $\mathbf{F}^{n,l}$     
   $\mathbf{F}^{n,l+1}$     
   $\delta \mathbf{F}^{n,l+1}$



# Level transfer operators

Conservative averaging (restriction):

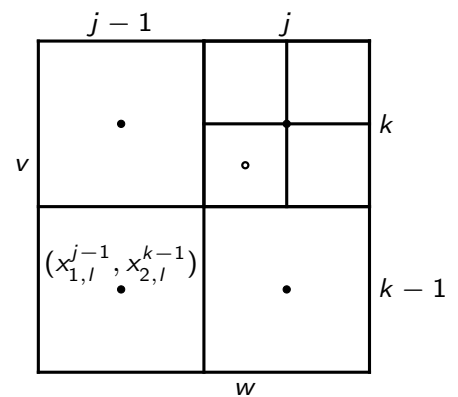
Replace cells on level  $l$  covered by level  $l + 1$ , i.e.

$G_l \cap G_{l+1}$ , by

$$\hat{\mathbf{Q}}_{jk}^l := \frac{1}{(r_{l+1})^2} \sum_{\kappa=0}^{r_{l+1}-1} \sum_{\iota=0}^{r_{l+1}-1} \mathbf{Q}_{v+\kappa, w+\iota}^{l+1}$$

Bilinear interpolation (prolongation):

$$\check{\mathbf{Q}}_{vw}^{l+1} := (1 - f_1)(1 - f_2) \mathbf{Q}_{j-1, k-1}^l + f_1(1 - f_2) \mathbf{Q}_{j, k-1}^l + (1 - f_1)f_2 \mathbf{Q}_{j-1, k}^l + f_1f_2 \mathbf{Q}_{j, k}^l$$



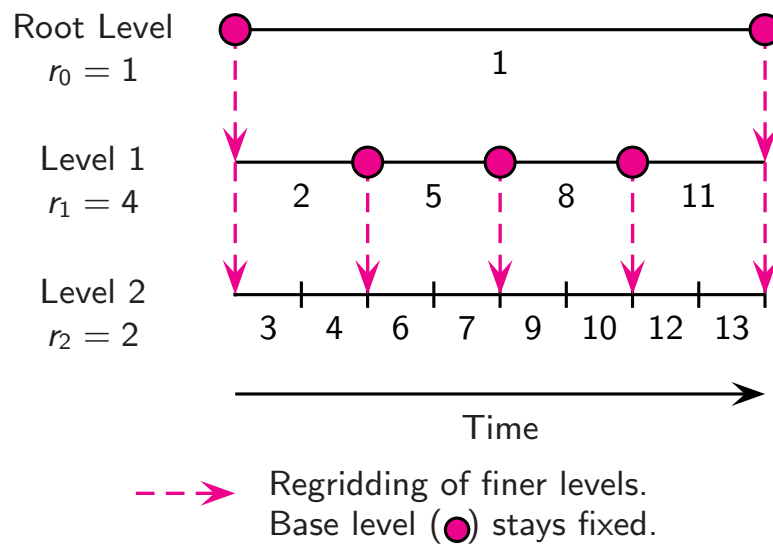
with factors  $f_1 := \frac{x_{1,l+1}^v - x_{1,l}^{j-1}}{\Delta x_{1,l}}$ ,  $f_2 := \frac{x_{2,l+1}^w - x_{2,l}^{k-1}}{\Delta x_{2,l}}$  derived from the spatial coordinates of the cell centers  $(x_{1,l}^{j-1}, x_{2,l}^{k-1})$  and  $(x_{1,l+1}^v, x_{2,l+1}^w)$ .

For boundary conditions on  $\tilde{l}_l^s$ : linear time interpolation

$$\tilde{\mathbf{Q}}^{l+1}(t + \kappa \Delta t_{l+1}) := \left(1 - \frac{\kappa}{r_{l+1}}\right) \check{\mathbf{Q}}^{l+1}(t) + \frac{\kappa}{r_{l+1}} \check{\mathbf{Q}}^{l+1}(t + \Delta t_l) \quad \text{for } \kappa = 0, \dots, r_{l+1}$$

## Recursive integration order

- ▶ Space-time interpolation of coarse data to set  $I_l^s, l > 0$
- ▶ Regridding:
  - ▶ Creation of new grids, copy existing cells on level  $l > 0$
  - ▶ Spatial interpolation to initialize new cells on level  $l > 0$



# The basic recursive algorithm

AdvanceLevel( $l$ )

Repeat  $r_l$  times

Set ghost cells of  $\mathbf{Q}'(t)$

If time to regrid?

Regrid( $l$ )

UpdateLevel( $l$ )

If level  $l+1$  exists?

Set ghost cells of  $\mathbf{Q}'(t + \Delta t_l)$

AdvanceLevel( $l+1$ )

Average  $\mathbf{Q}^{l+1}(t + \Delta t_l)$  onto  $\mathbf{Q}'(t + \Delta t_l)$

Correct  $\mathbf{Q}'(t + \Delta t_l)$  with  $\delta \mathbf{F}^{l+1}$

$t := t + \Delta t_l$

- ▶ Recursion
- ▶ Restriction and flux correction
- ▶ Re-organization of hierarchical data

Start - Start integration on level 0

$l = 0, r_0 = 1$

AdvanceLevel( $l$ )

[Berger and Colella, 1988][Berger and Oliger, 1984]

# Regridding algorithm

Regrid( $l$ ) - Regrid all levels  $\iota > l$

For  $\iota = l_f$  Downto  $l$  Do

Flag  $N^\iota$  according to  $\mathbf{Q}^\iota(t)$

If level  $\iota + 1$  exists?

Flag  $N^\iota$  below  $\check{G}^{\iota+2}$

Flag buffer zone on  $N^\iota$

Generate  $\check{G}^{\iota+1}$  from  $N^\iota$

$\check{G}_l := G_l$

For  $\iota = l$  To  $l_f$  Do

$C\check{G}_\iota := G_0 \setminus \check{G}_\iota$

$\check{G}_{\iota+1} := \check{G}_{\iota+1} \setminus C\check{G}_\iota^1$

Recompose( $l$ )

- ▶ Refinement flags:  
 $N' := \bigcup_m N(\partial G_{l,m})$
- ▶ Activate flags below higher levels
- ▶ Flag buffer cells of  $b > \kappa_r$  cells,  $\kappa_r$  steps between calls of Regrid( $l$ )
- ▶ Special cluster algorithm
- ▶ Use complement operation to ensure proper nesting condition

# Recomposition of data

Recompose( $l$ ) - Reorganize all levels  $\iota > l$

For  $\iota = l + 1$  To  $l_f + 1$  Do

Interpolate  $\mathbf{Q}^{\iota-1}(t)$  onto  $\check{\mathbf{Q}}^{\iota}(t)$

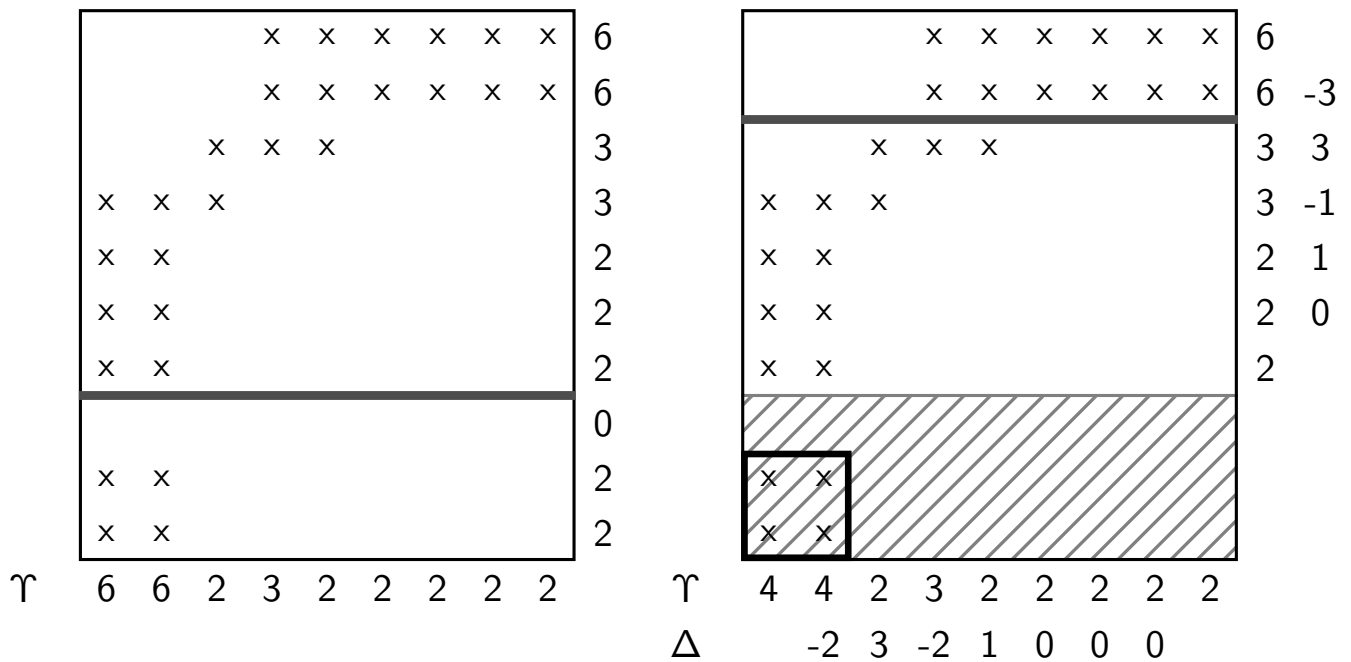
Copy  $\mathbf{Q}^{\iota}(t)$  onto  $\check{\mathbf{Q}}^{\iota}(t)$

Set ghost cells of  $\check{\mathbf{Q}}^{\iota}(t)$

$\mathbf{Q}^{\iota}(t) := \check{\mathbf{Q}}^{\iota}(t)$ ,  $G_{\iota} := \check{G}_{\iota}$

- ▶ Creates max. 1 level above  $l_f$ , but can remove multiple level if  $\check{G}_{\iota}$  empty (no coarsening!)
- ▶ Use spatial interpolation on entire data  $\check{\mathbf{Q}}^{\iota}(t)$
- ▶ Overwrite where old data exists
- ▶ Synchronization and physical boundary conditions

# Clustering by signatures

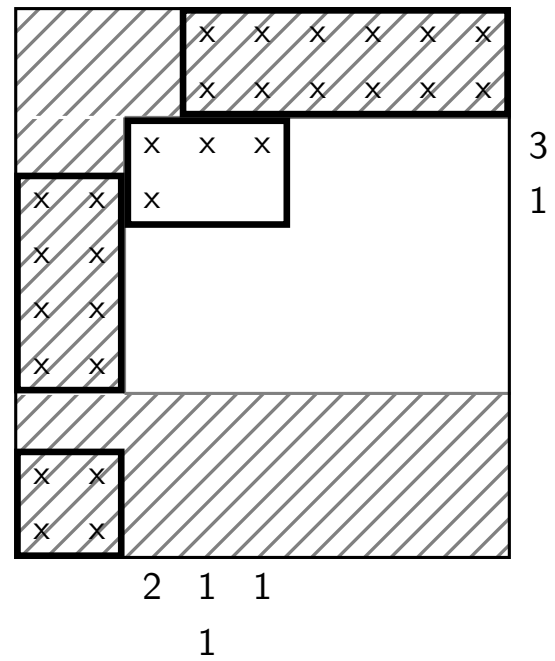
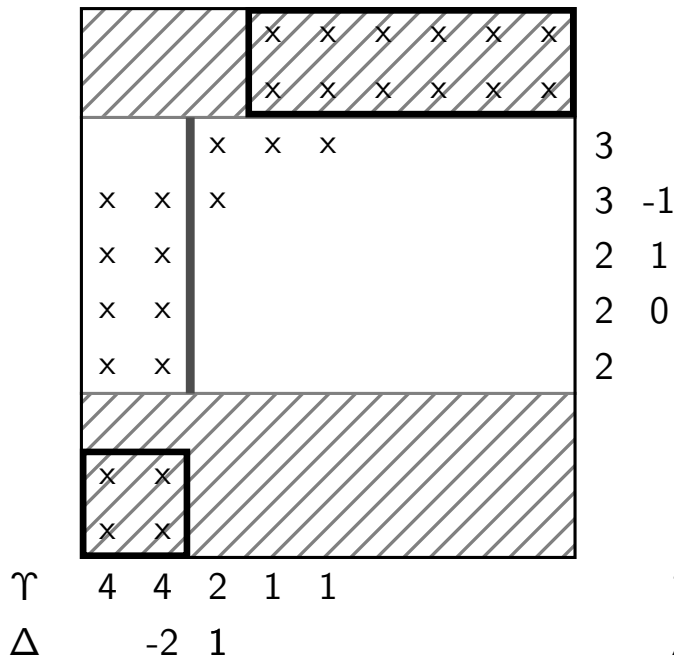


$\Upsilon$  Flagged cells per row/column

$\Delta$  Second derivative of  $\Upsilon$ ,  $\Delta = \Upsilon_{\nu+1} - 2\Upsilon_{\nu} + \Upsilon_{\nu-1}$

Technique from image detection: [Bell et al., 1994], see also

[Berger and Rigoutsos, 1991], [Berger, 1986]



Recursive generation of  $\check{G}_{l,m}$

1. 0 in  $\Upsilon$
2. Largest difference in  $\Delta$
3. Stop if ratio between flagged and unflagged cell  $> \eta_{tol}$

# Refinement criteria

Scaled gradient of scalar quantity  $w$

$$|w(\mathbf{Q}_{j+1,k}) - w(\mathbf{Q}_{jk})| > \epsilon_w, \quad |w(\mathbf{Q}_{j,k+1}) - w(\mathbf{Q}_{jk})| > \epsilon_w, \quad |w(\mathbf{Q}_{j+1,k+1}) - w(\mathbf{Q}_{jk})| > \epsilon_w$$

Heuristic error estimation [Berger, 1982]:

Local truncation error of scheme of order  $o$

$$\mathbf{q}(\mathbf{x}, t + \Delta t) - \mathcal{H}^{(\Delta t)}(\mathbf{q}(\cdot, t)) = \mathbf{C}\Delta t^{o+1} + O(\Delta t^{o+2})$$

For  $\mathbf{q}$  smooth after 2 steps  $\Delta t$

$$\mathbf{q}(\mathbf{x}, t + \Delta t) - \mathcal{H}_2^{(\Delta t)}(\mathbf{q}(\cdot, t - \Delta t)) = 2\mathbf{C}\Delta t^{o+1} + O(\Delta t^{o+2})$$

and after 1 step with  $2\Delta t$

$$\mathbf{q}(\mathbf{x}, t + \Delta t) - \mathcal{H}^{(2\Delta t)}(\mathbf{q}(\cdot, t - \Delta t)) = 2^{o+1}\mathbf{C}\Delta t^{o+1} + O(\Delta t^{o+2})$$

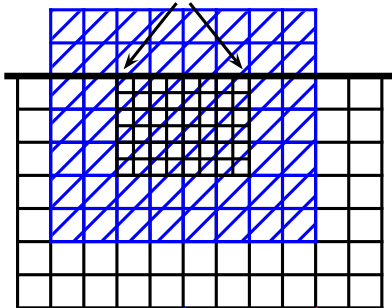
Gives

$$\mathcal{H}_2^{(\Delta t)}(\mathbf{q}(\cdot, t - \Delta t)) - \mathcal{H}^{(2\Delta t)}(\mathbf{q}(\cdot, t - \Delta t)) = (2^{o+1} - 2)\mathbf{C}\Delta t^{o+1} + O(\Delta t^{o+2})$$

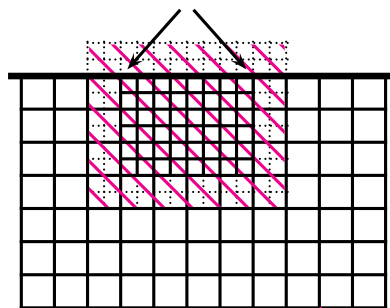


# Heuristic error estimation for FV methods

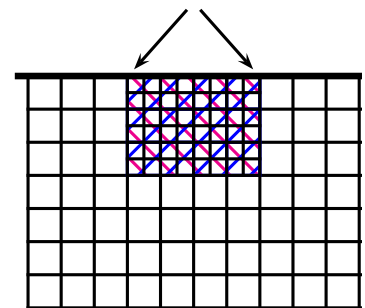
2. Create temporary Grid  
coarsened by factor 2  
Initialize with fine-grid-  
values of preceding  
time step



1. Error estimation on  
interior cells



3. Compare tempo-  
rary solutions



$$\begin{aligned} \mathcal{H}^{\Delta t_l} \mathbf{Q}^l(t_l - \Delta t_l) &= \mathcal{H}^{\Delta t_l} (\mathcal{H}^{\Delta t_l} \mathbf{Q}^l(t_l - \Delta t_l)) \\ &= \mathcal{H}_2^{\Delta t_l} \mathbf{Q}^l(t_l - \Delta t_l) \\ &= \mathcal{H}^{2\Delta t_l} \bar{\mathbf{Q}}^l(t_l - \Delta t_l) \end{aligned}$$

# Usage of heuristic error estimation

Current solution integrated tentatively 1 step with  $\Delta t_l$  and coarsened

$$\bar{Q}(t_l + \Delta t_l) := \text{Restrict} \left( \mathcal{H}_2^{\Delta t_l} \mathbf{Q}'(t_l - \Delta t_l) \right)$$

Previous solution coarsened and integrated 1 step with  $2\Delta t_l$

$$Q(t_l + \Delta t_l) := \mathcal{H}^{2\Delta t_l} \text{Restrict} \left( \mathbf{Q}'(t_l - \Delta t_l) \right)$$

Local error estimation of scalar quantity  $w$

$$\tau_{jk}^w := \frac{|w(\bar{Q}_{jk}(t + \Delta t)) - w(Q_{jk}(t + \Delta t))|}{2^{o+1} - 2}$$

In practice [Deiterding, 2003] use

$$\frac{\tau_{jk}^w}{\max(|w(Q_{jk}(t + \Delta t))|, S_w)} > \eta_w^r$$

# Outline

## The serial Berger-Colella SAMR method

- Block-based data structures
- Numerical update
- Conservative flux correction
- Level transfer operators
- The basic recursive algorithm
- Cluster algorithm
- Refinement criteria

## Parallel SAMR method

- Domain decomposition
- A parallel SAMR algorithm
- Partitioning

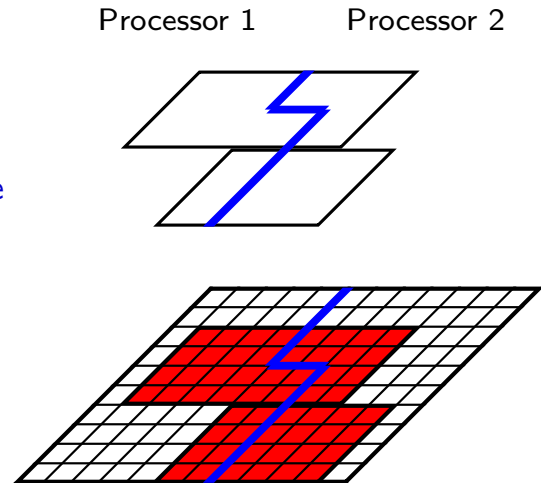
## Examples

- Euler equations

# Parallelization strategies

## Decomposition of the hierarchical data

- ▶ Distribution of each grid
- ▶ Separate distribution of each level, cf. [Rendleman et al., 2000]
- ▶ Rigorous domain decomposition
  - ▶ Data of all levels resides on same node
  - ▶ Grid hierarchy defines unique "floor-plan"
  - ▶ Redistribution of data blocks during reorganization of hierarchical data
  - ▶ Synchronization when setting ghost cells



# Rigorous domain decomposition formalized

Parallel machine with  $P$  identical nodes.  $P$  non-overlapping portions  $G_0^p$ ,  $p = 1, \dots, P$  as

$$G_0 = \bigcup_{p=1}^P G_0^p \quad \text{with} \quad G_0^p \cap G_0^q = \emptyset \quad \text{for } p \neq q$$

Higher level domains  $G_l$  follow decomposition of root level

$$G_l^p := G_l \cap G_0^p$$

With  $\mathcal{N}_l(\cdot)$  denoting number of cells, we estimate the workload as

$$\mathcal{W}(\Omega) = \sum_{l=0}^{l_{\max}} \left[ \mathcal{N}_l(G_l \cap \Omega) \prod_{\kappa=0}^l r_{\kappa} \right]$$

Equal work distribution necessitates

$$\mathcal{L}^p := \frac{P \cdot \mathcal{W}(G_0^p)}{\mathcal{W}(G_0)} \approx 1 \quad \text{for all } p = 1, \dots, P$$

[Deiterding, 2005]

# Ghost cell setting

Local synchronization

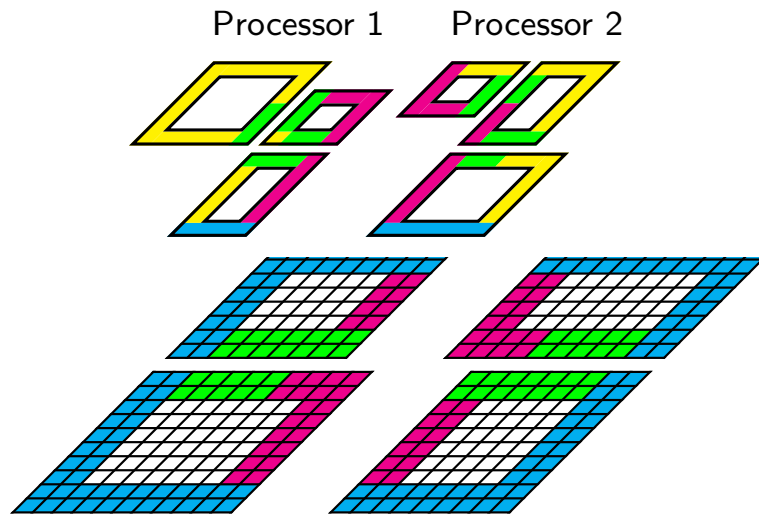
$$\tilde{S}_{l,m}^{s,p} = \tilde{G}_{l,m}^{s,p} \cap G_l^p$$

Parallel synchronization

$$\tilde{S}_{l,m}^{s,q} = \tilde{G}_{l,m}^{s,p} \cap G_l^q, q \neq p$$

Interpolation and physical boundary conditions remain strictly local

- ▶ Scheme  $\mathcal{H}(\Delta t_l)$  evaluated locally
- ▶ Restriction and prolongation local

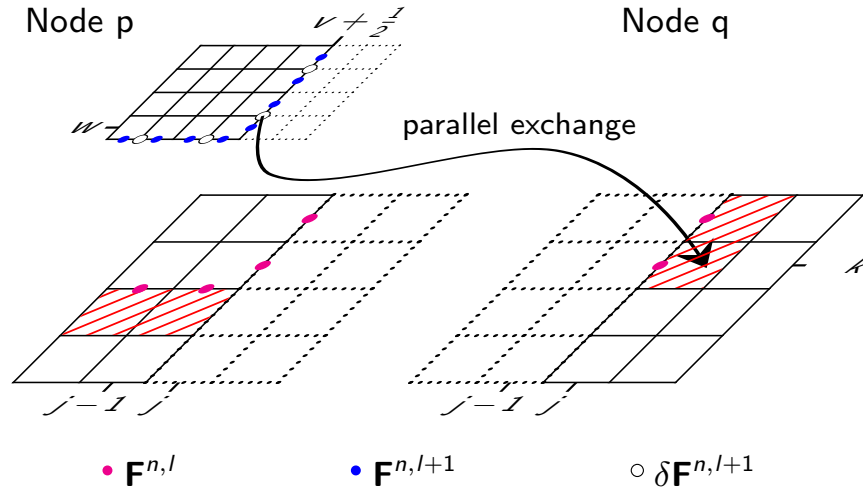


Ghost cell values:

- |   |   |
|---|---|
| <span style="display: inline-block; width: 15px; height: 15px; background-color: yellow; border: 1px solid black;"></span> Interpolation        | <span style="display: inline-block; width: 15px; height: 15px; background-color: pink; border: 1px solid black;"></span> Parallel synchronization |
| <span style="display: inline-block; width: 15px; height: 15px; background-color: green; border: 1px solid black;"></span> Local synchronization | <span style="display: inline-block; width: 15px; height: 15px; background-color: blue; border: 1px solid black;"></span> Physical boundary        |

# Parallel flux correction

1. Strictly local: Init  $\delta \mathbf{F}^{n,l+1}$  with  $\mathbf{F}^n(\bar{G}_{l,m} \cap \partial G_{l+1}, t)$
2. Strictly local: Add  $\mathbf{F}^n(\partial G_{l,m}, t)$  to  $\delta \mathbf{F}^{n,l}$
3. Parallel communication: Correct  $\mathbf{Q}^l(t + \Delta t_l)$  with  $\delta \mathbf{F}^{l+1}$



# The recursive algorithm in parallel

AdvanceLevel( $l$ )

Repeat  $r_l$  times

Set ghost cells of  $\mathbf{Q}^l(t)$

If time to regrid?

Regrid( $l$ )

UpdateLevel( $l$ )

If level  $l+1$  exists?

Set ghost cells of  $\mathbf{Q}^l(t + \Delta t_l)$

AdvanceLevel( $l+1$ )

Average  $\mathbf{Q}^{l+1}(t + \Delta t_l)$  onto  $\mathbf{Q}^l(t + \Delta t_l)$

Correct  $\mathbf{Q}^l(t + \Delta t_l)$  with  $\delta \mathbf{F}^{l+1}$

$t := t + \Delta t_l$

UpdateLevel( $l$ )

For all  $m = 1$  To  $M_l$  Do

$\mathbf{Q}(G_{l,m}^s, t) \xrightarrow{\mathcal{H}(\Delta t_l)} \mathbf{Q}(G_{l,m}, t + \Delta t_l), \mathbf{F}^n(\bar{G}_{l,m}, t)$

If level  $l > 0$

Add  $\mathbf{F}^n(\partial G_{l,m}, t)$  to  $\delta \mathbf{F}^{n,l}$

If level  $l+1$  exists

Init  $\delta \mathbf{F}^{n,l+1}$  with  $\mathbf{F}^n(\bar{G}_{l,m} \cap \partial G_{l+1}, t)$

- ▶ Numerical update strictly local
- ▶ Inter-level transfer local
- ▶ Parallel synchronization
- ▶ Application of  $\delta \mathbf{F}^{l+1}$  on  $\partial G_l^q$



# Regridding algorithm in parallel

Regrid( $l$ ) - Regrid all levels  $\iota > l$

```

For  $\iota = l_f$  Downto  $l$  Do
  Flag  $N^\iota$  according to  $Q^\iota(t)$ 
  If level  $\iota + 1$  exists?
    Flag  $N^\iota$  below  $\check{G}^{\iota+2}$ 
    Flag buffer zone on  $N^\iota$ 
    Generate  $\check{G}^{\iota+1}$  from  $N^\iota$ 
 $\check{G}_l := G_l$ 
For  $\iota = l$  To  $l_f$  Do
   $C\check{G}_\iota := G_0 \setminus \check{G}_\iota$ 
   $\check{G}_{\iota+1} := \check{G}_{\iota+1} \setminus C\check{G}_\iota^1$ 
Recompose( $l$ )

```

- ▶ Need a ghost cell overlap of  $b$  cells to ensure correct setting of refinement flags in parallel
- ▶ Two options exist (we choose the latter):
  - ▶ Global clustering algorithm
  - ▶ Local clustering algorithm and concatenation of new lists  $\check{G}^{\iota+1}$

# Recomposition algorithm in parallel

Recompose( $l$ ) - Reorganize all levels

Generate  $G_0^p$  from  $\{G_0, \dots, G_l, \check{G}_{l+1}, \dots, \check{G}_{l_f+1}\}$

For  $\iota = l + 1$  To  $l_f + 1$  Do

    If  $\iota > l$

$\check{G}_\iota^p := \check{G}_\iota \cap G_0^p$

        Interpolate  $\mathbf{Q}^{\iota-1}(t)$  onto  $\check{\mathbf{Q}}^\iota(t)$

    else

$\check{G}_\iota^p := G_\iota \cap G_0^p$

        If  $\iota > 0$

            Copy  $\delta \mathbf{F}^{n,\iota}$  onto  $\delta \check{\mathbf{F}}^{n,\iota}$

$\delta \mathbf{F}^{n,\iota} := \delta \check{\mathbf{F}}^{n,\iota}$

    If  $\iota \geq l$  then  $\kappa_\iota = 0$  else  $\kappa_\iota = 1$

    For  $\kappa = 0$  To  $\kappa_\iota$  Do

        Copy  $\mathbf{Q}^\iota(t)$  onto  $\check{\mathbf{Q}}^\iota(t)$

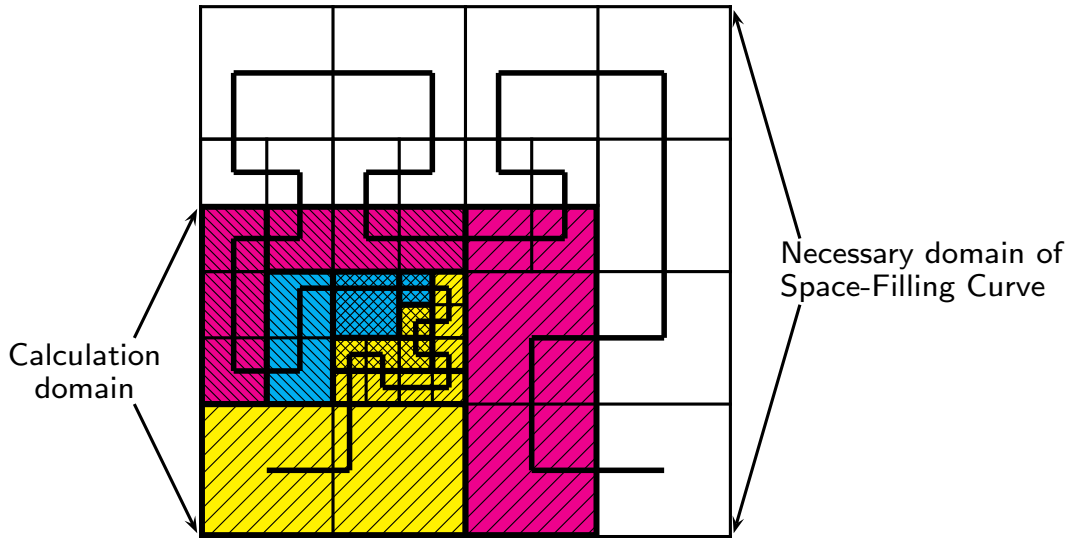
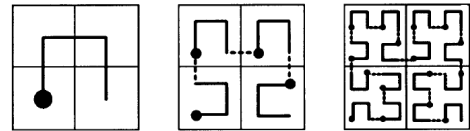
        Set ghost cells of  $\check{\mathbf{Q}}^\iota(t)$






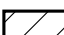
$\mathbf{Q}^\iota(t) := \check{\mathbf{Q}}^\iota(t)$

$G_\iota := \check{G}_\iota$

- ▶ Global redistribution can also be required when regridding higher levels and  $G_0, \dots, G_l$  do not change (drawback of domain decomposition)
- ▶ When  $\iota > l$  do nothing special
- ▶ For  $\iota \leq l$ , redistribute additionally
  - ▶ Flux corrections  $\delta \mathbf{F}^{n,\iota}$
  - ▶ Already updated time level  $\mathbf{Q}^\iota(t + \kappa \Delta t_\iota)$

# Space-filling curve algorithm



- |  |         |  |                 |
|--|---------|--|-----------------|
|   | Proc. 1 |   | High Workload   |
|   | Proc. 2 |   | Medium Workload |
|  | Proc. 3 |  | Low Workload    |

# Outline

## The serial Berger-Colella SAMR method

- Block-based data structures
- Numerical update
- Conservative flux correction
- Level transfer operators
- The basic recursive algorithm
- Cluster algorithm
- Refinement criteria

## Parallel SAMR method

- Domain decomposition
- A parallel SAMR algorithm
- Partitioning

## Examples

- Euler equations

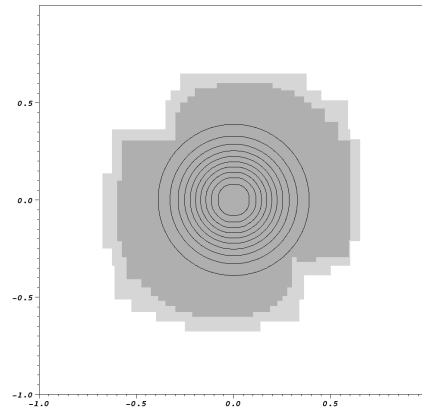
# SAMR accuracy verification

Gaussian density shape

$$\rho(x_1, x_2) = 1 + e^{-\left(\frac{\sqrt{x_1^2 + x_2^2}}{R}\right)^2}$$

is advected with constant velocities  $u_1 = u_2 \equiv 1$ ,  
 $p_0 \equiv 1$ ,  $R = 1/4$

- ▶ Domain  $[-1, 1] \times [-1, 1]$ , periodic boundary conditions,  $t_{end} = 2$
- ▶ Two levels of adaptation with  $r_{1,2} = 2$ , finest level corresponds to  $N \times N$  uniform grid



Use *locally* conservative interpolation

$$\check{\mathbf{Q}}_{v,w}^l := \mathbf{Q}_{ij}^l + f_1(\mathbf{Q}_{i+1,j}^l - \mathbf{Q}_{i-1,j}^l) + f_2(\mathbf{Q}_{i,j+1}^l - \mathbf{Q}_{i,j-1}^l)$$

with factor  $f_1 = \frac{x_{1,l+1}^v - x_{1,l}^j}{2\Delta x_{1,l}}$ ,  $f_2 = \frac{x_{2,l+1}^w - x_{2,l}^j}{2\Delta x_{2,l}}$  to also test flux correction

*This prolongation operator is not monotonicity preserving! Only applicable to smooth problems.*

# SAMR accuracy verification: results

VanLeer flux vector splitting with dimensional splitting, Minmod limiter

$N$	Unigrid		SAMR - fixup			SAMR - no fixup		
	Error	Order	Error	Order	$\Delta\rho$	Error	Order	$\Delta\rho$
20	0.10946400							
40	0.04239430	1.369						
80	0.01408160	1.590	0.01594820		0	0.01595980		2e-5
160	0.00492945	1.514	0.00526693	1.598	0	0.00530538	1.589	2e-5
320	0.00146132	1.754	0.00156516	1.751	0	0.00163837	1.695	-1e-5
640	0.00041809	1.805	0.00051513	1.603	0	0.00060021	1.449	-6e-5

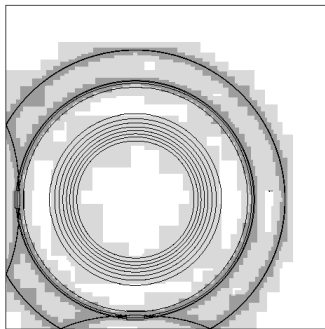
Fully two-dimensional Wave Propagation Method, Minmod limiter

$N$	Unigrid		SAMR - fixup			SAMR - no fixup		
	Error	Order	Error	Order	$\Delta\rho$	Error	Order	$\Delta\rho$
20	0.10620000							
40	0.04079600	1.380						
80	0.01348250	1.598	0.01536580		0	0.01538820		2e-5
160	0.00472301	1.513	0.00505406	1.604	0	0.00510499	1.592	5e-5
320	0.00139611	1.758	0.00147218	1.779	0	0.00152387	1.744	7e-5
640	0.00039904	1.807	0.00044500	1.726	0	0.00046587	1.710	6e-5

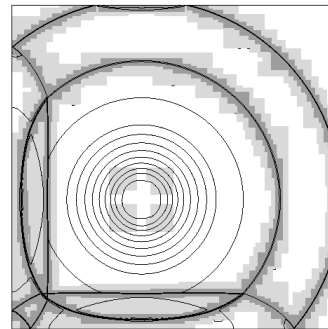
# Benchmark run: blast wave in 2D

- ▶ 2D-Wave-Propagation Method with Roe's approximate solver
- ▶ Base grid  $150 \times 150$
- ▶ 2 levels: factor 2, 4

Task [%]	$P=1$	$P=2$	$P=4$	$P=8$	$P=16$
Update by $\mathcal{H}(\cdot)$	86.6	83.4	76.7	64.1	51.9
Flux correction	1.2	1.6	3.0	7.9	10.7
Boundary setting	3.5	5.7	10.1	15.6	18.3
Recomposition	5.5	6.1	7.4	9.9	14.0
Misc.	4.9	3.2	2.8	2.5	5.1
<b>Time [min]</b>	<b>151.9</b>	<b>79.2</b>	<b>43.4</b>	<b>23.3</b>	<b>13.9</b>
<b>Efficiency [%]</b>	<b>100.0</b>	<b>95.9</b>	<b>87.5</b>	<b>81.5</b>	<b>68.3</b>



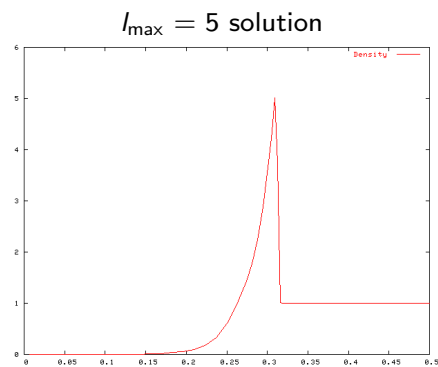
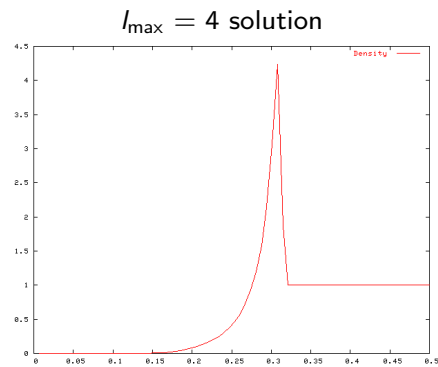
After 38 time steps



After 79 time steps

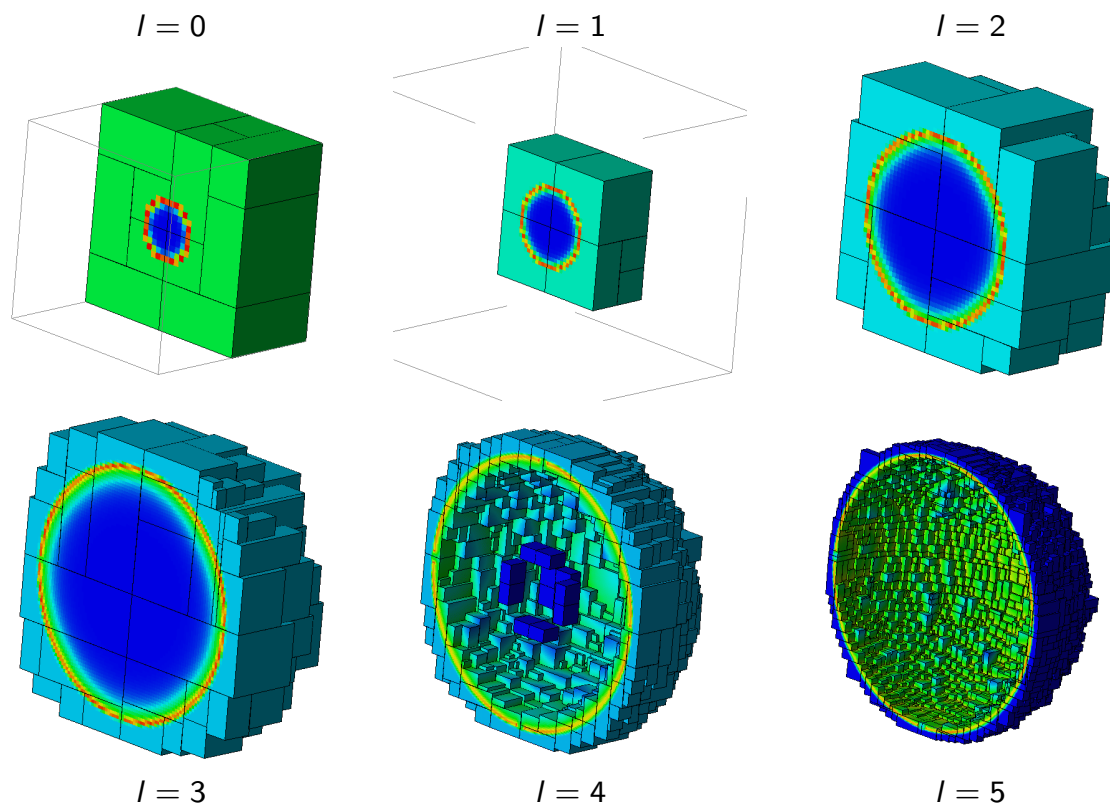
## Benchmark run 2: point-explosion in 3D

- ▶ Benchmark from the Chicago workshop on AMR methods, September 2003
- ▶ Sedov explosion - energy deposition in sphere of radius 4 finest cells
- ▶ 3D-Wave-Prop. Method with hybrid Roe-HLL scheme
- ▶ Base grid  $32^3$
- ▶ Refinement factor  $r_l = 2$
- ▶ Effective resolutions:  $128^3$ ,  $256^3$ ,  $512^3$ ,  $1024^3$
- ▶ Grid generation efficiency  $\eta_{tol} = 85\%$
- ▶ Proper nesting enforced
- ▶ Buffer of 1 cell





## Benchmark run 2: visualization of refinement



## Benchmark run 2: performance results

Number of grids and cells

$l$	$l_{\max} = 2$		$l_{\max} = 3$		$l_{\max} = 4$		$l_{\max} = 5$	
	Grids	Cells	Grids	Cells	Grids	Cells	Grids	Cells
0	28	32,768	28	32,768	33	32,768	34	32,768
1	8	32,768	14	32,768	20	32,768	20	32,768
2	63	115,408	49	116,920	43	125,680	50	125,144
3			324	398,112	420	555,744	193	572,768
4					1405	1,487,312	1,498	1,795,048
5							5,266	5,871,128
$\Sigma$		180,944		580,568		2,234,272		8,429,624

Breakdown of CPU time on 8 nodes SGI Altix 3000 (Linux-based shared memory system)

Task [%]	$l_{\max} = 2$		$l_{\max} = 3$		$l_{\max} = 4$		$l_{\max} = 5$	
Integration	73.7		77.2		72.9		37.8	
Fixup	2.6	46	3.1	58	2.6	42	2.2	45
Boundary	10.1	79	6.3	78	5.1	56	6.9	78
Recomposition	7.4		8.0		15.1		50.4	
Clustering	0.5		0.6		0.7		1.0	
Output/Misc	5.7		4.0		3.6		1.7	
Time [min]	0.5		5.1		73.0		2100.0	
Uniform [min]	5.4		160		~5,000		~180,000	
<b>Factor of AMR savings</b>	11		31		69		86	
Time steps	15		27		52		115	

# References I

- [Bell et al., 1994] Bell, J., Berger, M., Saltzman, J., and Welcome, M. (1994). Three-dimensional adaptive mesh refinement for hyperbolic conservation laws. *SIAM J. Sci. Comp.*, 15(1):127–138.
- [Berger, 1982] Berger, M. (1982). *Adaptive Mesh Refinement for Hyperbolic Differential Equations*. PhD thesis, Stanford University. Report No. STAN-CS-82-924.
- [Berger, 1986] Berger, M. (1986). Data structures for adaptive grid generation. *SIAM J. Sci. Stat. Comput.*, 7(3):904–916.
- [Berger and Colella, 1988] Berger, M. and Colella, P. (1988). Local adaptive mesh refinement for shock hydrodynamics. *J. Comput. Phys.*, 82:64–84.
- [Berger and Oliger, 1984] Berger, M. and Oliger, J. (1984). Adaptive mesh refinement for hyperbolic partial differential equations. *J. Comput. Phys.*, 53:484–512.
- [Berger and Rigoutsos, 1991] Berger, M. and Rigoutsos, I. (1991). An algorithm for point clustering and grid generation. *IEEE Transactions on Systems, Man, and Cybernetics*, 21(5):1278–1286.

# References II

- [Deiterding, 2003] Deiterding, R. (2003). *Parallel adaptive simulation of multi-dimensional detonation structures*. PhD thesis, Brandenburgische Technische Universität Cottbus.
- [Deiterding, 2005] Deiterding, R. (2005). Construction and application of an AMR algorithm for distributed memory computers. In Plewa, T., Linde, T., and Weirs, V. G., editors, *Adaptive Mesh Refinement - Theory and Applications*, volume 41 of *Lecture Notes in Computational Science and Engineering*, pages 361–372. Springer.
- [Rendleman et al., 2000] Rendleman, C. A., Beckner, V. E., Lijewski, M., Crutchfield, W., and Bell, J. B. (2000). Parallelization of structured, hierarchical adaptive mesh refinement algorithms. *Computing and Visualization in Science*, 3:147–157.

# Lecture 3

## Complex hyperbolic applications

Course *Block-structured Adaptive Mesh Refinement Methods for Conservation Laws*  
*Theory, Implementation and Application*

Ralf Deiterding

Computer Science and Mathematics Division  
Oak Ridge National Laboratory  
P.O. Box 2008 MS6367, Oak Ridge, TN 37831, USA

E-mail: [deiterdingr@ornl.gov](mailto:deiterdingr@ornl.gov)

# Outline

## Complex geometry

- Boundary aligned meshes
- Cartesian techniques
- Implicit geometry representation
- Accuracy / verification

## Combustion

- Equations and FV schemes
- Shock-induced combustion examples

## Fluid-structure interaction

- Coupling to a solid mechanics solver
- Rigid body motion
- Thin elastic structures
- Deforming thin structures

## Turbulence

- Large-eddy simulation

# Outline

## Complex geometry

- Boundary aligned meshes
- Cartesian techniques
- Implicit geometry representation
- Accuracy / verification

## Combustion

- Equations and FV schemes
- Shock-induced combustion examples

## Fluid-structure interaction

- Coupling to a solid mechanics solver
- Rigid body motion
- Thin elastic structures
- Deforming thin structures

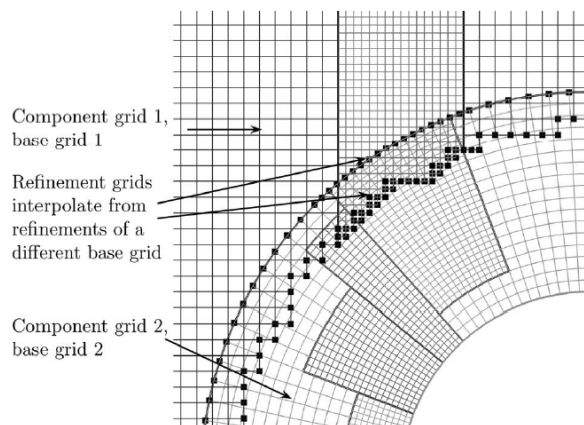
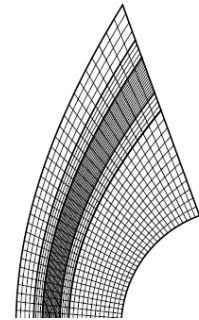
## Turbulence

- Large-eddy simulation

# SAMR on boundary aligned meshes

Analytic or stored geometric mapping of the coordinates  
(graphic from [Yamaleev and Carpenter, 2002])

- ▶ Topology remains unchanged and thereby entire SAMR algorithm
- ▶ Patch solver and interpolation need to consider geometry transformation
- ▶ Handles boundary layers well



Overlapping adaptive meshes  
[Henshaw and Schwendeman, 2003],  
[Meakin, 1995]

- ▶ Idea is to use a non-Cartesian structured grids only near boundary
- ▶ Very suitable for moving objects with boundary layers
- ▶ Interpolation between meshes is usually non-conservative



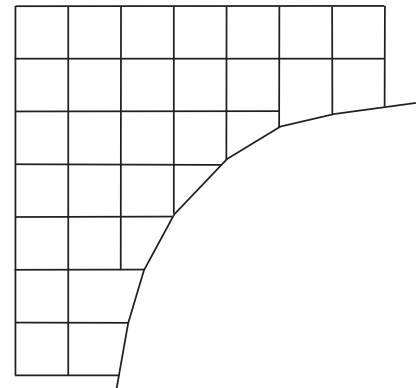
# Cut-cell techniques

Accurate embedded boundary method

$$V_j^{n+1} \mathbf{Q}_j^{n+1} = V_j^n \mathbf{Q}_j^n - \Delta t \left( A_{j+1/2}^{n+1/2} \mathbf{F}(\mathbf{Q}, j) - A_{j-1/2}^{n+1/2} \mathbf{F}(\mathbf{Q}, j-1) \right)$$

Methods that represent the boundary sharply:

- ▶ Cut-cell approach constructs appropriate finite volumes
- ▶ Conservative by construction. Correct boundary flux
- ▶ Key question: How to avoid small-cell time step restriction in explicit methods?
  - ▶ Cell merging: [Quirk, 1994a]
- ▶ Usually explicit geometry representation used [Aftosmis, 1997], but can also be implicit, cf. [Nourgaliev et al., 2003], [Murman et al., 2003]



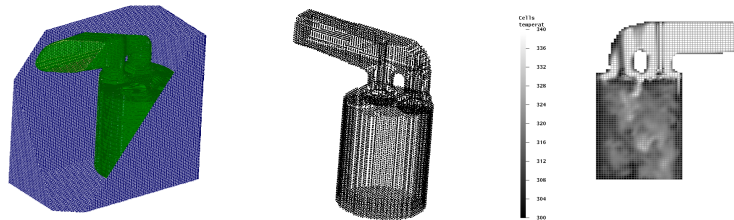
# Embedded boundary techniques

Volume of fluid methods that resemble a cut-cell technique on purely Cartesian mesh

- ▶ Redistribution of boundary flux achieves conservation and bypasses time step restriction: [Pember et al., 1999], [Berger and Helzel, 2002]

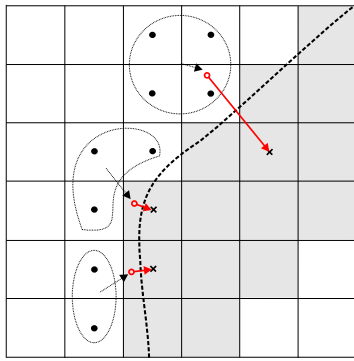
Methods that diffuse the boundary in one cell (good overview in [Mittal and Iaccarino, 2005]):

- ▶ Related to the immersed boundary method by Peskin, cf. [Roma et al., 1999]
- ▶ Boundary prescription often by internal ghost cell values, cf. [Tseng and Ferziger, 2003]
- ▶ Not conservative by construction but conservative correction possible
- ▶ Usually combined with implicit geometry representation



K. J. Richards et al., On the use of the immersed boundary method for engine modeling

# Level-set method for boundary embedding



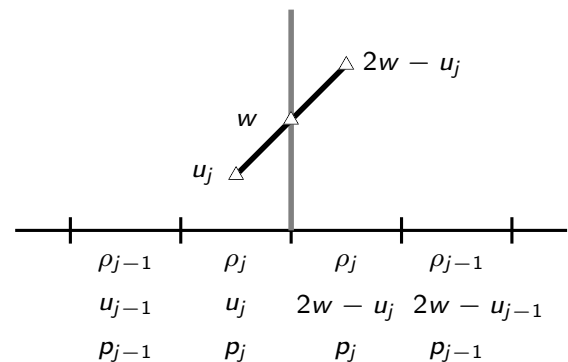
- ▶ Implicit boundary representation via distance function  $\varphi$ , normal  $\mathbf{n} = \nabla\varphi/|\nabla\varphi|$
- ▶ Complex boundary moving with local velocity  $\mathbf{w}$ , treat interface as moving rigid wall
- ▶ Construction of values in embedded boundary cells by interpolation / extrapolation

Interpolate / constant value extrapolate values at

$$\tilde{\mathbf{x}} = \mathbf{x} + 2\varphi\mathbf{n}$$

Velocity in ghost cells

$$\begin{aligned}\mathbf{u}' &= (2\mathbf{w} \cdot \mathbf{n} - \mathbf{u} \cdot \mathbf{n})\mathbf{n} + (\mathbf{u} \cdot \mathbf{t})\mathbf{t} \\ &= 2((\mathbf{w} - \mathbf{u}) \cdot \mathbf{n})\mathbf{n} + \mathbf{u}\end{aligned}$$



# Closest point transform algorithm

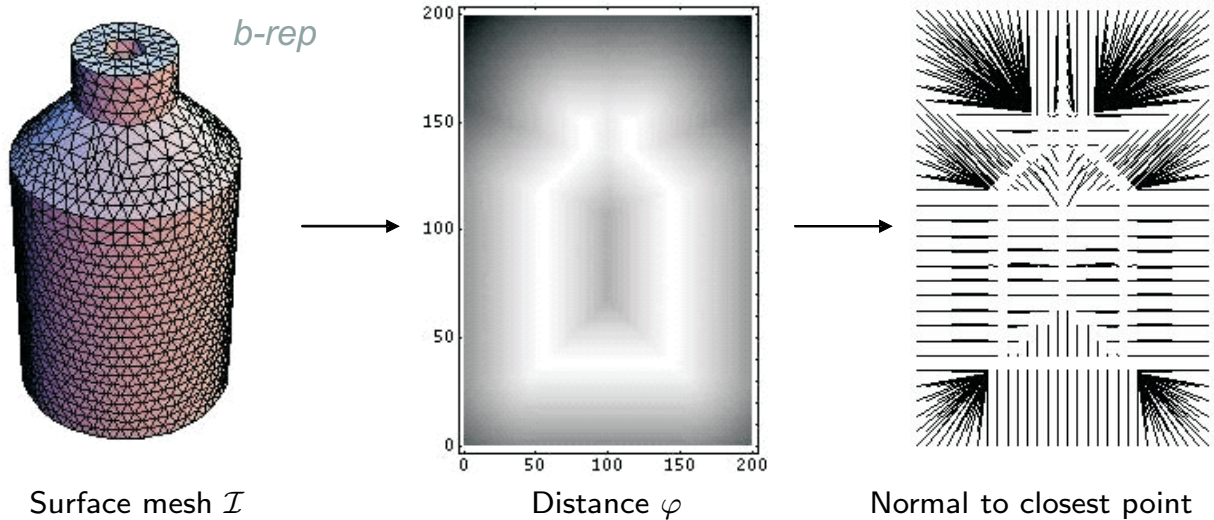
The signed distance  $\varphi$  to a surface  $\mathcal{I}$  satisfies the eikonal equation [Sethian, 1999]

$$|\nabla\varphi| = 1 \quad \text{with} \quad \varphi|_{\mathcal{I}} = 0$$

Solution smooth but non-differentiable across characteristics.

Distance computation trivial for non-overlapping elementary shapes but difficult to do efficiently for triangulated surface meshes:

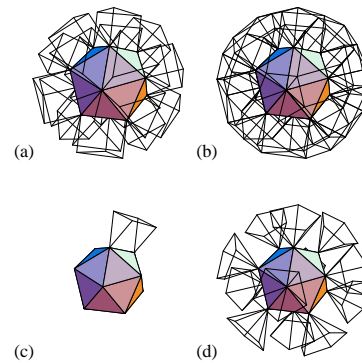
- ▶ Geometric solution approach with closest-point-transform algorithm [Mauch, 2003]



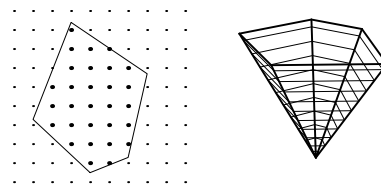
# The characteristic / scan conversion algorithm

1. Build the characteristic polyhedrons for the surface mesh
2. For each face/edge/vertex
  - 2.1 Scan convert the polyhedron.
  - 2.2 Compute distance to that primitive for the scan converted points
3. Computational complexity.
  - ▶  $O(m)$  to build the b-rep and the polyhedra.
  - ▶  $O(n)$  to scan convert the polyhedra and compute the distance, etc.
4. Problem reduction by evaluation only within specified max. distance

Characteristic polyhedra for faces, edges, and vertices



Slicing and scan conversion of apolygon



[Mauch, 2003], see also  
[Deiterding et al., 2006]

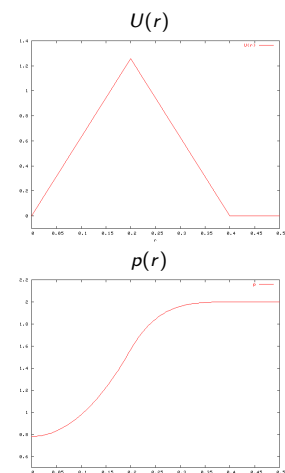
# Accuracy test: stationary vortex

Construct non-trivial *radially symmetric* and *stationary* solution by balancing hydrodynamic pressure and centripetal force per volume element, i.e.

$$\frac{d}{dr}p(r) = \rho(r) \frac{U(r)^2}{r}$$

For  $\rho_0 \equiv 1$  and the velocity field

$$U(r) = \alpha \cdot \begin{cases} 2r/R & \text{if } 0 < r < R/2, \\ 2(1 - r/R) & \text{if } R/2 \leq r \leq R, \\ 0 & \text{if } r > R, \end{cases}$$



one gets with boundary condition  $p(R) = p_0 \equiv 2$  the pressure distribution

$$p(r) = p_0 + 2\rho_0\alpha^2 \cdot \begin{cases} r^2/R^2 + 1 - 2\log 2 & \text{if } 0 < r < R/2, \\ r^2/R^2 + 3 - 4r/R + 2\log(r/R) & \text{if } R/2 \leq r \leq R, \\ 0 & \text{if } r > R. \end{cases}$$

Entire solution for Euler equations reads

$$\rho(x_1, x_2, t) = \rho_0, \quad u_1(x_1, x_2, t) = -U(r) \sin \phi, \quad u_2(x_1, x_2, t) = U(r) \cos \phi, \quad p(x_1, x_2, t) = p(r)$$

for all  $t \geq 0$  with  $r = \sqrt{(x_1 - x_{1,c})^2 + (x_2 - x_{2,c})^2}$  and  $\phi = \arctan \frac{x_2 - x_{2,c}}{x_1 - x_{1,c}}$

# Stationary vortex: results

Compute one full rotation, Roe solver, embedded slip wall boundary conditions

$x_{1,c} = 0.5$ ,  $x_{2,c} = 0.5$ ,  $R = 0.4$ ,  $t_{end} = 1$ ,  $\Delta h = \Delta x_1 = \Delta x_2 = 1/N$ ,  $\alpha = R\pi$

No embedded boundary

$N$	Wave Propagation		Godunov Splitting	
	Error	Order	Error	Order
20	0.0111235		0.0182218	
40	0.0037996	1.55	0.0090662	1.01
80	0.0013388	1.50	0.0046392	0.97
160	0.0005005	1.42	0.0023142	1.00

Marginal shear flow along embedded boundary,  $\alpha = R\pi$ ,  $R_G = R$ ,  $U_W = 0$

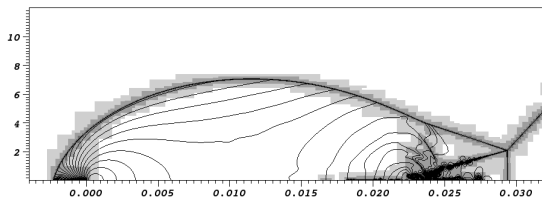
$N$	Wave Propagation			Godunov Splitting		
	Error	Order	Mass loss	Error	Order	Mass loss
20	0.0120056		0.0079236	0.0144203		0.0020241
40	0.0035074	1.78	0.0011898	0.0073070	0.98	0.0001300
80	0.0014193	1.31	0.0001588	0.0038401	0.93	-0.0001036
160	0.0005032	1.50	5.046e-05	0.0018988	1.02	-2.783e-06

Major shear flow along embedded boundary,  $\alpha = R\pi$ ,  $R_G = R/2$ ,  $U_W = 0$

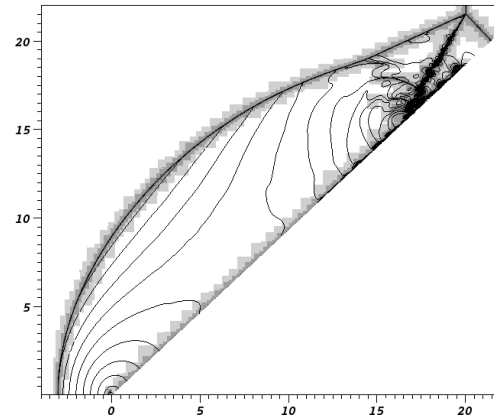
$N$	Wave Propagation			Godunov Splitting		
	Error	Order	Mass loss	Error	Order	Mass loss
20	0.0423925		0.0423925	0.0271446		0.0271446
40	0.0358735	0.24	0.0358735	0.0242260	0.16	0.0242260
80	0.0212340	0.76	0.0212340	0.0128638	0.91	0.0128638
160	0.0121089	0.81	0.0121089	0.0070906	0.86	0.0070906

# Verification: shock reflection

- ▶ Reflection of a Mach 2.38 shock in nitrogen at  $43^\circ$  wedge
- ▶ 2nd order MUSCL scheme with Roe solver, 2nd order multidimensional wave propagation method



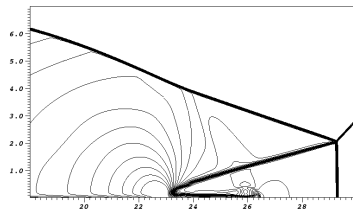
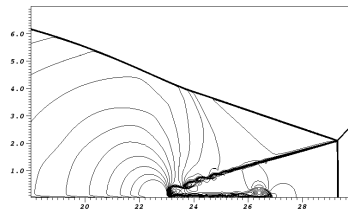
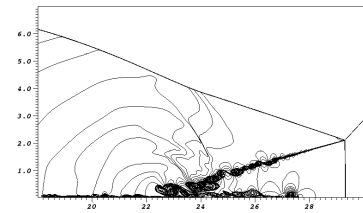
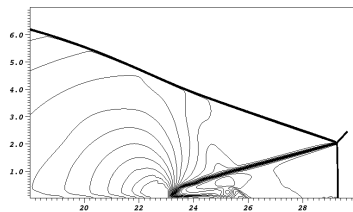
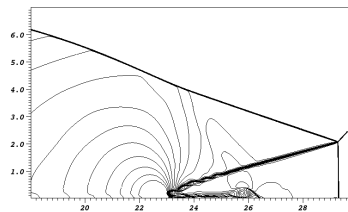
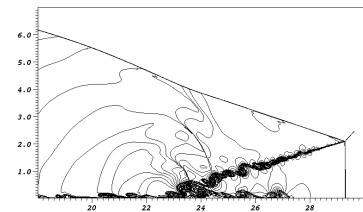
Cartesian base grid  $360 \times 160$  cells on domain of  $36 \text{ mm} \times 16 \text{ mm}$  with up to 3 refinement levels with  $r_l = 2, 4, 4$  and  $\Delta x_{1,2} = 3.125 \mu\text{m}$ , 38 h CPU



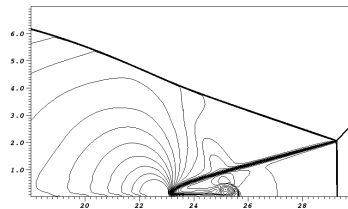
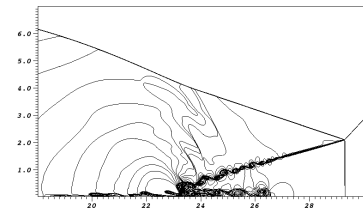
GFM base grid  $390 \times 330$  cells on domain of  $26 \text{ mm} \times 22 \text{ mm}$  with up to 3 refinement levels with  $r_l = 2, 4, 4$  and  $\Delta x_{e,1,2} = 2.849 \mu\text{m}$ , 200 h CPU



# Shock reflection: SAMR solution for Euler equations

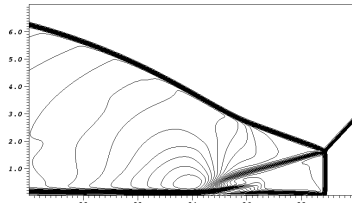
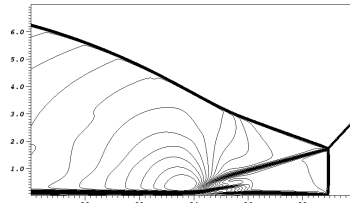
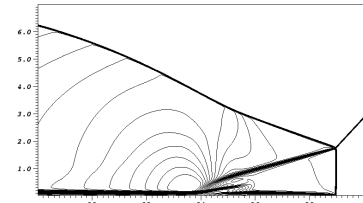
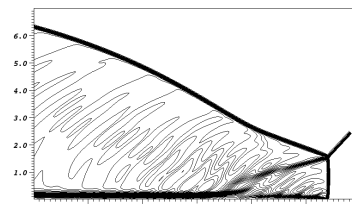
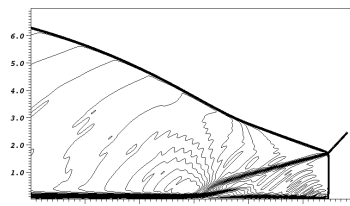
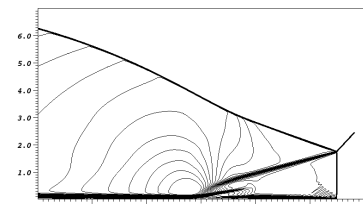

 $\Delta x = 25 \text{ mm}$ 

 $\Delta x = 12.5 \text{ mm}$ 

 $\Delta x = 3.125 \text{ mm}$ 

 $\Delta x_e = 22.8 \text{ mm}$ 

 $\Delta x_e = 11.4 \text{ mm}$ 

 $\Delta x_e = 2.849 \text{ mm}$ 

2nd order MUSCL scheme  
with Van Leer FVS, dimensional  
splitting


 $\Delta x = 12.5 \text{ mm}$ 

 $\Delta x = 3.125 \text{ mm}$

# Shock reflection: solution for Navier-Stokes equations

- ▶ No-slip boundary conditions enforced
- ▶ Conservative 2nd order centered differences to approximate stress tensor and heat flow

 $\Delta x = 50 \text{ mm}$  $\Delta x = 25 \text{ mm}$  $\Delta x = 12.5 \text{ mm, SAMR}$  $\Delta x_e = 45.6 \text{ mm}$  $\Delta x_e = 22.8 \text{ mm}$  $\Delta x_e = 11.4 \text{ mm, SAMR}$

# Outline

## Complex geometry

- Boundary aligned meshes
- Cartesian techniques
- Implicit geometry representation
- Accuracy / verification

## Combustion

- Equations and FV schemes
- Shock-induced combustion examples

## Fluid-structure interaction

- Coupling to a solid mechanics solver
- Rigid body motion
- Thin elastic structures
- Deforming thin structures

## Turbulence

- Large-eddy simulation

# Governing equations for premixed combustion

Euler equations with reaction terms

$$\begin{aligned}\frac{\partial \rho_i}{\partial t} + \frac{\partial}{\partial x_n} (\rho_i u_n) &= \dot{\omega}_i, \quad i = 1, \dots, K \\ \frac{\partial}{\partial t} (\rho u_k) + \frac{\partial}{\partial x_n} (\rho u_k u_n + \delta_{kn} p) &= 0, \quad k = 1, \dots, d \\ \frac{\partial}{\partial t} (\rho E) + \frac{\partial}{\partial x_n} (u_n (\rho E + p)) &= 0\end{aligned}$$

Ideal gas law and Dalton's law for gas-mixtures

$$p(\rho_1, \dots, \rho_K, T) = \sum_{i=1}^K p_i = \sum_{i=1}^K \rho_i \frac{\mathcal{R}}{W_i} T = \rho \frac{\mathcal{R}}{W} T \quad \text{with} \quad \sum_{i=1}^K \rho_i = \rho, Y_i = \frac{\rho_i}{\rho}$$

Caloric equation

$$h(Y_1, \dots, Y_K, T) = \sum_{i=1}^K Y_i h_i(T) \quad \text{with} \quad h_i(T) = h_i^0 + \int_0^T c_{pi}(s) ds$$

Computation of  $T = T(\rho_1, \dots, \rho_K, e)$  from implicit equation

$$\sum_{i=1}^K \rho_i h_i(T) - \mathcal{R} T \sum_{i=1}^K \frac{\rho_i}{W_i} - \rho e = 0$$

for *thermally perfect* gases with  $\gamma_i(T) = c_{pi}(T)/c_{vi}(T)$

# Chemistry

Arrhenius-Kinetics:

$$\dot{\omega}_i = \sum_{j=1}^M (\nu_{ji}^r - \nu_{ji}^f) \left[ k_j^f \prod_{n=1}^K \left( \frac{\rho_n}{W_n} \right)^{\nu_{jn}^f} - k_j^r \prod_{n=1}^K \left( \frac{\rho_n}{W_n} \right)^{\nu_{jn}^r} \right] \quad i = 1, \dots, K$$

- ▶ Parsing of mechanisms with Chemkin-II
- ▶ Evaluation of  $\dot{\omega}_i$  with automatically generated optimized Fortran-77 functions in the line of Chemkin-II

Integration of reaction rates: ODE integration in  $\mathcal{S}^{(\cdot)}$  for Euler equations with chemical reaction

- ▶ Standard implicit or semi-implicit ODE-solver subcycles within each cell
- ▶  $\rho, e, u_k$  remain unchanged!

$$\partial_t \rho_i = W_i \dot{\omega}_i(\rho_1, \dots, \rho_K, T) \quad i = 1, \dots, K$$

Use Newton or bisection method to compute  $T$  iteratively.

## Non-equilibrium mechanism for hydrogen-oxygen combustion

				$A$ [cm, mol, s]	$\beta$	$E_{act}$ [cal mol <sup>-1</sup> ]
1.	H + O <sub>2</sub>	→	O + OH	$1.86 \times 10^{14}$	0.00	16790.
2.	O + OH	→	H + O <sub>2</sub>	$1.48 \times 10^{13}$	0.00	680.
3.	H <sub>2</sub> + O	→	H + OH	$1.82 \times 10^{10}$	1.00	8900.
4.	H + OH	→	H <sub>2</sub> + O	$8.32 \times 10^{09}$	1.00	6950.
5.	H <sub>2</sub> O + O	→	OH + OH	$3.39 \times 10^{13}$	0.00	18350.
6.	OH + OH	→	H <sub>2</sub> O + O	$3.16 \times 10^{12}$	0.00	1100.
7.	H <sub>2</sub> O + H	→	H <sub>2</sub> + OH	$9.55 \times 10^{13}$	0.00	20300.
8.	H <sub>2</sub> + OH	→	H <sub>2</sub> O + H	$2.19 \times 10^{13}$	0.00	5150.
9.	H <sub>2</sub> O <sub>2</sub> + OH	→	H <sub>2</sub> O + HO <sub>2</sub>	$1.00 \times 10^{13}$	0.00	1800.
10.	H <sub>2</sub> O + HO <sub>2</sub>	→	H <sub>2</sub> O <sub>2</sub> + OH	$2.82 \times 10^{13}$	0.00	32790.
...	...		...	...	...	...
30.	OH + M	→	O + H + M	$7.94 \times 10^{19}$	-1.00	103720.
31.	O <sub>2</sub> + M	→	O + O + M	$5.13 \times 10^{15}$	0.00	115000.
32.	O + O + M	→	O <sub>2</sub> + M	$4.68 \times 10^{15}$	-0.28	0.
33.	H <sub>2</sub> + M	→	H + H + M	$2.19 \times 10^{14}$	0.00	96000.
34.	H + H + M	→	H <sub>2</sub> + M	$3.02 \times 10^{15}$	0.00	0.

Third body efficiencies:  $f(\text{O}_2) = 0.40$ ,  $f(\text{H}_2\text{O}) = 6.50$

C. K. Westbrook. Chemical kinetics of hydrocarbon oxidation in gaseous detonations. *J. Combustion and Flame*, 46:191–210, 1982.

# Riemann solver for combustion

(S1) Calculate standard Roe-averages  $\hat{\rho}$ ,  $\hat{u}_n$ ,  $\hat{H}$ ,  $\hat{Y}_i$ ,  $\hat{T}$ .

(S2) Compute  $\hat{\gamma} := \hat{c}_p / \hat{c}_v$  with  $\hat{c}_{\{p,v\}i} = \frac{1}{T_R - T_L} \int_{T_L}^{T_R} c_{\{p,v\}i}(\tau) d\tau$ .

(S3) Calculate  $\hat{\phi}_i := (\hat{\gamma} - 1) \left( \frac{\hat{u}^2}{2} - \hat{h}_i \right) + \hat{\gamma} R_i \hat{T}$  with standard Roe-averages  $\hat{e}_i$  or  $\hat{h}_i$ .

(S4) Calculate  $\hat{c} := \left( \sum_{i=1}^K \hat{Y}_i \hat{\phi}_i - (\hat{\gamma} - 1) \hat{u}^2 + (\hat{\gamma} - 1) \hat{H} \right)^{1/2}$ .

(S5) Use  $\Delta \mathbf{q} = \mathbf{q}_R - \mathbf{q}_L$  and  $\Delta p$  to compute the wave strengths  $a_m$ .

(S6) Calculate  $\mathcal{W}_1 = a_1 \hat{\mathbf{r}}_1$ ,  $\mathcal{W}_2 = \sum_{\ell=2}^{K+d} a_\ell \hat{\mathbf{r}}_\ell$ ,  $\mathcal{W}_3 = a_{K+d+1} \hat{\mathbf{r}}_{K+d+1}$ .

(S7) Evaluate  $s_1 = \hat{u}_1 - \hat{c}$ ,  $s_2 = \hat{u}_1$ ,  $s_3 = \hat{u}_1 + \hat{c}$ .

(S8) Evaluate  $\rho_{L/R}^*$ ,  $u_{1,L/R}^*$ ,  $e_{L/R}^*$ ,  $c_{1,L/R}^*$  from  $\mathbf{q}_L^* = \mathbf{q}_L + \mathcal{W}_1$  and  $\mathbf{q}_R^* = \mathbf{q}_R - \mathcal{W}_3$ .

(S9) If  $\rho_{L/R}^* \leq 0$  or  $e_{L/R}^* \leq 0$  use  $\mathbf{F}_{HLL}(\mathbf{q}_L, \mathbf{q}_R)$  and go to (S12).

(S10) Entropy correction: Evaluate  $|\tilde{s}_\ell|$ .

$$\mathbf{F}_{Roe}(\mathbf{q}_L, \mathbf{q}_R) = \frac{1}{2} (\mathbf{f}(\mathbf{q}_L) + \mathbf{f}(\mathbf{q}_R) - \sum_{\ell=1}^3 |\tilde{s}_\ell| \mathcal{W}_\ell)$$

(S11) Positivity correction: Replace  $\mathbf{F}_i$  by

$$\mathbf{F}_i^* = \mathbf{F}_\rho \cdot \begin{cases} Y_i^l, & \mathbf{F}_\rho \geq 0, \\ Y_i^r, & \mathbf{F}_\rho < 0. \end{cases}$$

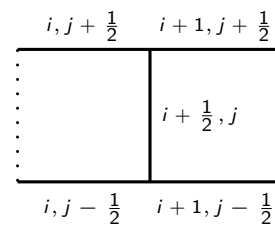
(S12) Evaluate maximal signal speed by  $S = \max(|s_1|, |s_3|)$ .

# Riemann solver for combustion: carbuncle fix

Entropy corrections [Harten, 1983]  
[Harten and Hyman, 1983]

1.  $|\tilde{s}_\ell| = \begin{cases} |s_\ell| & \text{if } |s_\ell| \geq 2\eta \\ \frac{|s_\ell|^2}{4\eta} + \eta & \text{otherwise} \end{cases}$   
 $\eta = \frac{1}{2} \max_\ell \{ |s_\ell(\mathbf{q}_R) - s_\ell(\mathbf{q}_L)| \}$
2. Replace  $|s_\ell|$  by  $|\tilde{s}_\ell|$  only if  
 $s_\ell(\mathbf{q}_L) < 0 < s_\ell(\mathbf{q}_R)$

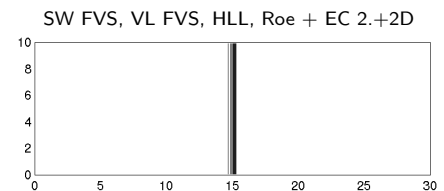
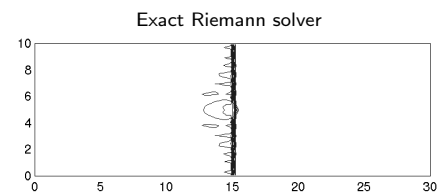
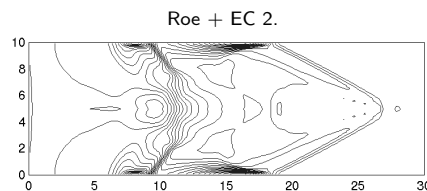
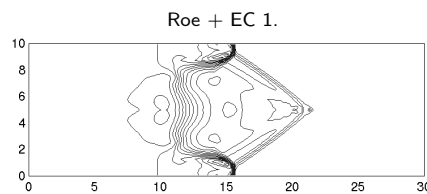
2D modification of entropy correction  
[Sanders et al., 1998]:



$$\tilde{\eta}_{i+1/2,j} = \max \{ \eta_{i+1/2,j}, \eta_{i,j-1/2}, \eta_{i,j+1/2}, \eta_{i+1,j-1/2}, \eta_{i+1,j+1/2} \}$$

Carbuncle phenomenon

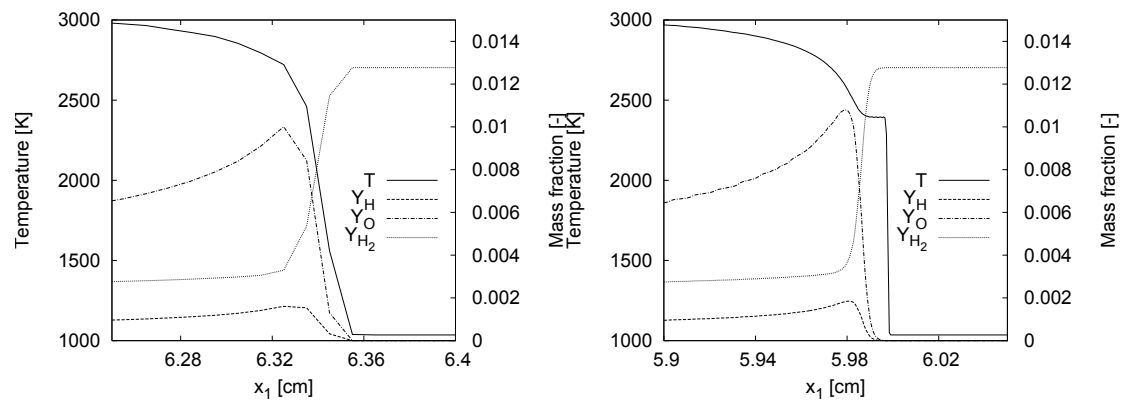
- [Quirk, 1994b]
- Test from [Deiterding, 2003]





# Detonations - motivation for SAMR

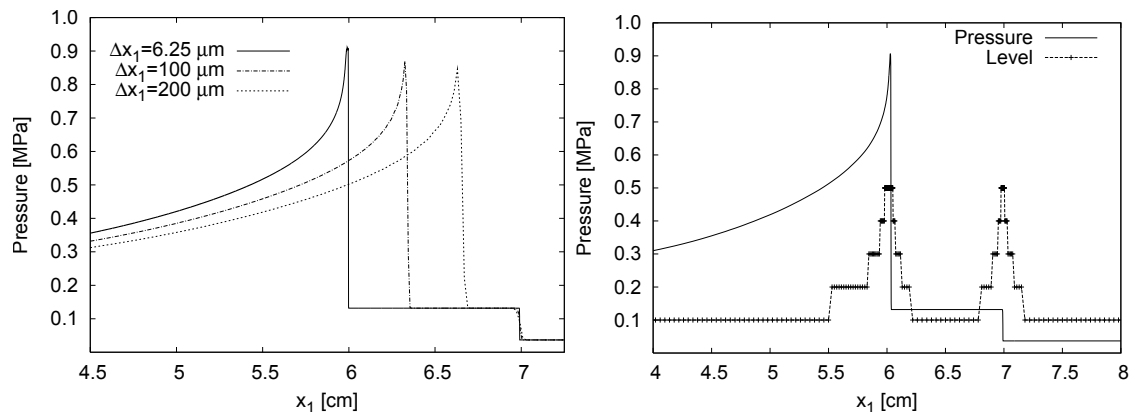
- ▶ Extremely high spatial resolution in reaction zone necessary.
- ▶ Minimal spatial resolution:  $7 - 8 \text{ Pts}/l_{ig} \rightarrow \Delta x_1 \approx 0.2 - 0.175 \text{ mm}$
- ▶ Uniform grids for typical geometries:  $> 10^7 \text{ Pts}$  in 2D,  $> 10^9 \text{ Pts}$  in 3D  $\rightarrow$  Self-adaptive finite volume method (AMR)



Approximation of  $\text{H}_2 : \text{O}_2$  detonation at  $\sim 1.5 \text{ Pts}/l_{ig}$  (left) and  $\sim 24 \text{ Pts}/l_{ig}$  (right)

# Detonation ignition in a shock tube

- ▶ Shock-induced detonation ignition of  $\text{H}_2 : \text{O}_2 : \text{Ar}$  mixture at molar ratios 2:1:7 in closed 1d shock tube
- ▶ Insufficient resolution leads to inaccurate results
- ▶ Reflected shock is captured correctly by FV scheme, detonation is resolution dependent
- ▶ Fine mesh necessary in the induction zone at the head of the detonation

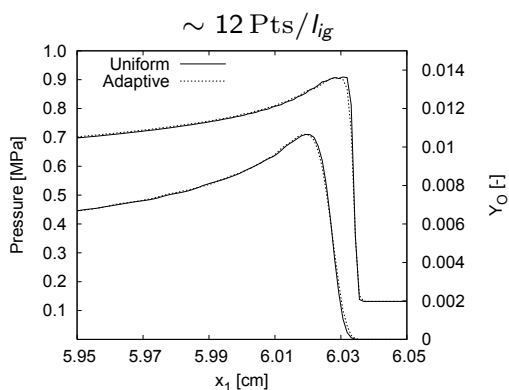


Left: Comparison of pressure distribution  $t = 170 \mu\text{s}$  after shock reflection. Right: Domains of refinement levels

# Detonation ignition in 1d - adaptive vs. uniform

Uniformly refined vs. dynamic adaptive simulations (Intel Xeon 3.4 GHz CPU)

$\Delta x_1 [\mu\text{m}]$	Uniform			Adaptive			
	Cells	$t_m [\mu\text{s}]$	Time [s]	$l_{max}$	$r_l$	$t_m [\mu\text{s}]$	Time [s]
400	300	166.1	31				
200	600	172.6	90	2	2	172.6	99
100	1200	175.5	277	3	2,2	175.8	167
50	2400	176.9	858	4	2,2,2	177.3	287
25	4800	177.8	2713	4	2,2,4	177.9	393
12.5	9600	178.3	9472	5	2,2,2,4	178.3	696
6.25	19200	178.6	35712	5	2,2,4,4	178.6	1370



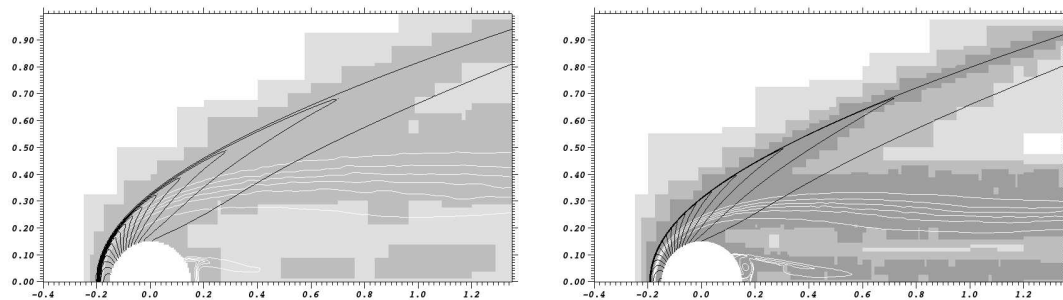
Refinement criteria:

$Y_i$	$S_{Y_i} \cdot 10^{-4}$	$\eta_{Y_i}^r \cdot 10^{-3}$
O <sub>2</sub>	10.0	2.0
H <sub>2</sub> O	7.8	8.0
H	0.16	5.0
O	1.0	5.0
OH	1.8	5.0
H <sub>2</sub>	1.3	2.0

$\epsilon_\rho = 0.07 \text{ kg m}^{-3}$ ,  $\epsilon_p = 50 \text{ kPa}$

# Shock-induced combustion around a sphere

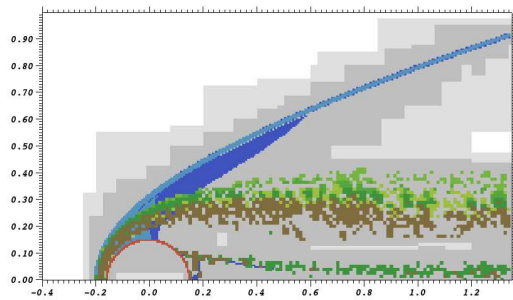
- ▶ Spherical projectile of radius 1.5 mm travels with constant velocity  $v_I = 2170.6 \text{ m/s}$  through  $\text{H}_2 : \text{O}_2 : \text{Ar}$  mixture (molar ratios 2:1:7) at 6.67 kPa and  $T = 298 \text{ K}$
- ▶ Cylindrical symmetric simulation on AMR base mesh of  $70 \times 40$  cells
- ▶ Comparison of 3-level computation with refinement factors 2,2 ( $\sim 5 \text{ Pts}/l_{ig}$ ) and a 4-level computation with refinement factors 2,2,4 ( $\sim 19 \text{ Pts}/l_{ig}$ ) at  $t = 350 \mu\text{s}$
- ▶ Higher resolved computation captures combustion zone visibly better and at slightly different position (see below)



Iso-contours of  $p$  (black) and  $Y_{\text{H}_2}$  (white) on refinement domains for 3-level (left) and 4-level computation (right)

# Combustion around a sphere - adaptation

Refinement indicators on  $l = 2$  at  $t = 350 \mu\text{s}$ .  
Blue:  $\epsilon_\rho$ , light blue:  $\epsilon_p$ , green shades:  $\eta_{Y_i}^r$ ,  
red: embedded boundary

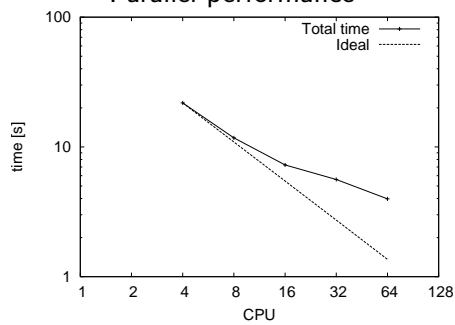


Refinement criteria:

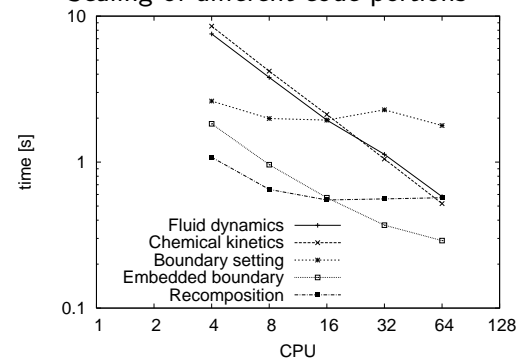
$Y_i$	$S_{Y_i} \cdot 10^{-4}$	$\eta_{Y_i}^r \cdot 10^{-4}$
O <sub>2</sub>	10.0	4.0
H <sub>2</sub> O	5.8	3.0
H	0.2	10.0
O	1.4	10.0
OH	2.3	10.0
H <sub>2</sub>	1.3	4.0

$$\epsilon_\rho = 0.02 \text{ kg m}^{-3}, \epsilon_p = 16 \text{ kPa}$$

Parallel performance



Scaling of different code portions

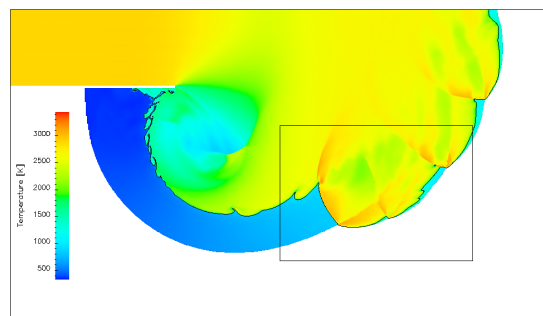


# Detonation diffraction

- ▶ CJ detonation for  
 $\text{H}_2 : \text{O}_2 : \text{Ar}/2 : 1 : 7$  at  
 $T_0 = 298 \text{ K}$  and  $p_0 = 10 \text{ kPa}$ .  
Cell width  $\lambda_c = 1.6 \text{ cm}$
- ▶ Adaption criteria (similar as before):
  1. Scaled gradients of  $\rho$  and  $p$
  2. Error estimation in  $Y_i$  by Richardson extrapolation
- ▶  $25 \text{ Pts}/l_{ig}$ . 5 refinement levels (2,2,2,4).
- ▶ Adaptive computations use up to  $\sim 2.2 \text{ M}$  instead of  $\sim 150 \text{ M}$  cells (uniform grid)
- ▶  $\sim 3850 \text{ h CPU}$  ( $\sim 80 \text{ h real time}$ ) on 48 nodes Athlon 1.4GHz

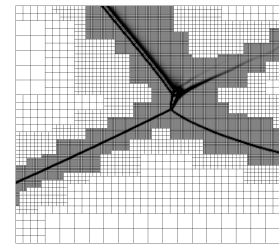
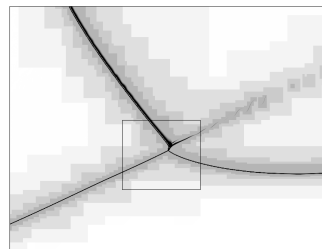
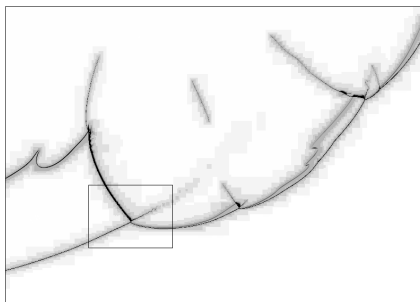
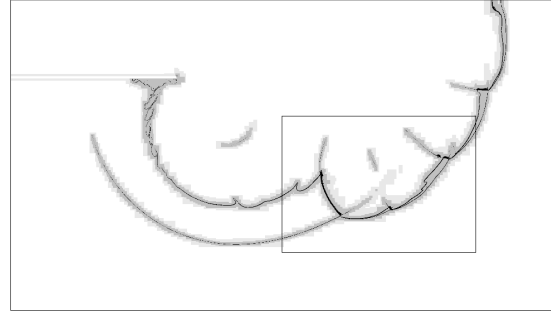
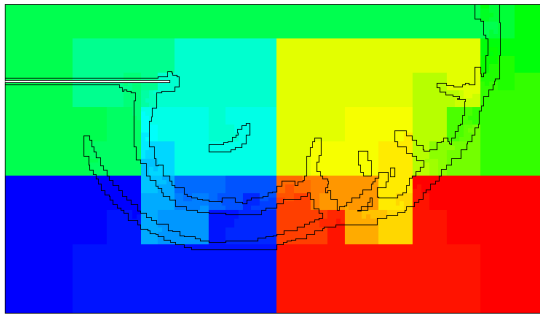


E. Schultz. *Detonation diffraction through an abrupt area expansion*. PhD thesis, California Institute of Technology, Pasadena, California, April 2000.



# Detonation diffraction - adaptation

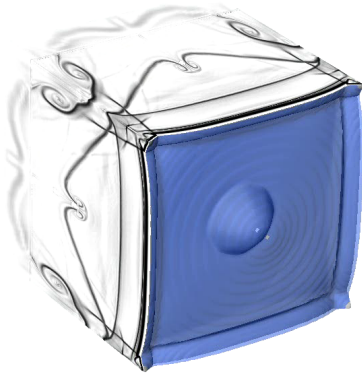
Final distribution to 48 nodes and density distribution on four refinement levels



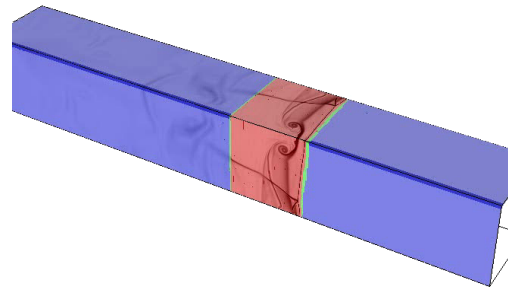
# Detonation cell structure in 3D

- ▶ Simulation of only one quadrant
- ▶  $44.8 \text{ Pts}/l_{ig}$  for  $\text{H}_2 : \text{O}_2 : \text{Ar}$  CJ detonation
- ▶ SAMR base grid  $400 \times 24 \times 24$ , 2 additional refinement levels (2, 4)
- ▶ Simulation uses  $\sim 18 \text{ M}$  cells instead of  $\sim 118 \text{ M}$  (unigrid)
- ▶  $\sim 51,000 \text{ h}$  CPU on 128 CPU Compaq Alpha.  
 $\mathcal{H}$ : 37.6 %,  $\mathcal{S}$ : 25.1 %

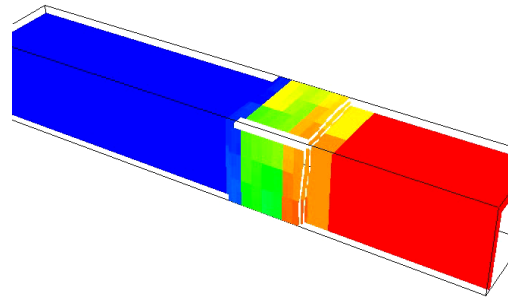
Schlieren and isosurface of  $Y_{\text{OH}}$



Schlieren on refinement levels



Distribution to 128 processors





# Outline

## Complex geometry

- Boundary aligned meshes
- Cartesian techniques
- Implicit geometry representation
- Accuracy / verification

## Combustion

- Equations and FV schemes
- Shock-induced combustion examples

## Fluid-structure interaction

- Coupling to a solid mechanics solver
- Rigid body motion
- Thin elastic structures
- Deforming thin structures

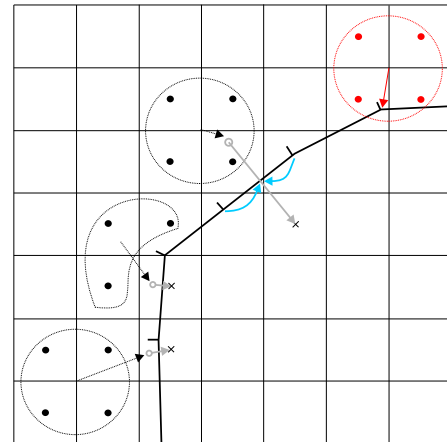
## Turbulence

- Large-eddy simulation

# Construction of coupling data

- ▶ Moving boundary/interface is treated as a moving contact discontinuity and represented by level set  
[Fedkiw, 2002][Arienti et al., 2003]
- ▶ One-sided construction of mirrored ghost cell and new FEM nodal point values
- ▶ FEM ansatz-function interpolation to obtain intermediate surface values
- ▶ Explicit coupling possible if geometry and velocities are prescribed for the more compressible medium  
[Specht, 2000]

$$\begin{aligned}
 u_n^F &:= u_n^S(t)|_{\mathcal{I}} \\
 \text{UpdateFluid}(\Delta t) \\
 \sigma_{nn}^S &:= p^F(t + \Delta t)|_{\mathcal{I}} \\
 \text{UpdateSolid}(\Delta t) \\
 t &:= t + \Delta t
 \end{aligned}$$



Coupling conditions on interface

$$\left. \begin{aligned}
 u_n^S &= u_n^F \\
 \sigma_{nn}^S &= p^F \\
 \sigma_{nm}^S &= 0
 \end{aligned} \right|_{\mathcal{I}}$$

# Usage of SAMR

- ▶ Eulerian SAMR + non-adaptive Lagrangian FEM scheme
- ▶ Exploit SAMR time step refinement for effective coupling to solid solver
  - ▶ Lagrangian simulation is called only at level  $l_c \leq l_{\max}$
  - ▶ SAMR refines solid boundary at least at level  $l_c$
  - ▶ Additional levels can be used resolve geometric ambiguities
- ▶ Nevertheless: Inserting sub-steps accommodates for time step reduction from the solid solver within an SAMR cycle
- ▶ Communication strategy:
  - ▶ Updated boundary info from solid solver must be received before regridding operation
  - ▶ Boundary data is sent to solid when highest level available
- ▶ Inter-solver communication (point-to-point or globally) managed on the fly special coupling module

# SAMR algorithm for FSI coupling

AdvanceLevel( $l$ )

Repeat  $r_l$  times

Set ghost cells of  $\mathbf{Q}'(t)$

CPT( $\varphi^l, C^l, \mathcal{I}, \delta_l$ )

If time to regrid?

Regrid( $l$ )

UpdateLevel( $l$ )

If level  $l+1$  exists?

Set ghost cells of  $\mathbf{Q}'(t + \Delta t_l)$

AdvanceLevel( $l+1$ )

Average  $\mathbf{Q}^{l+1}(t + \Delta t_l)$  onto  $\mathbf{Q}'(t + \Delta t_l)$

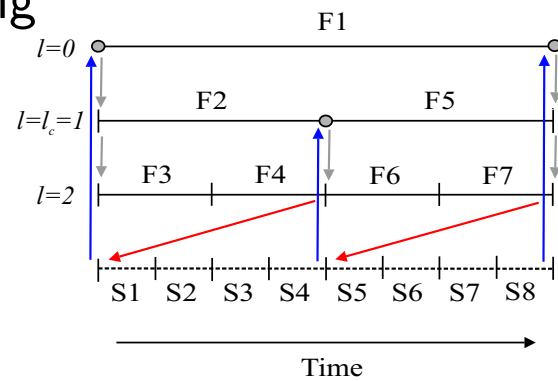
If  $l = l_c$ ?

SendInterfaceData( $p^F(t + \Delta t_l)|_{\mathcal{I}}$ )

If  $(t + \Delta t_l) < (t_0 + \Delta t_0)$ ?

ReceiveInterfaceData( $\mathcal{I}, \mathbf{u}^S|_{\mathcal{I}}$ )

$t := t + \Delta t_l$



- ▶ Call CPT algorithm before Regrid( $l$ )
- ▶ Include also call to CPT( $\cdot$ ) into Recompose( $l$ ) to ensure consistent level set data on levels that have changed
- ▶ Communicate boundary data on coupling level  $l_c$

# Fluid and solid update / exchange of time steps

FluidStep( )

$$\Delta\tau_F := \min_{l=0, \dots, l_{\max}} (R_l \cdot \text{StableFluidTimeStep}(l), \Delta\tau_S)$$

$$\Delta t_l := \Delta\tau_F / R_l \text{ for } l = 0, \dots, L$$

ReceiveInterfaceData( $\mathcal{I}$ ,  $\mathbf{u}^S|_{\mathcal{I}}$ )

AdvanceLevel(0)

SolidStep( )

$$\Delta\tau_S := \min(K \cdot R_{l_c} \cdot \text{StableSolidTimeStep}(), \Delta\tau_F)$$

Repeat  $R_{l_c}$  times

$$t_{\text{end}} := t + \Delta\tau_S / R_{l_c}, \quad \Delta t := \Delta\tau_S / (K R_{l_c})$$

While  $t < t_{\text{end}}$

    SendInterfaceData( $\mathcal{I}(t)$ ,  $\vec{u}^S|_{\mathcal{I}}(t)$ )

    ReceiveInterfaceData( $p^F|_{\mathcal{I}}$ )

    UpdateSolid( $p^F|_{\mathcal{I}}$ ,  $\Delta t$ )

$t := t + \Delta t$

$\Delta t := \min(\text{StableSolidTimeStep}(), t_{\text{end}} - t)$

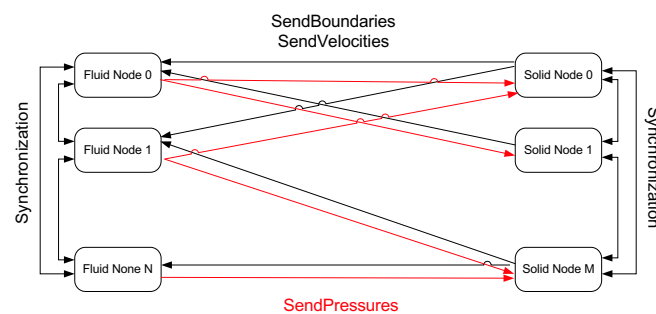
with  $R_l = \prod_{\iota=0}^l r_{\iota}$

- Time step stays constant for  $R_{l_c}$  steps, which corresponds to one fluid step at level 0

# Parallelization strategy for coupled simulations

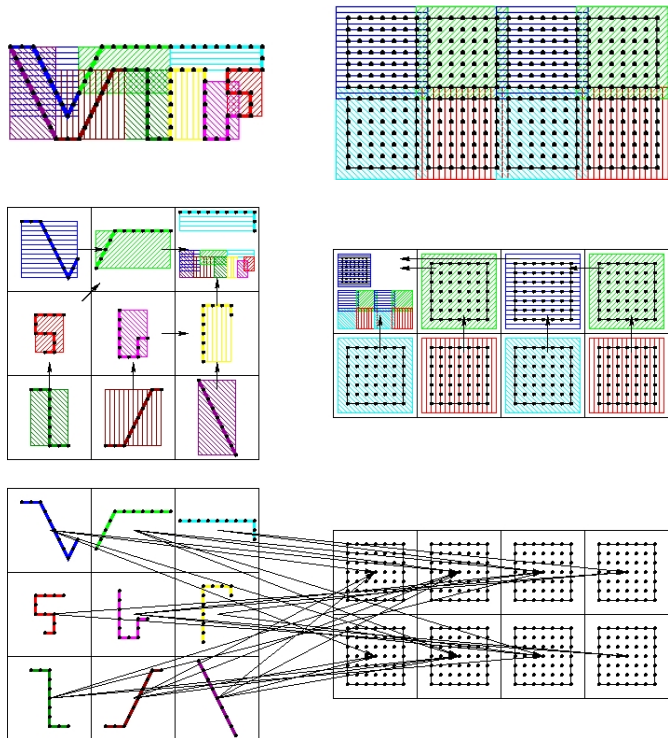
Coupling of an Eulerian FV fluid Solver and a Lagrangian FEM Solver:

- ▶ Distribute both meshes separately and copy necessary nodal values and geometry data to fluid nodes
- ▶ Setting of ghost cell values becomes strictly local operation
- ▶ Construct new nodal values strictly local on fluid nodes and transfer them back to solid nodes
- ▶ Only surface data is transferred
- ▶ Asynchronous communication ensures scalability
- ▶ Generic encapsulated implementation guarantees reusability



# Eulerian/Lagrangian communication module

1. Put bounding boxes around each solid processors piece of the boundary and around each fluid processors grid
2. Gather, exchange and broadcast of bounding box information
3. Optimal point-to-point communication pattern, non-blocking



# Lift-up of a spherical body

Cylindrical body hit by Mach 3 shockwave, 2D test case by [Falcovitz et al., 1997]

Schlieren plot of density



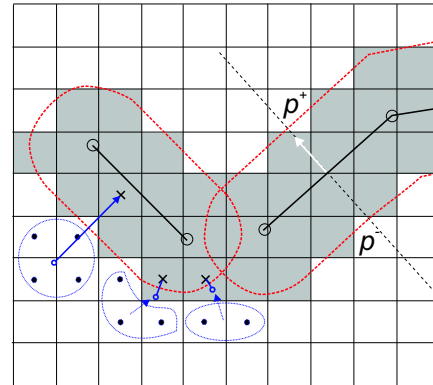
Refinement levels





# Treatment of thin structures

- ▶ Thin boundary structures or lower-dimensional shells require “thickening” to apply embedded boundary method
- ▶ Unsigned distance level set function  $\varphi$
- ▶ Treat cells with  $0 < \varphi < d$  as ghost fluid cells



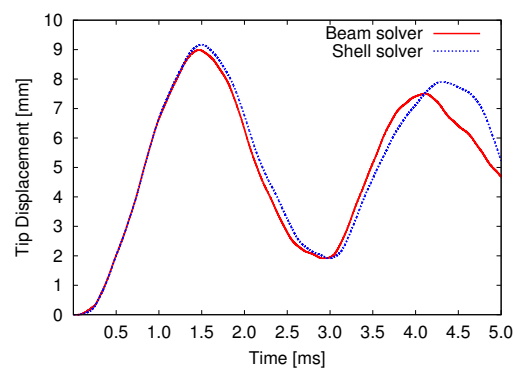
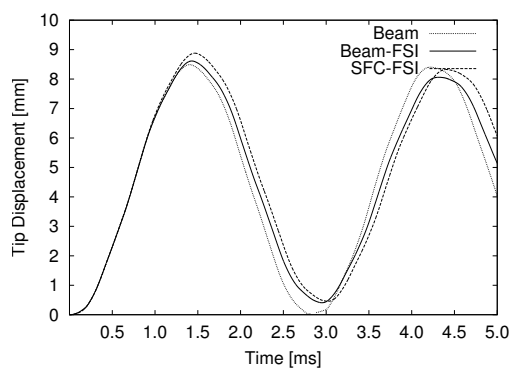
- ▶ Leaving  $\varphi$  unmodified ensures correctness of  $\nabla \varphi$
- ▶ Use face normal in shell element to evaluate in  $\Delta p = p^+ - p^-$
- ▶ Utilize finite difference solver using the beam equation

$$\rho_s h \frac{\partial^2 w}{\partial t^2} + EI \frac{\partial^4 w}{\partial \bar{x}^4} = p^F$$

to verify FSI algorithms

# FSI verification by elastic vibration

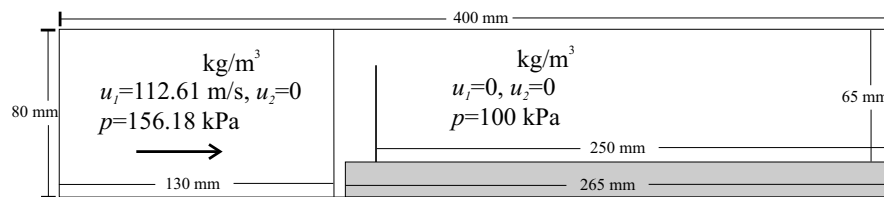
- ▶ Thin steel plate (thickness  $h = 1$  mm, length 50 mm), clamped at lower end
- ▶  $\rho_s = 7600 \text{ kg/m}^3$ ,  $E = 220 \text{ GPa}$ ,  $I = h^3/12$ ,  $\nu = 0.3$
- ▶ Modeled with beam solver (101 points) and thin-shell FEM solver (325 triangles) by F. Cirak
- ▶ Left: Coupling verification with constant instantaneous loading by  $\Delta p = 100 \text{ kPa}$
- ▶ Right: FSI verification with Mach 1.21 shockwave in air ( $\gamma = 1.4$ )



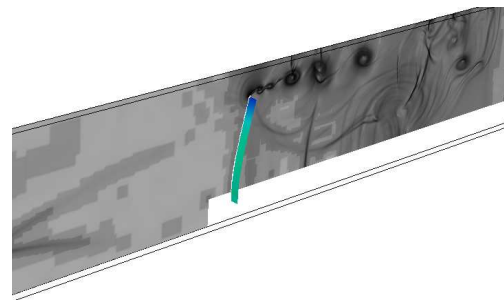
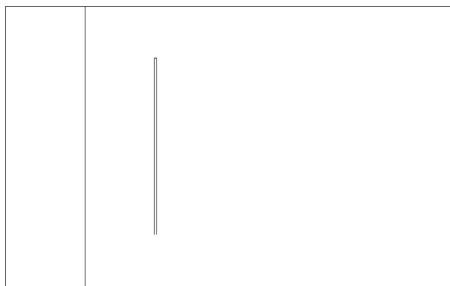
# Shock-driven elastic panel motion

Test case suggested by [Giordano et al., 2005]

- ▶ Forward facing step geometry, fixed walls everywhere except at inflow



- ▶ SAMR base mesh  $320 \times 64(\times 2)$ ,  $r_{1,2} = 2$
- ▶ Intel 3.4GHz Xeon dual processors, GB Ethernet interconnect
  - ▶ Beam-FSI: 12.25 h CPU on 3 fluid CPU + 1 solid CPU
  - ▶ FEM-FSI: 322 h CPU on 14 fluid CPU + 2 solid CPU



$t = 1.56$  ms after impact

# Detonation-driven plastic deformation

Chapman-Jouguet detonation in a tube filled with a stoichiometric ethylene and oxygen ( $C_2H_4 + 3 O_2$ , 295 K) mixture. Euler equations with single exothermic reaction  $A \rightarrow B$

$$\partial_t \rho + \partial_{x_n}(\rho u_n) = 0, \quad \partial_t(\rho u_k) + \partial_{x_n}(\rho u_k u_n + \delta_{kn} p) = 0, \quad k = 1, \dots, d$$

$$\partial_t(\rho E) + \partial_{x_n}(u_n(\rho E + p)) = 0, \quad \partial_t(Y \rho) + \partial_{x_n}(Y \rho u_n) = \psi$$

with

$$p = (\gamma - 1)(\rho E - \frac{1}{2} \rho u_n u_n - \rho Y q_0) \quad \text{and} \quad \psi = -k Y \rho \exp\left(\frac{-E_A \rho}{p}\right)$$

modeled with heuristic detonation model by [Mader, 1979]

$$V := \rho^{-1}, \quad V_0 := \rho_0^{-1}, \quad V_{CJ} := \rho_{CJ}^{-1}$$

$$Y' := 1 - (V - V_0)/(V_{CJ} - V_0)$$

If  $0 \leq Y' \leq 1$  and  $Y > 10^{-8}$  then

If  $Y < Y'$  and  $Y' < 0.9$  then  $Y' := 0$

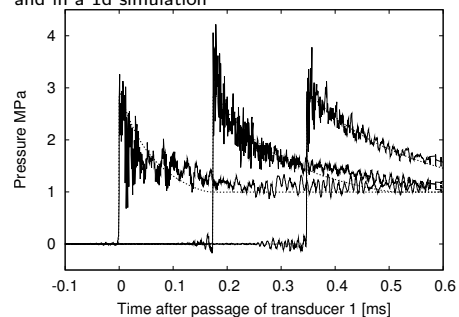
If  $Y' < 0.99$  then  $p' := (1 - Y') p_{CJ}$

else  $p' := p$

$$\rho_A := Y' \rho$$

$$E := p' / (\rho(\gamma - 1)) + Y' q_0 + \frac{1}{2} u_n u_n$$

Comparison of the pressure traces in the experiment and in a 1d simulation

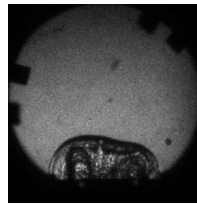


# Tube with flaps

- ▶ Fluid: VanLeer FVS
  - ▶ Detonation model with  $\gamma = 1.24$ ,  $p_{CJ} = 3.3$  MPa,  $D_{CJ} = 2376$  m/s
  - ▶ AMR base level:  $104 \times 80 \times 242$ ,  $r_{1,2} = 2$ ,  $r_3 = 4$
  - ▶  $\sim 4 \cdot 10^7$  cells instead of  $7.9 \cdot 10^9$  cells (uniform)
  - ▶ Tube and detonation fully refined
  - ▶ Thickening of 2D mesh: 0.81 mm on both sides (real 0.445 mm)
- ▶ Solid: thin-shell solver by F. Cirak
  - ▶ Aluminum, J2 plasticity with hardening, rate sensitivity, and thermal softening
  - ▶ Mesh: 8577 nodes, 17056 elements
- ▶ 16+2 nodes 2.2 GHz AMD Opteron quad processor, PCI-X 4x Infiniband network,  $\sim 4320$  h CPU to  $t_{end} = 450 \mu s$



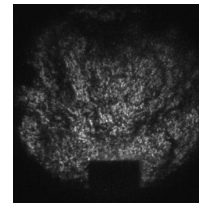
0.032 ms



0.030 ms

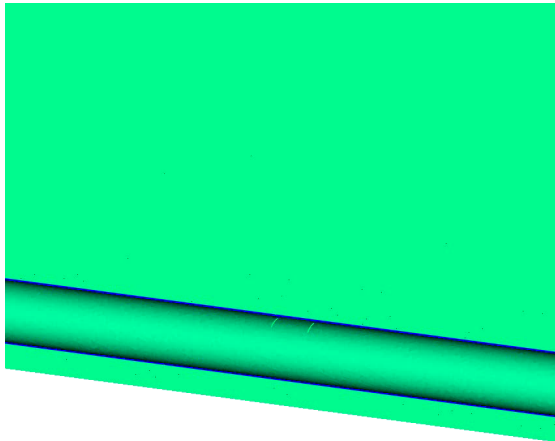


0.212 ms

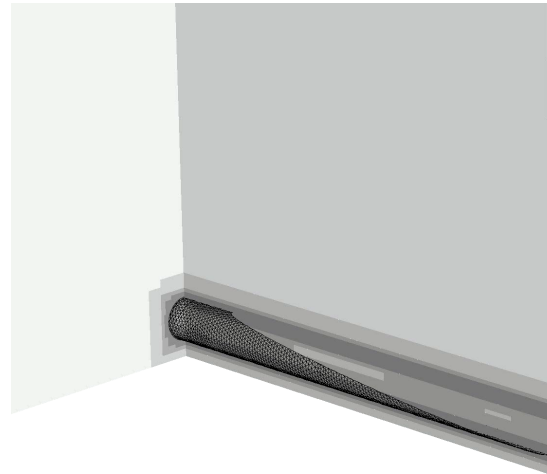


0.210 ms

## Tube with flaps: results



Fluid density and displacement in y-direction in solid



Schlieren plot of fluid density on refinement levels

[Cirak et al., 2007]

# Underwater explosion modeling

Volume fraction based two-component model with  $\sum_{i=1}^m \alpha^i = 1$ , that defines mixture quantities as

$$\rho = \sum_{i=1}^m \alpha^i \rho^i, \quad \rho u_n = \sum_{i=1}^m \alpha^i \rho^i u_n^i, \quad \rho e = \sum_{i=1}^m \alpha^i \rho^i e^i$$

Assuming total pressure  $p = (\gamma - 1) \rho e - \gamma p_\infty$  and speed of sound  $c = (\gamma(p + p_\infty)/\rho)^{1/2}$  yields

$$\frac{p}{\gamma - 1} = \sum_{i=1}^m \frac{\alpha^i p^i}{\gamma^i - 1}, \quad \frac{\gamma p_\infty}{\gamma - 1} = \sum_{i=1}^m \frac{\alpha^i \gamma^i p_\infty^i}{\gamma^i - 1}$$

and the overall set of equations [Shyue, 1998]

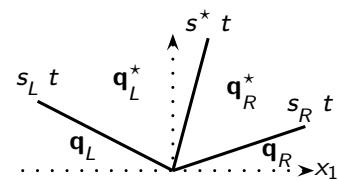
$$\partial_t \rho + \partial_{x_n}(\rho u_n) = 0, \quad \partial_t(\rho u_k) + \partial_{x_n}(\rho u_k u_n + \delta_{kn} p) = 0, \quad \partial_t(\rho E) + \partial_{x_n}(u_n(\rho E + p)) = 0$$

$$\frac{\partial}{\partial t} \left( \frac{1}{\gamma - 1} \right) + u_n \frac{\partial}{\partial x_n} \left( \frac{1}{\gamma - 1} \right) = 0, \quad \frac{\partial}{\partial t} \left( \frac{\gamma p_\infty}{\gamma - 1} \right) + u_n \frac{\partial}{\partial x_n} \left( \frac{\gamma p_\infty}{\gamma - 1} \right) = 0$$

Oscillation free at contacts: [Abgrall and Karni, 2001][Shyue, 2006]

# Approximate Riemann solver

Use HLLC approach because of robustness and positivity preservation

$$\mathbf{q}^{HLLC}(x_1, t) = \begin{cases} \mathbf{q}_L, & x_1 < s_L t, \\ \mathbf{q}_L^*, & s_L t \leq x_1 < s^* t, \\ \mathbf{q}_R^*, & s^* t \leq x_1 \leq s_R t, \\ \mathbf{q}_R, & x_1 > s_R t, \end{cases}$$


Wave speed estimates [Davis, 1988]  $s_L = \min\{u_{1,L} - c_L, u_{1,R} - c_R\}$ ,

$s_R = \max\{u_{1,L} + c_L, u_{1,R} + c_R\}$

Unknown state [Toro et al., 1994]

$$s^* = \frac{p_R - p_L + s_L u_{1,L}(s_L - u_{1,L}) - \rho_R u_{1,R}(s_R - u_{1,R})}{\rho_L(s_L - u_{1,L}) - \rho_R(s_R - u_{1,R})}$$

$$\mathbf{q}_\tau^* = \left[ \eta, \eta s^*, \eta u_2, \eta \left[ \frac{(\rho E)_\tau}{\rho_\tau} + (s^* - u_{1,\tau}) \left( s_\tau + \frac{p_\tau}{\rho_\tau(s_\tau - u_{1,\tau})} \right) \right], \frac{1}{\gamma_\tau - 1}, \frac{\gamma_\tau p_{\infty,\tau}}{\gamma_\tau - 1} \right]^T$$

$$\eta = \rho_\tau \frac{s_\tau - u_{1,\tau}}{s_\tau - s^*}, \quad \tau = \{L, R\}$$

Evaluate waves as  $\mathcal{W}_1 = \mathbf{q}_L^* - \mathbf{q}_L$ ,  $\mathcal{W}_2 = \mathbf{q}_R^* - \mathbf{q}_L^*$ ,  $\mathcal{W}_3 = \mathbf{q}_R - \mathbf{q}_R^*$  and  $\lambda_1 = s_L$ ,

$\lambda_2 = s^*$ ,  $\lambda_3 = s_R$  to compute the fluctuations  $\mathcal{A}^- \Delta = \sum_{\lambda_\nu < 0} \lambda_\nu \mathcal{W}_\nu$ ,

$\mathcal{A}^+ \Delta = \sum_{\lambda_\nu \geq 0} \lambda_\nu \mathcal{W}_\nu$  for  $\nu = \{1, 2, 3\}$

Overall scheme: Wave Propagation method [Shyue, 2006]



# Underwater explosion FSI simulations

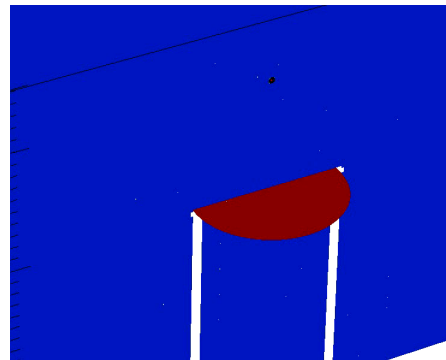
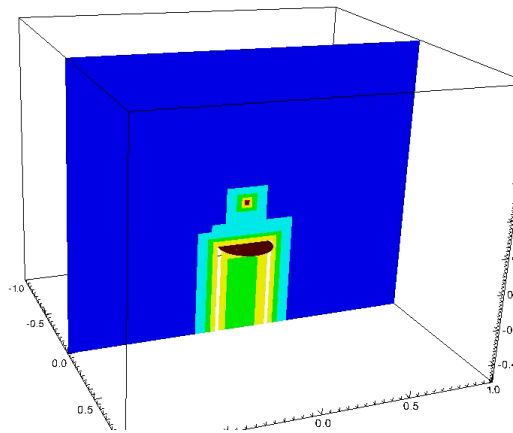
- ▶ Air:  $\gamma^A = 1.4$ ,  $p_\infty^A = 0$ ,  $\rho^A = 1.29 \text{ kg/m}^3$
- ▶ Water:  $\gamma^W = 7.415$ ,  $p_\infty^W = 296.2 \text{ MPa}$ ,  $\rho^W = 1027 \text{ kg/m}^3$
- ▶ Cavitation modeling with pressure cut-off model at  $p = -1 \text{ MPa}$
- ▶ 3D simulation of deformation of air backed aluminum plate with  $r = 85 \text{ mm}$ ,  $h = 3 \text{ mm}$  from underwater explosion
  - ▶ Water basin [Ashani and Ghamsari, 2008]  $2 \text{ m} \times 1.6 \text{ m} \times 2 \text{ m}$
  - ▶ Explosion modeled as energy increase ( $m_{C4} \cdot 6.06 \text{ MJ/kg}$ ) in sphere with  $r=5\text{mm}$
  - ▶  $\rho_s = 2719 \text{ kg/m}^3$ ,  $E = 69 \text{ GPa}$ ,  $\nu = 0.33$ , J2 plasticity model, yield stress  $\sigma_y = 217.6 \text{ MPa}$
- ▶ 3D simulation of copper plate  $r = 32 \text{ mm}$ ,  $h = 0.25 \text{ mm}$  rupturing due to water hammer
  - ▶ Water-filled shocktube  $1.3 \text{ m}$  with driver piston [Deshpande et al., 2006]
  - ▶ Piston simulated with separate level set, see [Deiterding et al., 2009] for pressure wave
  - ▶  $\rho_s = 8920 \text{ kg/m}^3$ ,  $E = 130 \text{ GPa}$ ,  $\nu = 0.31$ , J2 plasticity model,  $\sigma_y = 38.5 \text{ MPa}$ , cohesive interface model, max. tensile stress  $\sigma_c = 525 \text{ MPa}$

# Underwater explosion simulation

- ▶ AMR base grid  $50 \times 40 \times 50$ ,  $r_{1,2,3} = 2$ ,  $r_4 = 4$ ,  $l_c = 3$ , highest level restricted to initial explosion center, 3rd and 4th level to plate vicinity
- ▶ Triangular mesh with 8148 elements
- ▶ Computations of 1296 coupled time steps to  $t_{end} = 1$  ms
- ▶ 10+2 nodes 3.4 GHz Intel Xeon dual processor,  $\sim 130$  h CPU

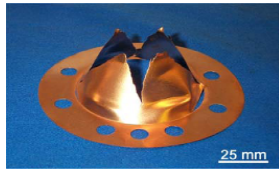
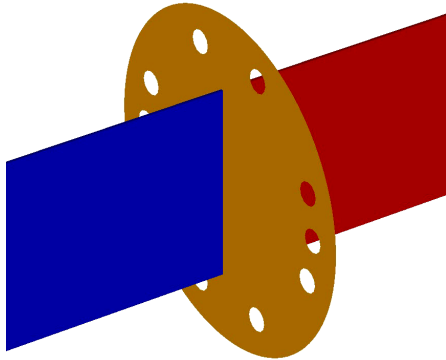
Maximal deflection [mm]

	Exp.	Sim.
20 g, $d = 25$ cm	28.83	25.88
30 g, $d = 30$ cm	30.09	27.31

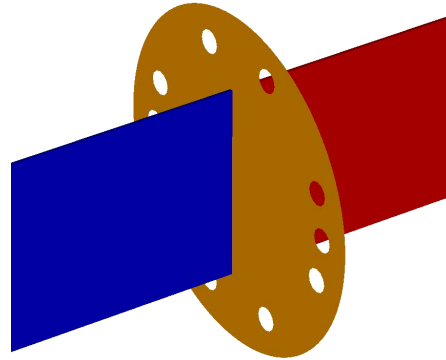


# Plate in underwater shocktube

- ▶ AMR base mesh  $374 \times 20 \times 20$ ,  $r_{1,2} = 2$ ,  $l_c = 2$ , solid mesh: 8896 triangles
- ▶  $\sim 1250$  coupled time steps to  $t_{end} = 1$  ms
- ▶ 6+6 nodes 3.4 GHz Intel Xeon dual processor,  $\sim 800$  h CPU



$p_0 = 64$  MPa



$p_0 = 173$  MPa

# Outline

## Complex geometry

- Boundary aligned meshes
- Cartesian techniques
- Implicit geometry representation
- Accuracy / verification

## Combustion

- Equations and FV schemes
- Shock-induced combustion examples

## Fluid-structure interaction

- Coupling to a solid mechanics solver
- Rigid body motion
- Thin elastic structures
- Deforming thin structures

## Turbulence

- Large-eddy simulation

# Favre-averaged Navier-Stokes equations

$$\begin{aligned}\frac{\partial \bar{\rho}}{\partial t} + \frac{\partial}{\partial x_n} (\bar{\rho} \tilde{u}_n) &= 0 \\ \frac{\partial}{\partial t} (\bar{\rho} \tilde{u}_k) + \frac{\partial}{\partial x_n} (\bar{\rho} \tilde{u}_k \tilde{u}_n + \delta_{kn} \bar{p} - \tilde{\tau}_{kn} + \sigma_{kn}) &= 0 \\ \frac{\partial \bar{\rho} \tilde{E}}{\partial t} + \frac{\partial}{\partial x_n} (\tilde{u}_n (\bar{\rho} \tilde{E} + \bar{p}) + \tilde{q}_n - \tilde{\tau}_{nj} \tilde{u}_j + \sigma_n^e) &= 0 \\ \frac{\partial}{\partial t} (\bar{\rho} \tilde{Y}_i) + \frac{\partial}{\partial x_n} (\bar{\rho} \tilde{Y}_i \tilde{u}_n + \tilde{J}_n^i + \sigma_n^i) &= 0\end{aligned}$$

with stress tensor

$$\tilde{\tau}_{kn} = \tilde{\mu} \left( \frac{\partial \tilde{u}_n}{\partial x_k} + \frac{\partial \tilde{u}_k}{\partial x_n} \right) - \frac{2}{3} \tilde{\mu} \frac{\partial \tilde{u}_j}{\partial x_j} \delta_{in} ,$$

heat conduction

$$\tilde{q}_n = -\tilde{\lambda} \frac{\partial \tilde{T}}{\partial x_n} ,$$

and inter-species diffusion

$$\tilde{J}_n^i = -\bar{\rho} \tilde{D}_i \frac{\partial \tilde{Y}_i}{\partial x_n}$$

Favre-filtering

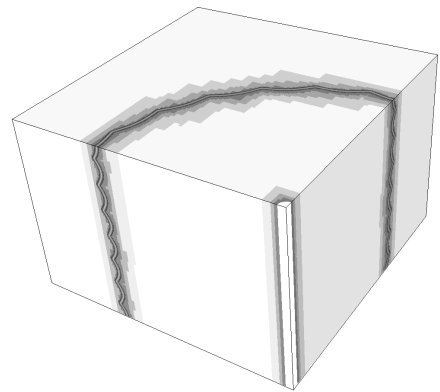
$$\tilde{\phi} = \frac{\overline{\rho \phi}}{\bar{\rho}} \quad \text{with} \quad \bar{\phi}(\mathbf{x}, t; \Delta_c) = \int_{\Omega} G(\mathbf{x} - \mathbf{x}'; \Delta_c) \phi(\mathbf{x}', t) d\mathbf{x}'$$

# Numerical solution approach

- ▶ Subgrid terms  $\sigma_{kn}$ ,  $\sigma_n^e$ ,  $\sigma_n^i$  are computed by Pullin's stretched-vortex model
- ▶ Cutoff  $\Delta_c$  is set to local SAMR resolution  $\Delta x_l$
- ▶ It remains to solve the Navier-Stokes equations in the hyperbolic regime
  - ▶ 3rd order WENO method (hybridized with a tuned centered difference stencil) for convection
  - ▶ 2nd order conservative centered differences for diffusion

Example: Cylindrical Richtmyer-Meshkov instability

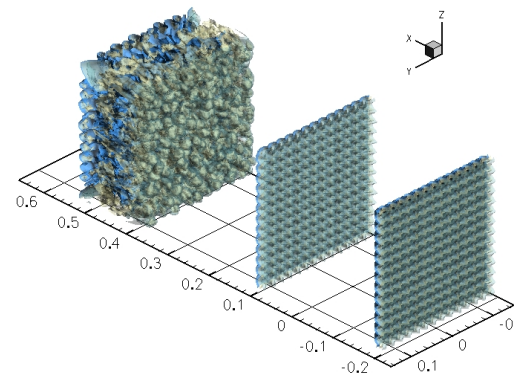
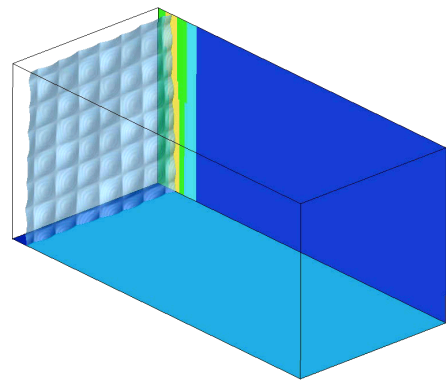
- ▶ Sinusoidal interface between two gases hit by shock wave
- ▶ Objective is correctly predict turbulent mixing
- ▶ Embedded boundary method used to regularize apex
- ▶ AMR base grid  $95 \times 95 \times 64$  cells,  $r_{1,2,3} = 2$
- ▶  $\sim 70,000$  h CPU on 32 AMD 2.5GHZ-quad-core nodes



# Planar Richtmyer-Meshkov instability

- ▶ Perturbed Air-SF6 interface shocked and re-shocked by Mach 1.5 shock
- ▶ Containment of turbulence in refined zones
- ▶ 96 CPUs IBM SP2-Power3
- ▶ WENO-TCD scheme with LES model
- ▶ AMR base grid  $172 \times 56 \times 56$ ,  $r_{1,2} = 2$ , 10 M cells in average instead of 3 M (uniform)

Task	2ms (%)	5ms (%)	10ms (%)
Integration	45.3	65.9	52.0
Boundary setting	44.3	28.6	41.9
Flux correction	7.2	3.4	4.1
Interpolation	0.9	0.4	0.3
Reorganization	1.6	1.2	1.2
Misc.	0.6	0.5	0.5
Max. imbalance	1.25	1.23	1.30



# Flux correction for Runge-Kutta method

Recall Runge-Kutta temporal update

$$\tilde{\mathbf{Q}}_j^v = \alpha_v \mathbf{Q}_j^n + \beta_v \tilde{\mathbf{Q}}_j^{v-1} + \gamma_v \frac{\Delta t}{\Delta x_k} \Delta \mathbf{F}^k(\tilde{\mathbf{Q}}^{v-1})$$

rewrite scheme as

$$\mathbf{Q}^{n+1} = \mathbf{Q}^n - \sum_{v=1}^{\Upsilon} \varphi_v \frac{\Delta t}{\Delta x_k} \Delta \mathbf{F}^k(\tilde{\mathbf{Q}}^{v-1}) \quad \text{with} \quad \varphi_v = \gamma_v \prod_{\nu=v+1}^{\Upsilon} \beta_\nu$$

Flux correction to be used [Pantano et al., 2007]

1.  $\delta \mathbf{F}_{i-\frac{1}{2},j}^{1,l+1} := -\varphi_1 \mathbf{F}_{i-\frac{1}{2},j}^{1,l}(\tilde{\mathbf{Q}}^0), \quad \delta \mathbf{F}_{i-\frac{1}{2},j}^{1,l+1} := \delta \mathbf{F}_{i-\frac{1}{2},j}^{1,l+1} - \sum_{v=2}^{\Upsilon} \varphi_v \mathbf{F}_{i-\frac{1}{2},j}^{1,l}(\tilde{\mathbf{Q}}^{v-1})$
2.  $\delta \mathbf{F}_{i-\frac{1}{2},j}^{1,l+1} := \delta \mathbf{F}_{i-\frac{1}{2},j}^{1,l+1} + \frac{1}{r_{l+1}^2} \sum_{m=0}^{r_{l+1}-1} \sum_{v=1}^{\Upsilon} \varphi_v \mathbf{F}_{v+\frac{1}{2},w+m}^{1,l+1} \left( \tilde{\mathbf{Q}}^{v-1}(t + \kappa \Delta t_{l+1}) \right)$

Storage-efficient SSPRK(3,3):

$v$	$\alpha_v$	$\beta_v$	$\gamma_v$	$\varphi_v$
1	1	0	1	$\frac{1}{6}$
2	$\frac{3}{4}$	$\frac{1}{4}$	$\frac{1}{4}$	$\frac{1}{6}$
3	$\frac{1}{2}$	$\frac{2}{3}$	$\frac{2}{3}$	$\frac{2}{3}$



# References I

- [Abgrall and Karni, 2001] Abgrall, R. and Karni, S. (2001). Computations of compressible multifluids. *J. Comput. Phys.*, 169:594–523.
- [Aftosmis, 1997] Aftosmis, M. J. (1997). Solution adaptive Cartesian grid methods for aerodynamic flows with complex geometries. Technical Report Lecture Series 1997-2, von Karman Institute for Fluid Dynamics.
- [Arienti et al., 2003] Arienti, M., Hung, P., Morano, E., and Shepherd, J. E. (2003). A level set approach to Eulerian-Lagrangian coupling. *J. Comput. Phys.*, 185:213–251.
- [Ashani and Ghamsari, 2008] Ashani, J. Z. and Ghamsari, A. K. (2008). Theoretical and experimental analysis of plastic response of isotropic circular plates subjected to underwater explosion loading. *Mat.-wiss. u. Werkstofftechn.*, 39(2):171–175.
- [Berger and Helzel, 2002] Berger, M. J. and Helzel, C. (2002). Grid aligned h-box methods for conservation laws in complex geometries. In *Proc. 3rd Intl. Symp. Finite Volumes for Complex Applications*, Porquerolles.
- [Cirak et al., 2007] Cirak, F., Deiterding, R., and Mauch, S. P. (2007). Large-scale fluid-structure interaction simulation of viscoplastic and fracturing thin shells subjected to shocks and detonations. *Computers & Structures*, 85(11-14):1049–1065.

## References II

- [Davis, 1988] Davis, S. F. (1988). Simplified second-order Godunov-type methods. *SIAM J. Sci. Stat. Comp.*, 9:445–473.
- [Deiterding, 2003] Deiterding, R. (2003). *Parallel adaptive simulation of multi-dimensional detonation structures*. PhD thesis, Brandenburgische Technische Universität Cottbus.
- [Deiterding et al., 2009] Deiterding, R., Cirak, F., and Mauch, S. P. (2009). Efficient fluid-structure interaction simulation of viscoplastic and fracturing thin-shells subjected to underwater shock loading. In Hartmann, S., Meister, A., Schäfer, M., and Turek, S., editors, *Int. Workshop on Fluid-Structure Interaction. Theory, Numerics and Applications, Herrsching am Ammersee 2008*, pages 65–80. kassel university press GmbH.
- [Deiterding et al., 2006] Deiterding, R., Radovitzky, R., Mauch, S. P., Noels, L., Cummings, J. C., and Meiron, D. I. (2006). A virtual test facility for the efficient simulation of solid materials under high energy shock-wave loading. *Engineering with Computers*, 22(3-4):325–347.
- [Deshpande et al., 2006] Deshpande, V. S., Heaver, A., and Fleck, N. A. (2006). An underwater shock simulator. *Royal Society of London Proceedings Series A*, 462(2067):1021–1041.

## References III

- [Falcovitz et al., 1997] Falcovitz, J., Alfandary, G., and Hanoch, G. (1997). A two-dimensional conservation laws scheme for compressible flows with moving boundaries. *J. Comput. Phys.*, 138:83–102.
- [Fedkiw, 2002] Fedkiw, R. P. (2002). Coupling an Eulerian fluid calculation to a Lagrangian solid calculation with the ghost fluid method. *J. Comput. Phys.*, 175:200–224.
- [Giordano et al., 2005] Giordano, J., Jourdan, G., Burtschell, Y., Medale, M., Zeitoun, D. E., and Houas, L. (2005). Shock wave impacts on deforming panel, an application of fluid-structure interaction. *Shock Waves*, 14(1-2):103–110.
- [Harten, 1983] Harten, A. (1983). High resolution schemes for hyperbolic conservation laws. *J. Comput. Phys.*, 49:357–393.
- [Harten and Hyman, 1983] Harten, A. and Hyman, J. M. (1983). Self adjusting grid methods for one-dimensional hyperbolic conservation laws. *J. Comput. Phys.*, 50:235–269.
- [Henshaw and Schwendeman, 2003] Henshaw, W. D. and Schwendeman, D. W. (2003). An adaptive numerical scheme for high-speed reactive flow on overlapping grids. *J. Comput. Phys.*, 191:420–447.

## References IV

- [Mader, 1979] Mader, C. L. (1979). *Numerical modeling of detonations*. University of California Press, Berkeley and Los Angeles, California.
- [Mauch, 2003] Mauch, S. P. (2003). *Efficient Algorithms for Solving Static Hamilton-Jacobi Equations*. PhD thesis, California Institute of Technology.
- [Meakin, 1995] Meakin, R. L. (1995). An efficient means of adaptive refinement within systems of overset grids. In *12th AIAA Computational Fluid Dynamics Conference, San Diego*, AIAA-95-1722-CP.
- [Mittal and Iaccarino, 2005] Mittal, R. and Iaccarino, G. (2005). Immersed boundary methods. *Annu. Rev. Fluid Mech.*, 37:239–261.
- [Murman et al., 2003] Murman, S. M., Aftosmis, M. J., and Berger, M. J. (2003). Implicit approaches for moving boundaries in a 3-d Cartesian method. In *41st AIAA Aerospace Science Meeting*, AIAA 2003-1119.
- [Nourgaliev et al., 2003] Nourgaliev, R. R., Dinh, T. N., and Theofanis, T. G. (2003). On capturing of interfaces in multimaterial compressible flows using a level-set-based Cartesian grid method. Technical Report 05/03-1, Center for Risk Studies and Safety, UC Santa Barbara.

# References V

- [Pantano et al., 2007] Pantano, C., Deiterding, R., Hill, D. J., and Pullin, D. I. (2007). A low-numerical dissipation patch-based adaptive mesh refinement method for large-eddy simulation of compressible flows. *J. Comput. Phys.*, 221(1):63–87.
- [Pember et al., 1999] Pember, R. B., Bell, J. B., Colella, P., Crutchfield, W. Y., and Welcome, M. L. (1999). An adaptive Cartesian grid method for unsteady compressible flows in irregular regions. *J. Comput. Phys.*, 120:287–304.
- [Quirk, 1994a] Quirk, J. J. (1994a). An alternative to unstructured grids for computing gas dynamics flows around arbitrarily complex two-dimensional bodies. *Computers Fluids*, 23:125–142.
- [Quirk, 1994b] Quirk, J. J. (1994b). A contribution to the great Riemann solver debate. *Int. J. Numer. Meth. Fluids*, 18:555–574.
- [Roma et al., 1999] Roma, A. M., Perskin, C. S., and Berger, M. J. (1999). An adaptive version of the immersed boundary method. *J. Comput. Phys.*, 153:509–534.
- [Sanders et al., 1998] Sanders, R., Morano, E., and Druguett, M.-C. (1998). Multidimensional dissipation for upwind schemes: Stability and applications to gas dynamics. *J. Comput. Phys.*, 145:511–537.

## References VI

- [Sethian, 1999] Sethian, J. A. (1999). *Level set methods and fast marching methods*. Cambridge University Press, Cambridge, New York.
- [Shyue, 1998] Shyue, K.-M. (1998). An efficient shock-capturing algorithm for compressible multicomponent problems. *J. Comput. Phys.*, 142:208–242.
- [Shyue, 2006] Shyue, K.-M. (2006). A volume-fraction based algorithm for hybrid barotropic and non-barotropic two-fluid flow problems. *Shock Waves*, 15:407–423.
- [Specht, 2000] Specht, U. (2000). *Numerische Simulation mechanischer Wellen an Fluid-Festkörper-Mediengrenzen*. Number 398 in VDI Reihe 7. VDU Verlag, Düsseldorf.
- [Toro et al., 1994] Toro, E. F., Spruce, M., and Speares, W. (1994). Restoration of the contact surface in the HLL-Riemann solver. *Shock Waves*, 4:25–34.
- [Tseng and Ferziger, 2003] Tseng, Y.-H. and Ferziger, J. H. (2003). A ghost-cell immersed boundary method for flow in complex geometry. *J. Comput. Phys.*, 192:593–623.
- [Yamaleev and Carpenter, 2002] Yamaleev, N. K. and Carpenter, M. H. (2002). On accuracy of adaptive grid methods for captured shocks. *J. Comput. Phys.*, 181:280–316.

# Lecture 4a

## Using the SAMR approach for elliptic and parabolic problems

Course *Block-structured Adaptive Mesh Refinement Methods for Conservation Laws*  
*Theory, Implementation and Application*

Ralf Deiterding

Computer Science and Mathematics Division  
Oak Ridge National Laboratory  
P.O. Box 2008 MS6367, Oak Ridge, TN 37831, USA

E-mail: [deiterdingr@ornl.gov](mailto:deiterdingr@ornl.gov)

# Outline

## Adaptive geometric multigrid methods

- Linear iterative methods for Poisson-type problems

- Multi-level algorithms

- Multigrid algorithms on SAMR data structures

- Example

## Comments on parabolic problems



# Poisson equation

$$\begin{aligned}\Delta q(\mathbf{x}) &= \psi(\mathbf{x}), \quad \mathbf{x} \in \Omega \subset \mathbb{R}^d, \quad q \in C^2(\Omega), \quad \psi \in C^0(\Omega) \\ q &= \psi^\Gamma(\mathbf{x}), \quad \mathbf{x} \in \partial\Omega\end{aligned}$$

Discrete Poisson equation in 2D:

$$\frac{Q_{j+1,k} - 2Q_{jk} + Q_{j-1,k}}{\Delta x_1^2} + \frac{Q_{j,k+1} - 2Q_{jk} + Q_{j,k-1}}{\Delta x_2^2} = \psi_{jk}$$

Operator

$$\mathcal{A}(Q_{\Delta x_1, \Delta x_2}) = \begin{bmatrix} \frac{1}{\Delta x_1^2} & -\left(\frac{2}{\Delta x_1^2} + \frac{2}{\Delta x_2^2}\right) & \frac{1}{\Delta x_2^2} \\ \frac{1}{\Delta x_2^2} & -\left(\frac{2}{\Delta x_1^2} + \frac{2}{\Delta x_2^2}\right) & \frac{1}{\Delta x_1^2} \end{bmatrix} Q(x_{1,j}, x_{2,k}) = \psi_{jk}$$

$$Q_{jk} = \frac{1}{\sigma} \left[ (Q_{j+1,k} + Q_{j-1,k})\Delta x_2^2 + (Q_{j,k+1} + Q_{j,k-1})\Delta x_1^2 - \Delta x_1^2 \Delta x_2^2 \psi_{jk} \right]$$

$$\text{with } \sigma = \frac{2\Delta x_1^2 + 2\Delta x_2^2}{\Delta x_1^2 \Delta x_2^2}$$

# Iterative methods

Jacobi iteration

$$Q_{jk}^{m+1} = \frac{1}{\sigma} \left[ (Q_{j+1,k}^m + Q_{j-1,k}^m) \Delta x_2^2 + (Q_{j,k+1}^m + Q_{j,k-1}^m) \Delta x_1^2 - \Delta x_1^2 \Delta x_2^2 \psi_{jk} \right]$$

Lexicographical Gauss-Seidel iteration (use updated values when they become available)

$$Q_{jk}^{m+1} = \frac{1}{\sigma} \left[ (Q_{j+1,k}^m + Q_{j-1,k}^{m+1}) \Delta x_2^2 + (Q_{j,k+1}^m + Q_{j,k-1}^{m+1}) \Delta x_1^2 - \Delta x_1^2 \Delta x_2^2 \psi_{jk} \right]$$

Efficient parallelization / patch-wise application not possible!

Checker-board or Red-Black Gauss Seidel iteration

1.  $Q_{jk}^{m+1} = \frac{1}{\sigma} \left[ (Q_{j+1,k}^m + Q_{j-1,k}^m) \Delta x_2^2 + (Q_{j,k+1}^m + Q_{j,k-1}^m) \Delta x_1^2 - \Delta x_1^2 \Delta x_2^2 \psi_{jk} \right]$   
for  $j + k \bmod 2 = 0$
2.  $Q_{jk}^{m+1} = \frac{1}{\sigma} \left[ (Q_{j+1,k}^{m+1} + Q_{j-1,k}^{m+1}) \Delta x_2^2 + (Q_{j,k+1}^{m+1} + Q_{j,k-1}^{m+1}) \Delta x_1^2 - \Delta x_1^2 \Delta x_2^2 \psi_{jk} \right]$   
for  $j + k \bmod 2 = 1$

Gauss-Seidel methods require  $\sim 1/2$  of iterations than Jacobi method, however, iteration count still proportional to number of unknowns [Hackbusch, 1994]

# Smoothing vs. solving

$\nu$  iterations with iterative linear solver

$$Q^{m+\nu} = \mathcal{S}(Q^m, \psi, \nu)$$

Defect after  $m$  iterations

$$d^m = \psi - \mathcal{A}(Q^m)$$

Defect after  $m + \nu$  iterations

$$d^{m+\nu} = \psi - \mathcal{A}(Q^{m+\nu}) = \psi - \mathcal{A}(Q^m + v_\nu^m) = d^m - \mathcal{A}(v_\nu^m)$$

with correction

$$v_\nu^m = \mathcal{S}(\vec{0}, d^m, \nu)$$

Neglecting the sub-iterations in the smoother we write

$$Q^{n+1} = Q^n + v = Q^n + \mathcal{S}(d^n)$$

Observation: Oscillations are damped faster on coarser grid.

Coarse grid correction:

$$Q^{n+1} = Q^n + v = Q^n + \mathcal{P}\mathcal{SR}(d^n)$$

where  $\mathcal{R}$  is suitable restriction operator and  $\mathcal{P}$  a suitable prolongation operator

# Two-grid correction method

Relaxation on current grid:

$$\bar{Q} = \mathcal{S}(Q^n, \psi, \nu)$$

$$Q^{n+1} = \bar{Q} + \mathcal{PS}(\vec{0}, \cdot, \mu) \mathcal{R}(\psi - \mathcal{A}(\bar{Q}))$$

Algorithm:

$$\bar{Q} := \mathcal{S}(Q^n, \psi, \nu)$$

$$d := \psi - \mathcal{A}(\bar{Q})$$

$$d_c := \mathcal{R}(d)$$

$$v_c := \mathcal{S}(0, d_c, \mu)$$

$$v := \mathcal{P}(v_c)$$

$$Q^{n+1} := \bar{Q} + v$$

with smoothing:

$$d := \psi - \mathcal{A}(Q)$$

$$v := \mathcal{S}(0, d, \nu)$$

$$r := d - \mathcal{A}(v)$$

$$d_c := \mathcal{R}(r)$$

$$v_c := \mathcal{S}(0, d_c, \mu)$$

$$v := v + \mathcal{P}(v_c)$$

$$Q^{n+1} := Q + v$$

with pre- and post-iteration:

$$d := \psi - \mathcal{A}(Q)$$

$$v := \mathcal{S}(0, d, \nu_1)$$

$$r := d - \mathcal{A}(v)$$

$$d_c := \mathcal{R}(r)$$

$$v_c := \mathcal{S}(0, d_c, \mu)$$

$$v := v + \mathcal{P}(v_c)$$

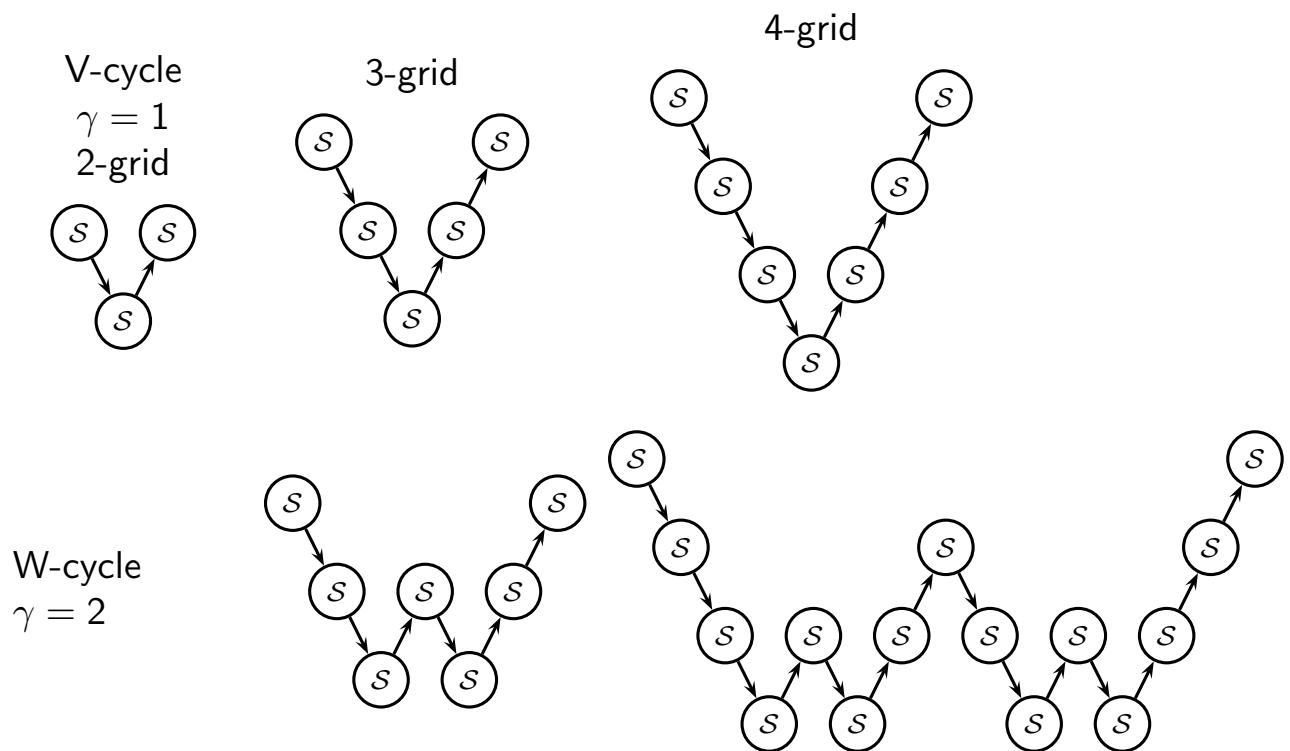
$$d := d - \mathcal{A}(v)$$

$$r := \mathcal{S}(0, d, \nu_2)$$

$$Q^{n+1} := Q + v + r$$

[Hackbusch, 1985]

# Multi-level methods and cycles



[Hackbusch, 1985] [Wesseling, 1992] ...

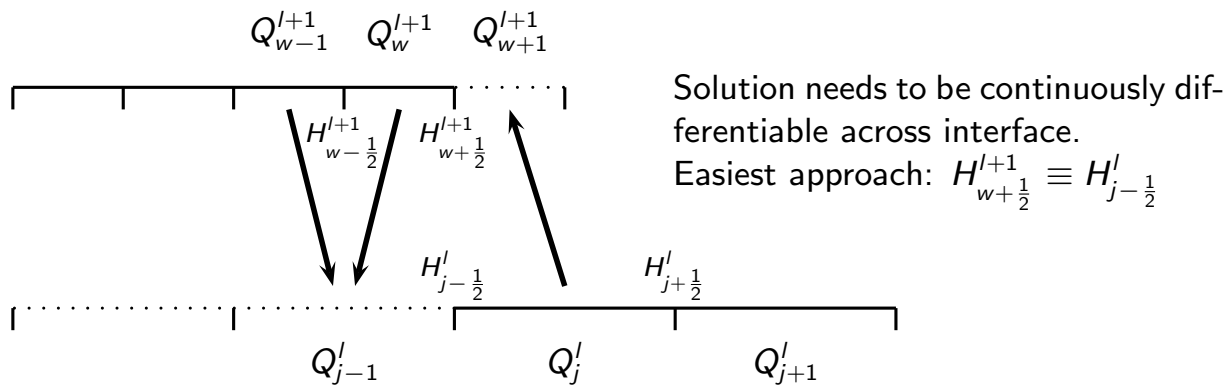
# Stencil modification at coarse-fine boundaries in 1D

1D Example: Cell  $j$ ,  $\psi - \nabla \cdot \nabla q = 0$

$$d_j^l = \psi_j - \frac{1}{\Delta x_l} \left( \frac{1}{\Delta x_l} (Q_{j+1}^l - Q_j^l) - \frac{1}{\Delta x_l} (Q_j^l - Q_{j-1}^l) \right) = \psi_j - \frac{1}{\Delta x_l} \left( H_{j+\frac{1}{2}}^l - H_{j-\frac{1}{2}}^l \right)$$

$H$  is approximation to derivative of  $Q^l$ .

Consider 2-level situation with  $r_{l+1} = 2$ :



No specific modification necessary for 1D vertex-based stencils, cf.  
[Bastian, 1996]

# Stencil modification at coarse-fine boundaries in 1D II

Set  $H_{w+\frac{1}{2}}^{l+1} = H_{\mathcal{I}}$ . Inserting  $Q$  gives

$$\frac{Q_{w+1}^{l+1} - Q_w^{l+1}}{\Delta x_{l+1}} = \frac{Q_j^l - Q_w^{l+1}}{\frac{3}{2}\Delta x_{l+1}}$$

from which we readily derive

$$Q_{w+1}^{l+1} = \frac{2}{3}Q_j^l + \frac{1}{3}Q_w^{l+1}$$

for the boundary cell on  $l+1$ . We use the flux correction procedure to enforce  $H_{w+\frac{1}{2}}^{l+1} \equiv H_{j-\frac{1}{2}}^l$  and thereby  $H_{j-\frac{1}{2}}^l \equiv H_{\mathcal{I}}$ .

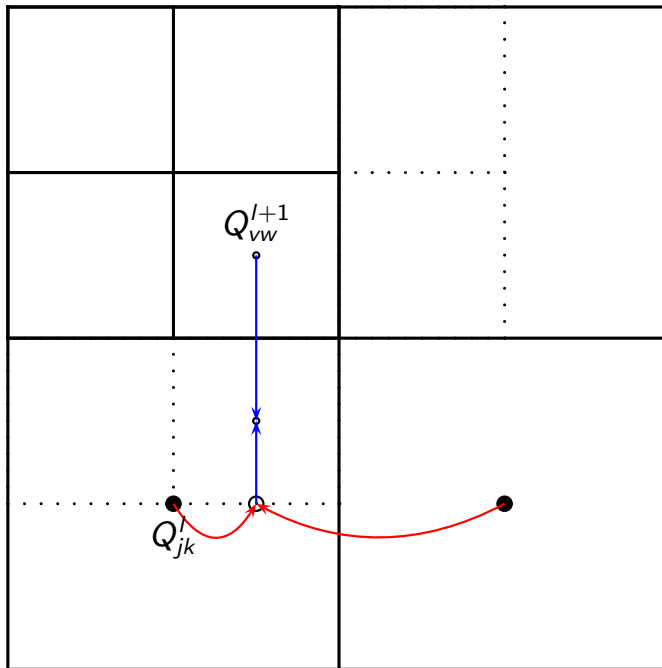
Correction pass [Martin, 1998]

1.  $\delta H_{j-\frac{1}{2}}^{l+1} := -H_{j-\frac{1}{2}}^l$
2.  $\delta H_{j-\frac{1}{2}}^{l+1} := \delta H_{j-\frac{1}{2}}^{l+1} + H_{w+\frac{1}{2}}^{l+1} = -H_{j-\frac{1}{2}}^l + (Q_j^l - Q_w^{l+1})/\frac{3}{2}\Delta x_{l+1}$
3.  $\check{d}_j^l := d_j^l + \frac{1}{\Delta x_l} \delta H_{j-\frac{1}{2}}^{l+1}$

yields

$$\check{d}_j^l = \psi_j - \frac{1}{\Delta x_l} \left( \frac{1}{\Delta x_l} (Q_{j+1}^l - Q_j^l) - \frac{2}{3\Delta x_{l+1}} (Q_j^l - Q_w^{l+1}) \right)$$

# Stencil modification at coarse-fine boundaries: 2D



$$Q_{v,w-1}^{l+1} = \frac{1}{3} Q_{vw}^{l+1} + \frac{2}{3} \left( \frac{3}{4} Q_{jk}^l + \frac{1}{4} Q_{j+1,k}^l \right)$$

In general:

$$Q_{v,w-1}^{l+1} = \left( 1 - \frac{2}{r_{l+1} + 1} \right) Q_{vw}^{l+1} + \frac{2}{r_{l+1} + 1} \left( (1-f) Q_{jk}^l + f Q_{j+1,k}^l \right)$$

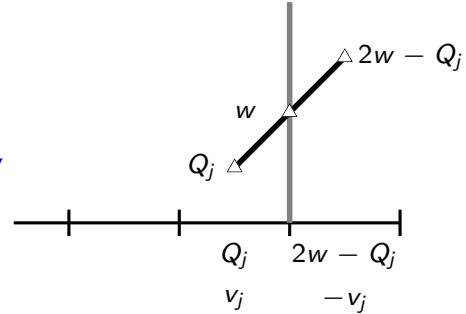
with

$$f = \frac{x_{1,l+1}^v - x_{1,l}^j}{\Delta x_{1,l}}$$



# Components of an SAMR multigrid method

- ▶ Stencil operators
  - ▶ Application of defect  $d^l = \psi^l - \mathcal{A}(Q^l)$  on each grid  $G_{l,m}$  of level  $l$
  - ▶ Computation of correction  $v^l = \mathcal{S}(0, d^l, \nu)$  on each grid of level  $l$
- ▶ Boundary (ghost cell) operators
  - ▶ Synchronization of  $Q^l$  and  $v^l$  on  $\tilde{S}_l^1$
  - ▶ Specification of Dirichlet boundary conditions for a finite volume discretization for  $Q^l \equiv w$  and  $v^l \equiv w$  on  $\tilde{P}_l^1$
  - ▶ Specification of  $v^l \equiv 0$  on  $\tilde{I}_l^1$
  - ▶ Specification of  $Q_l = \frac{(r_l-1)Q^{l+1} + 2Q^l}{r_l+1}$  on  $\tilde{I}_l^1$
- ▶ Coarse-fine boundary flux accumulation and application of  $\delta H^{l+1}$  on defect  $d^l$
- ▶ Standard prolongation and restriction on grids between adjacent levels
- ▶ Adaptation criteria
  - ▶ E.g., standard restriction to project solution on 2x coarsened grid, then use local error estimation
- ▶ Looping instead of time steps and check of convergence



# Additive geometric multigrid algorithm

AdvanceLevelMG( $l$ ) - Correction Scheme

Set ghost cells of  $Q^l$

Calculate defect  $d^l$  from  $Q^l, \psi^l$

$$d^l := \psi^l - \mathcal{A}(Q^l)$$

If ( $l < l_{\max}$ )

    Calculate updated defect  $r^{l+1}$  from  $v^{l+1}, d^{l+1}$

$$r^{l+1} := d^{l+1} - \mathcal{A}(v^{l+1})$$

    Restrict  $d^{l+1}$  onto  $d^l$

$$d^l := \mathcal{R}_l^{l+1}(r^{l+1})$$

Do  $\nu_1$  smoothing steps to get correction  $v^l$

$$v^l := \mathcal{S}(0, d^l, \nu_1)$$

If ( $l > l_{\min}$ )

    Do  $\gamma > 1$  times

        AdvanceLevelMG( $l - 1$ )

    Set ghost cells of  $v^{l-1}$

    Prolongate and add  $v^{l-1}$  to  $v^l$

$$v^l := v^l + \mathcal{P}_l^{l-1}(v^{l-1})$$

    If ( $\nu_2 > 0$ )

        Set ghost cells of  $v^l$

        Update defect  $d^l$  according to  $v^l$

$$d^l := d^l - \mathcal{A}(v^l)$$

        Do  $\nu_2$  post-smoothing steps to get  $r^l$

$$r^l := \mathcal{S}(v^l, d^l, \nu_2)$$

        Add additional correction  $r^l$  to  $v^l$

$$v^l := v^l + r^l$$

Add correction  $v^l$  to  $Q^l$

$$Q^l := Q^l + v^l$$

# Additive Geometric Multiplicative Multigrid Algorithm

Start - Start iteration on level  $l_{max}$

```
For  $l = l_{max}$  Downto  $l_{min} + 1$  Do
    Restrict  $Q^l$  onto  $Q^{l-1}$ 
    Regrid(0)
    AdvanceLevelMG( $l_{max}$ )
```

See also: [Trottenberg et al., 2001], [Canu and Ritzdorf, 1994]

Vertex-based: [Brandt, 1977], [Briggs et al., 2001]

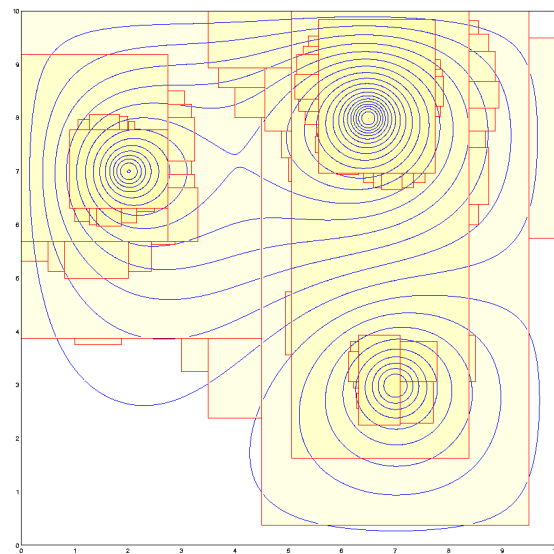
# Example

On  $\Omega = [0, 10] \times [0, 10]$  use hat function

$$\psi = \begin{cases} -A_n \cos\left(\frac{\pi r}{2R_n}\right), & r < R_n \\ 0 & \text{elsewhere} \end{cases}$$

with  $r = \sqrt{(x_1 - X_n)^2 + (x_2 - Y_n)^2}$   
to define three sources with

n	$A_n$	$R_n$	$X_n$	$Y_n$
1	0.3	0.3	6.5	8.0
2	0.2	0.3	2.0	7.0
3	-0.1	0.4	7.0	3.0



	$128 \times 128$	$1024 \times 1024$	$1024 \times 1024$
$l_{max}$	3	0	0
$l_{min}$	-4	-7	-4
$\nu_1$	5	5	5
$\nu_2$	5	5	5
V-Cycles	15	16	341
Time [sec]	9.4	27.7	563

Stop at  $\|d^l\|_{max} < 10^{-7}$  for  $l \geq 0$ ,  $\gamma = 1$ ,  $r_l = 2$

## Some comments on parabolic problems

- ▶ Consequences of time step refinement
- ▶ Level-wise elliptic solves vs. global solve
- ▶ If time step refinement is used an elliptic flux correction is unavoidable.
- ▶ The correction is explained in Bell, J. (2004). Block-structured adaptive mesh refinement. Lecture 2. Available at <https://ccse.lbl.gov/people/jbb/shortcourse/lecture2.pdf>.

# References I

- [Bastian, 1996] Bastian, P. (1996). *Parallele adaptive Mehrgitterverfahren*. Teubner Skripten zur Numerik. B. G. Teubner, Stuttgart.
- [Brandt, 1977] Brandt, A. (1977). Multi-level adaptive solutions to boundary-value problems. *Mathematics of Computations*, 31(183):333–390.
- [Briggs et al., 2001] Briggs, W. L., Henson, V. E., and McCormick, S. F. (2001). *A Multigrid Tutorial*. Society for Industrial and Applied Mathematics, 2nd edition.
- [Canu and Ritzdorf, 1994] Canu, J. and Ritzdorf, H. (1994). Adaptive, block-structured multigrid on local memory machines. In Hackbusch, W. and Wittum, G., editors, *Adaptive Methods-Algorithms, Theory and Applications*, pages 84–98, Braunschweig/Wiesbaden. Proceedings of the Ninth GAMM-Seminar, Vieweg & Sohn.
- [Hackbusch, 1985] Hackbusch, W. (1985). *Multi-Grid Methods and Applications*. Springer Verlag, Berlin, Heidelberg.
- [Hackbusch, 1994] Hackbusch, W. (1994). *Iterative solution of large sparse systems of equations*. Springer Verlag, New York.

## References II

- [Martin, 1998] Martin, D. F. (1998). *A cell-centered adaptive projection method for the incompressible Euler equations*. PhD thesis, University of California at Berkeley.
- [Trottenberg et al., 2001] Trottenberg, U., Oosterlee, C., and Schüller, A. (2001). *Multigrid*. Academic Press, San Antonio.
- [Wesseling, 1992] Wesseling, P. (1992). *An introduction to multigrid methods*. Wiley, Chichester.

# Lecture 4b

## Design of SAMR Systems, Advanced Parallelization, Usage

Course *Block-structured Adaptive Mesh Refinement Methods for Conservation Laws*  
*Theory, Implementation and Application*

Ralf Deiterding

Computer Science and Mathematics Division  
Oak Ridge National Laboratory  
P.O. Box 2008 MS6367, Oak Ridge, TN 37831, USA

E-mail: [deiterdingr@ornl.gov](mailto:deiterdingr@ornl.gov)



# Outline

## Available SAMR software

- Simplified block-based AMR
- General patch-based SAMR

## AMROC

- Overview
- Layered software structure

## Massively parallel SAMR

- Performance data from AMROC
- Scalability bottlenecks

## Usage of AMROC

- Short overview

# Simplified structured designs

*Distributed memory parallelization fully supported if not otherwise states.*

- ▶ PARAMESH (Parallel Adaptive Mesh Refinement)
  - ▶ Library based on uniform refinement blocks [MacNeice et al., 2000]
  - ▶ Both multigrid and explicit algorithms considered
  - ▶ <http://sourceforge.net/projects/paramesh>
- ▶ Flash code (AMR code for astrophysical thermonuclear flashes)
  - ▶ Built on PARAMESH
  - ▶ Solves the magneto-hydrodynamic equations with self-gravitation
  - ▶ <http://flash.uchicago.edu/website/home>
- ▶ Uintah (AMR code for simulation of accidental fires and explosions)
  - ▶ Only explicit algorithms considered
  - ▶ FSI coupling Material Point Method and ICE Method (Implicit, Continuous fluid, Eulerian)
  - ▶ <http://www.uintah.utah.edu>
- ▶ DAGH/Grace [Parashar and Browne, 1997]
  - ▶ Just C++ data structures but no methods
  - ▶ All grids are aligned to bases mesh coarsened by factor 2
  - ▶ <http://userweb.cs.utexas.edu/users/dagh>

# Systems that support general SAMR

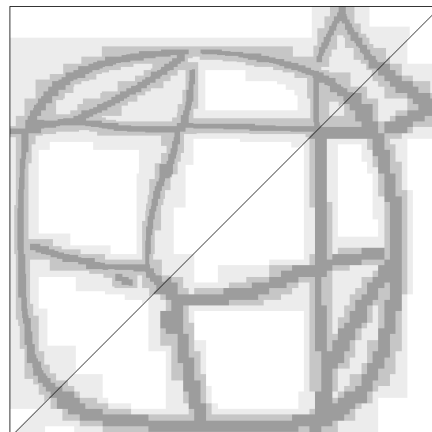
- ▶ SAMRAI - Structured Adaptive Mesh Refinement Application Infrastructure
  - ▶ Very mature SAMR system [Hornung et al., 2006]
  - ▶ Explicit algorithms directly supported, implicit methods through interface to Hypr package
  - ▶ Mapped geometry and some embedded boundary support
  - ▶ <https://computation.llnl.gov/casc/SAMRAI>
- ▶ BoxLib, AmrLib, MGLib, HGProj
  - ▶ Berkley-Lab-AMR collection of C++ classes by J. Bell et al., 50,000 LOC [Rendleman et al., 2000]
  - ▶ Both multigrid and explicit algorithms supported
  - ▶ <https://ccse.lbl.gov/Software> (no codes available)
- ▶ Chombo
  - ▶ Redesign and extension of BoxLib by P. Colella et al.
  - ▶ Both multigrid and explicit algorithms demonstrated
  - ▶ Some embedded boundary support
  - ▶ <https://seesar.lbl.gov/anag/chombo>

## Further SAMR software

- ▶ Overture (Object-oriented tools for solving PDEs in complex geometries)
  - ▶ Overlapping meshes for complex geometries by W. Henshaw et al. [Brown et al., 1997]
  - ▶ Explicit and implicit algorithms supported
  - ▶ <https://computation.llnl.gov/casc/Overture>
- ▶ AMRClaw within Clawpack [Berger and LeVeque, 1998]
  - ▶ Serial 2D Fortran 77 code for the explicit Wave Propagation method with own memory management
  - ▶ <http://www.clawpack.org>
- ▶ Amrita by J. Quirk
  - ▶ Only 2D explicit finite volume methods supported
  - ▶ Embedded boundary algorithm
  - ▶ <http://www.amrita-cfd.org>
- ▶ Cell-based Cartesian AMR: RAGE
  - ▶ Embedded boundary method
  - ▶ Explicit and implicit algorithms
  - ▶ [Gittings et al., 2008]

# AMROC

- ▶ “Adaptive Mesh Refinement in Object-oriented C++”
- ▶ ~ 46,000 LOC for C++ SAMR kernel, ~ 140,000 total C++, C, Fortran-77
- ▶ uses parallel hierarchical data structures that have evolved from DAGH
- ▶ Right: point explosion in box, 4 level, Euler computation, 7 compute nodes
- ▶ V1.0: <http://amroc.sourceforge.net>



	$l_{\max}$	Level 0	Level 1	Level 2	Level 3	Level 4
AMROC's DAGH grids/cells	1	43/22500	145/38696			
	2	42/22500	110/48708	283/83688		
	3	36/22500	78/54796	245/109476	582/165784	
	4	41/22500	88/56404	233/123756	476/220540	1017/294828
Original DAGH grids/cells	1	238/22500	125/41312			
	2	494/22500	435/48832	190/105216		
	3	695/22500	650/55088	462/133696	185/297984	
	4	875/22500	822/57296	677/149952	428/349184	196/897024

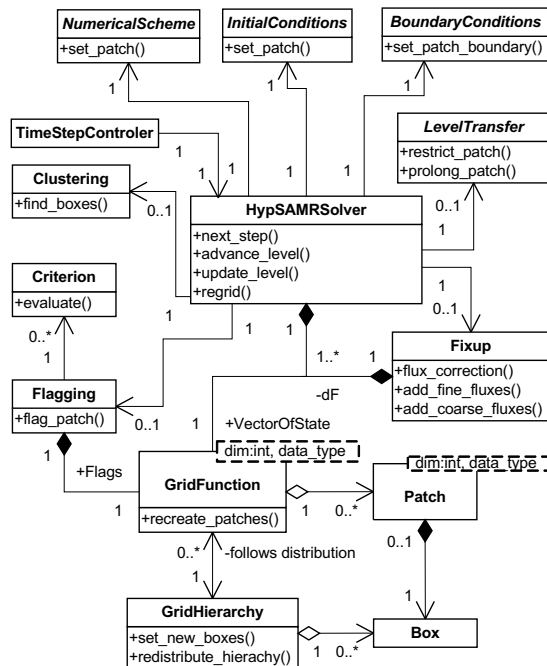
Comparison of number of cells and grids in DAGH and AMROC

# The Virtual Test Facility

- ▶ Implements all described algorithms beside multigrid methods
- ▶ AMROC V2.0 plus solid mechanics solvers
- ▶ Implements explicit SAMR with different finite volume solvers
- ▶ Embedded boundary method, FSI coupling
- ▶ ~ 430,000 lines of code total in C++, C, Fortran-77, Fortran-90
- ▶ autoconf / automake environment with support for typical parallel high-performance system
- ▶ <http://www.cacr.caltech.edu/asc>
- ▶ [Deiterding et al., 2006][Deiterding et al., 2007]

# UML design of AMROC

- ▶ Classical framework approach with generic main program in C++
- ▶ Customization / modification in Problem.h include file by derivation from base classes and redefining virtual interface functions
- ▶ Predefined, scheme-specific classes (with F77 interfaces) provided for standard simulations
- ▶ Standard simulations require only linking to F77 functions for initial and boundary conditions, source terms. No C++ knowledge required
- ▶ Interface mimics Clawpack
- ▶ Expert usage (algorithm modification, advanced output, etc.) in C++



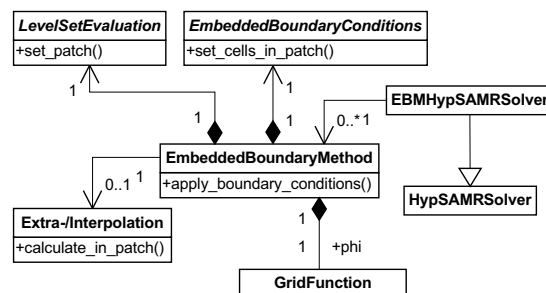
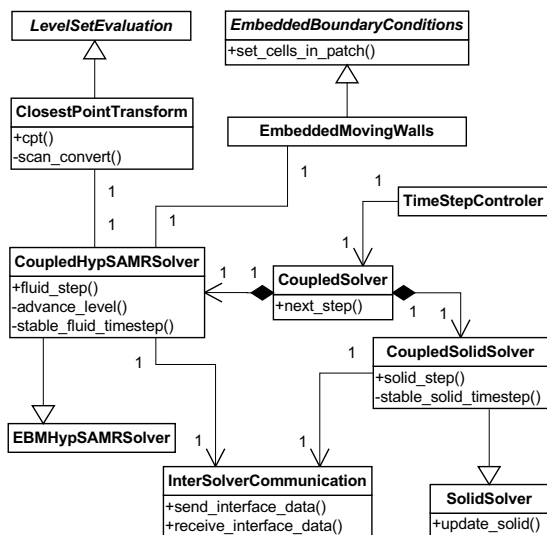
# Commonalities in software design

- ▶ Index coordinate system based on  $\Delta x_{n,l} \cong \prod_{\kappa=l+1}^{l_{\max}} r_{\kappa}$  to uniquely identify a cell within the hierarchy
- ▶ `Box<dim>`, `BoxList<dim>` class that define rectangular regions  $G_{m,l}$  by `lowerleft`, `upperright`, `stepsize` and specify topological operations  $\cap$ ,  $\cup$ ,  $\setminus$
- ▶ `Patch<dim,type>` class that assigns data to a rectangular grid  $G_{m,l}$
- ▶ A class, here `GridFunction<dim,type>`, that defines topological relations between lists of `Patch` objects to implement synchronization, restriction, prolongation, re-distribution
- ▶ Hierarchical parallel data structures are typically C++, routines on patches often Fortran



# Embedded boundary method / FSI coupling

- ▶ Multiple independent EmbeddedBoundaryMethod objects possible
- ▶ Specialization of GFM boundary conditions, level set description in scheme-specific F77 interface classes



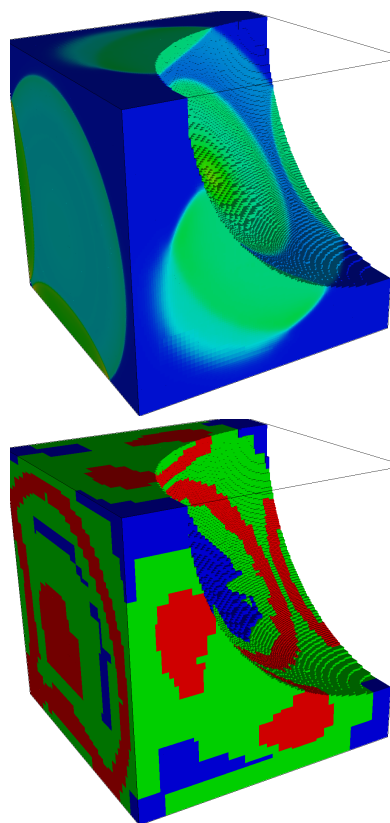
- ▶ Coupling algorithm implemented in further derived HypSAMRSolver class
- ▶ Level set evaluation always with CPT algorithm
- ▶ Parallel communication through efficient non-blocking communication module
- ▶ Time step selection for both solvers through CoupledSolver class

# Performance assessment

- ▶ Test run on 2.2 GHz AMD Opteron quad-core cluster connected with Infiniband
- ▶ Cartesian test configuration
- ▶ Spherical blast wave, Euler equations, 3rd order WENO scheme, 3-step Runge-Kutta update
- ▶ AMR base grid  $64^3$ ,  $r_{1,2} = 2$ , 89 time steps on coarsest level
- ▶ With embedded boundary method: 96 time steps on coarsest level
- ▶ Redistribute in parallel every 2nd base level step
- ▶ Uniform grid  $256^3 = 16.8 \cdot 10^6$  cells

Level	Grids	Cells
0	115	262,144
1	373	1,589,808
2	2282	5,907,064

Grid and cells used on 16 CPUs



# Cost of SAMR (AMROC V2.0)

- ▶ Flux correction is negligible
- ▶ Clustering is negligible (already local approach). For the complexities of a scalable global clustering algorithm see [Gunney et al., 2007]
- ▶ Costs for GFM constant around  $\sim 36\%$
- ▶ Main costs: Regrid(1) operation and ghost cell synchronization

CPU's	16	32	64
Time per step	32.44s	18.63s	11.87s
Uniform	59.65s	29.70s	15.15s
Integration	73.46%	64.69%	50.44%
Flux Correction	1.30%	1.49%	2.03%
Boundary Setting	13.72%	16.60%	20.44%
Regridding	10.43%	15.68%	24.25%
Clustering	0.34%	0.32%	0.26%
Output	0.29%	0.53%	0.92%
Misc.	0.46%	0.44%	0.47%

CPU's	16	32	64
Time per step	43.97s	25.24s	16.21s
Uniform	69.09s	35.94s	18.24s
Integration	59.09%	49.93%	40.20%
Flux Correction	0.82%	0.80%	1.14%
Boundary Setting	19.22%	25.58%	28.98%
Regridding	7.21%	9.15%	13.46%
Clustering	0.25%	0.23%	0.21%
GFM Find Cells	2.04%	1.73%	1.38%
GFM Interpolation	6.01%	10.39%	7.92%
GFM Overhead	0.54%	0.47%	0.37%
GFM Calculate	0.70%	0.60%	0.48%
Output	0.23%	0.52%	0.74%
Misc.	0.68%	0.62%	0.58%

# AMROC scalability tests

## Basic test configuration

- ▶ Spherical blast wave, Euler equations, 3D wave propagation method
- ▶ AMR base grid  $32^3$  with  $r_{1,2} = 2, 4$ . 5 time steps on coarsest level
- ▶ Uniform grid  $256^3 = 16.8 \cdot 10^6$  cells, 19 time steps
- ▶ Flux correction deactivated
- ▶ No volume I/O operations
- ▶ Tests run IBM BG/P (mode VN)

## Weak scalability test

- ▶ Reproduction of configuration each 64 CPUs
- ▶ On 1024 CPUs:  $128 \times 64 \times 64$  base grid,  $> 33,500$  Grids,  $\sim 61 \cdot 10^6$  cells, uniform  $1024 \times 512 \times 512 = 268 \cdot 10^6$  cells

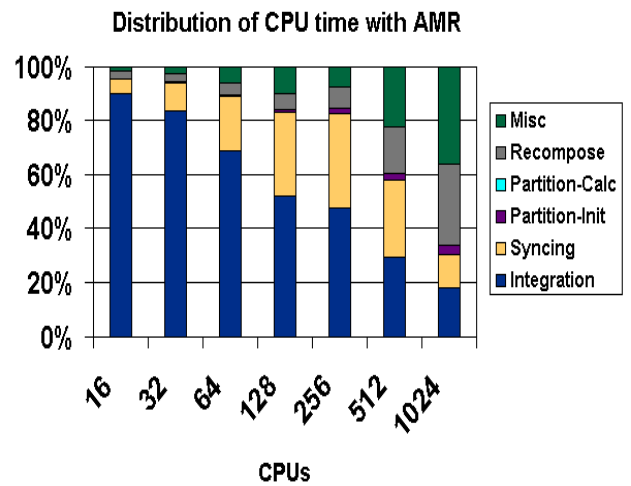
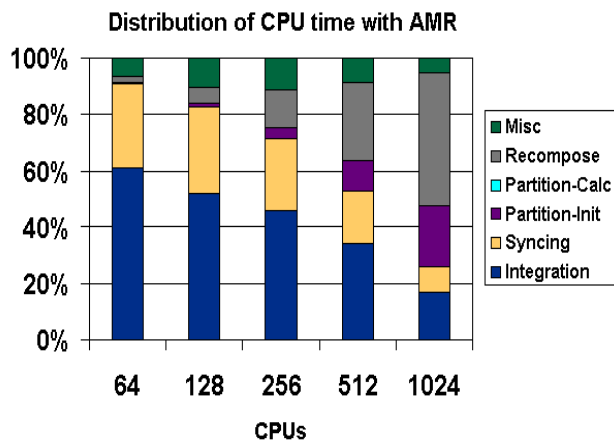
Level	Grids	Cells
0	606	32,768
1	575	135,312
2	910	3,639,040

## Strong scalability test

- ▶  $64 \times 32 \times 32$  base grid, uniform  $512 \times 256 \times 256 = 33.6 \cdot 10^6$  cells

Level	Grids	Cells
0	1709	65,536
1	1735	271,048
2	2210	7,190,208

# Scalability tests AMROC V2.0



- ▶ Syncing: Parallel communication portion of boundary setting
- ▶ Recompose: topological list operations, construction of boundary info, redistribution of data blocks
- ▶ Partition-Init, Partition-Calc: construction of space filling curve
- ▶ Costs for Partition-Init and Recompose increase dramatically for large problem size

# Topological list operations

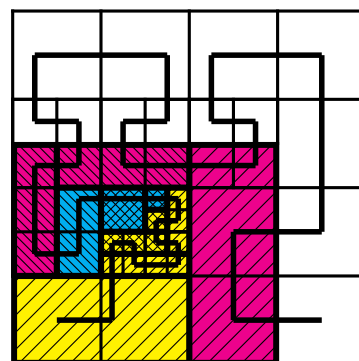
*Weak scalability problems are due to non-parallel sub-algorithms!*

- ▶ Operations  $\cap$ ,  $\setminus$  on two box lists have complexity  $O(NM)$
- ▶ Costs of operations in `Recompose(1)`, that use global box lists  $G_l$ , increase quadratically, cf. [Wissink et al., 2003]
- ▶ Solution
  - ▶ Clip  $G_l$  with properly chosen quadratic bounding box around  $G_l^p$  before using  $\cap$ ,  $\setminus$
- ▶ All topological operations in `Recompose(1)` involving global lists can be reduced to local ones
- ▶ Present code V2.1 $\beta$  still uses `MPI_allgather()` to communicate global lists to all nodes
- ▶ Global view is particularly useful to evaluate new local portion of hierarchy and for data redistribution

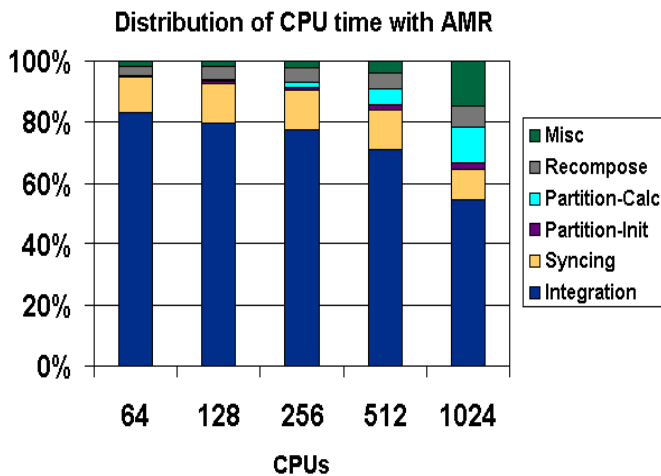
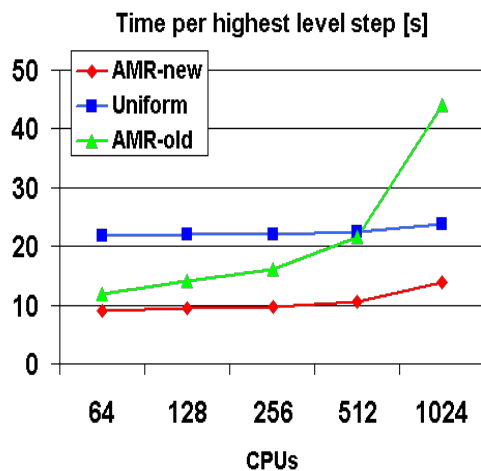
# Construction of space-filling curve

## Computation of space filling curve

- ▶ Partition-Init
  1. Compute aggregated workload for new grid hierarchy  $G_l$  and project result onto level 0
  2. Construct recursively SFC-units until work in each unit is homogeneous, GuCFactor defines minimal coarseness relative to level-0 grid
- ▶ Partition-Calc
  1. Compute entire workload and new work for each processor
  2. Go sequentially through SFC-ordered list of partitioning units and assign units to processors, refine partition if necessary and possible
- ▶ Ensure scalability of Partition-Init by creating SFC-units strictly local
- ▶ Currently still use of `MPI_allgather()` to create globally identical input for Partition-Calc



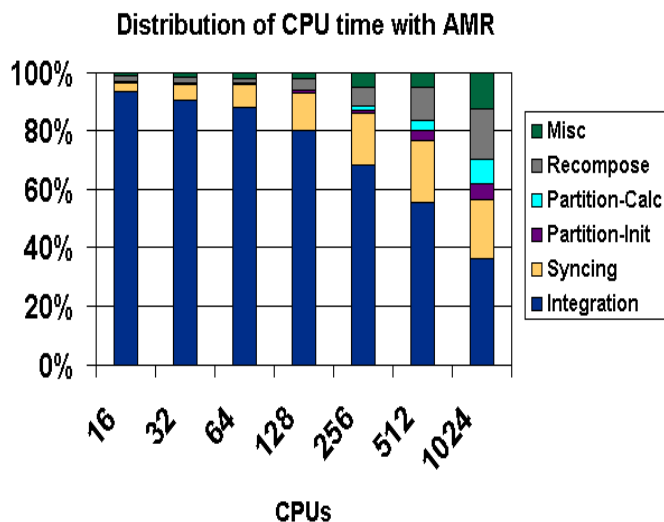
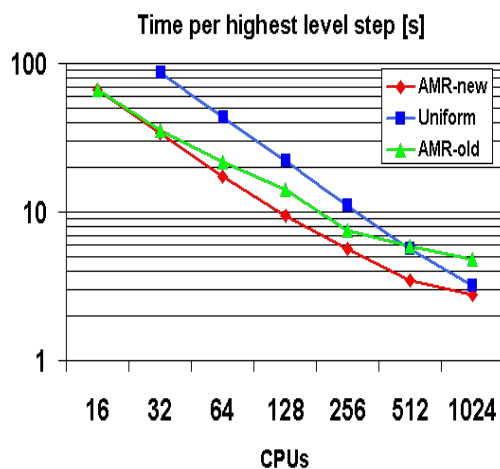
# Weak scalability test V2.1 $\beta$



- ▶ Overall performance improvement for 1024 CPUs by  $\sim 69\%$
- ▶ Absolute costs for Syncing are almost constant
- ▶ 1024 required usage of -DUAL option due to usage of global lists data structures in Partition-Calc and Recompose



# Strong scalability test V2.1 $\beta$



- ▶ Overall performance improvement for 1024 CPUs by 43 %
- ▶ Improved partitioning algorithm allowed usage of GuCFactor=1 instead of 2 before and full parallel data redistribution in every Regrid(1) instead of every 2nd level-0 step

# To-Do

## Comments

- ▶ Scalability of V2.1 $\beta$  for finite volume methods is comparable to results reported from Chombo and SAMRAI
- ▶ Significantly better scalability has so far only been reported for shallow hierarchies [Greenough et al., 2005] and/or tailored parameters choices

## Next step

- ▶ Eliminate aggregation of global box list data (that currently uses simply `MPI_allgather()`)
  - ▶ Partition-Calc: assignment of SFC-ordered sequence and refinement could be executed sequentially on each node
  - ▶ Global topology lists: assemble only those portions of global lists on each node that are relevant for the subsequent operations. Use Cartesian bounding box information to construct irregular point-to-point communication pattern for list data between nodes

## Future work

- ▶ Large-scale hierarchical I/O
- ▶ Hybrid parallelization (considering accelerators), cf. [Schive et al., 2010], [Jourdon, 2005]

# Quick start with AMROC V2.0 I

Standard Linux development system assumed! See `install_vtf.pdf` for details.

1. Unpack `hdf4_src.tgz` into home directory: `cd; tar -xvzf hdf4_src.tgz`
2. `cd asc; ./build_hdf4.sh`
3. If last step successful `libdf.a`, `libjpeg.a`, `libmfhdf.a`, `libsz.a`, `libz.a` are in `$HOME/asc/hdf4/lib`.
4. Unpack `AMROC-Clawpack-1.0.tgz` into `$HOME/asc`:  
`cd $HOME/asc; tar -xvzf AMROC-Clawpack-1.0.tgz`
5. With `mpicc`, `mpicxx` commands
  - 5.1 `cd vtf`
  - 5.2 `./configure -C --enable-opt=yes --enable-mpi=yes`  
`HDF4_DIR=$HOME/asc/hdf4`  
If `autoconf`, `automake` are available add  
`--enable-maintainer-mode` to last line
  - 5.3 `cd gnu-opt-mpi`

# Quick start with AMROC V2.0 II

5.4 make

5.5 source ../ac/paths.sh

5.6 Optional unit test

5.6.1 ../amroc/testrun.sh -m make -r 4 -s

5.6.2 ../amroc/testrun.sh -c

6. Without MPI

6.1 cd vtf

6.2 ./configure -C --enable-opt=yes --enable-mpi=no

HDF4\_DIR=\$HOME/asc/hdf4

If autoconf, automake are available add

--enable-maintainer-mode to last line

6.3 cd gnu-opt

6.4 make

6.5 source ../ac/paths.sh

6.6 Optional unit test

6.6.1 ../amroc/testrun.sh -m make -r 0 -s

6.6.2 ../amroc/testrun.sh -c

# Quick start with AMROC V2.0 III

## 7. Realistic example

- 7.1 Change to compilation directory gnu-opt/gnu-opt-mpi:  
`cd amroc/clawpack/applications/euler/2d/SphereLift0ff`
- 7.2 `make`
- 7.3 Change to corresponding directory with solver.in: `cd`  
`vtf/amroc/clawpack/applications/euler/2d/SphereLift0ff`
- 7.4 `./run.py` or `./run.py 2` (if you have compiled with MPI on a dual-core system)
- 7.5 `gnuplot Density.gnu` shows density evolution of lower boundary
- 7.6 Create binary VTK files for Paraview or VisIt: `hdf2tab.sh "-f display_file_visit.in"`
- 7.7 Execute VisIt or Paraview and load the VTK files for visualization.

# Quick start with AMROC V2.0 IV

## 8. FSI example (requires MPI)

- 8.1 `cd`  
    `$HOME/asc/gnu-opt-mpi/vtf/fsi/beam-amroc/VibratingBeam`
- 8.2 `make`
- 8.3 `cd $HOME/asc/vtf/fsi/beam-amroc/VibratingBeam`
- 8.4 `./run.py 4`  
    Change LastNode entry in `solver.in` for different processor number.
- 8.5 `hdf2tab.sh`
- 8.6 Execute VisIt or Paraview and load the VTK files for visualization.

## 9. For further documentation see <http://www.cacr.caltech.edu/asc>

# References I

- [Berger and LeVeque, 1998] Berger, M. and LeVeque, R. (1998). Adaptive mesh refinement using wave-propagation algorithms for hyperbolic systems. *SIAM J. Numer. Anal.*, 35(6):2298–2316.
- [Brown et al., 1997] Brown, D. L., Henshaw, W. D., and Quinlan, D. J. (1997). Overture: An object oriented framework for solving partial differential equations. In *Proc. ISCOPE 1997, appeared in Scientific Computing in Object-Oriented Parallel Environments*, number 1343 in Springer Lecture Notes in Computer Science.
- [Deiterding et al., 2007] Deiterding, R., Cirak, F., Mauch, S. P., and Meiron, D. I. (2007). A virtual test facility for simulating detonation- and shock-induced deformation and fracture of thin flexible shells. *Int. J. Multiscale Computational Engineering*, 5(1):47–63.
- [Deiterding et al., 2006] Deiterding, R., Radovitzky, R., Mauch, S. P., Noels, L., Cummings, J. C., and Meiron, D. I. (2006). A virtual test facility for the efficient simulation of solid materials under high energy shock-wave loading. *Engineering with Computers*, 22(3-4):325–347.

## References II

- [Gittings et al., 2008] Gittings, M., Weaver, R., Clover, M., Betlach, T., Byrne, N., Coker, R., Dendy, E., Hueckstaedt, R., New, K., Oakes, R., Rantal, D., and Stefan, R. (2008). The RAGE radiation-hydrodynamics code. *Comput. Sci. Disc.*, 1. doi:10.1088/1749-4699/1/1/015005.
- [Greenough et al., 2005] Greenough, J. A., de Supinski, B. R., Yates, R. K., Rendleman, C. A., Skinner, D., Beckner, V., Lijewski, M., Bell, J., and Sexton, J. C. (2005). Performance of a block structured, hierarchical adaptive mesh refinement code on the 64k node IBM BlueGene/L computer. Technical Report LBNL-57500, Ernest Orlando Lawrence Berkeley National Laboratory, Berkeley.
- [Gunney et al., 2007] Gunney, B. T., Wissink, A. M., and Hysoma, D. A. (2007). Parallel clustering algorithms for structured AMR. *J. Parallel and Distributed Computing*, 66(11):1419–1430.
- [Hornung et al., 2006] Hornung, R. D., Wissink, A. M., and Kohn, S. H. (2006). Managing complex data and geometry in parallel structured AMR applications. *Engineering with Computers*, 22:181–195.



## References III

- [Jourdon, 2005] Jourdon, H. (2005). HERA: A hydrodynamic AMR platform for multi-physics simulation. In Plewa, T., Linde, T., and Weirs, V. G., editors, *Adaptive Mesh Refinement - Theory and Applications*, volume 41 of *Lecture Notes in Computational Science and Engineering*, pages 283–294. Springer.
- [MacNeice et al., 2000] MacNeice, P., Olson, K. M., Mobarrry, C., deFainchtein, R., and Packer, C. (2000). PARAMESH: A parallel adaptive mesh refinement community toolkit. *Computer Physics Communications*, 126:330–354.
- [Parashar and Browne, 1997] Parashar, M. and Browne, J. C. (1997). System engineering for high performance computing software: The HDDA/DAGH infrastructure for implementation of parallel structured adaptive mesh refinement. In *Structured Adaptive Mesh Refinement Grid Methods*, IMA Volumes in Mathematics and its Applications. Springer.
- [Rendleman et al., 2000] Rendleman, C. A., Beckner, V. E., Lijewski, M., Crutchfield, W., and Bell, J. B. (2000). Parallelization of structured, hierarchical adaptive mesh refinement algorithms. *Computing and Visualization in Science*, 3:147–157.

## References IV

- [Schive et al., 2010] Schive, H.-Y., Tsai, Y.-C., and Chiueh, T. (2010). GAMER: a GPU-accelerated adaptive mesh refinement code for astrophysics. *Astrophysical J. Supplement Series*, 186:457–484.
- [Wissink et al., 2003] Wissink, A., Hysom, D., and Hornung, R. (2003). Enhancing scalability of parallel structured amr calculations. In *Proc. 17th Int. Conf. Supercomputing*, pages 336–347.